

HIGHER ORDER STABILIZED SURFACE FINITE  
ELEMENT METHODS FOR  
DIFFUSION-CONVECTION-REACTION EQUATIONS ON  
SURFACES WITH AND WITHOUT BOUNDARY

**Dissertation**

zur Erlangung des akademischen Grades

**doctor rerum naturalium**

**(Dr. rer. nat.)**

von Dipl.-Tech.-Math. Kristin Simon  
geboren am 30.11.1987 in Nordhausen

genehmigt durch die Fakultät für Mathematik  
der Otto-von-Guericke-Universität Magdeburg

Gutachter: Prof. Dr. rer. nat. habil. Lutz Tobiska  
Prof. Dr. rer. nat. habil. Arnd Meyer

eingereicht am 13. April 2017

Verteidigung am 25. August 2017



## Danksagung

Vor allen Anderen möchte ich meinem Betreuer Prof. Tobiska danken. Ohne seine Führung und Unterstützung wäre diese Doktorarbeit nicht möglich gewesen. Ich bin ihm für all die Zeit und Energie, die er in gemeinsame Diskussionen und Nachforschungen zu meinem Thema gesteckt hat, tief verbunden. Seine Ratschläge waren und sind eine große Hilfe; nicht nur in der Forschung und im akademischen Bereich sondern auch darüber hinaus.

Ich möchte mich bei all meinen Kollegen aus dem Institut für Analysis und Numerik sowie dem Graduiertenkolleg für den ergiebigen Austausch von Ideen, Gedanken und Problemen bedanken. Ein besondere Dank gebührt dabei Alina Bondarava, Andreas Hahn und Klim Kavaliou, die stets Zeit fanden auftretende Schwierigkeiten und unerwartete Ergebnisse zu diskutieren.

Ich möchte meine tiefe Dankbarkeit gegenüber meinen Eltern, deren stetige Ermutigungen und kontinuierliche Unterstützung mich dahin brachten, wo ich heute stehe, und gegenüber Martin Köhler, der mich jeder Zeit unterstützt und mir den Rücken frei gehalten hat, zum Ausdruck bringen. Ich danke auch dem Rest meiner Familie und meinen Freunden für ihre offenen Ohren und aufmunternden Worte.

Weiterhin bin ich dem Graduiertenkolleg *Micro-Macro-Interactions in structured Media and Particle Systems* für die finanzielle Unterstützung während meiner Dissertation zu Dank verpflichtet.



### Acknowledgement

First of all I give thanks to my supervisor Prof. Tobiska. Without his advice and support this PhD thesis would not have been possible. I am deeply grateful for all the time and energy he spent in joint discussions and study on my topic. His guidance was and is of great assistance not only for research and academia but also beyond.

I want to thank all of my colleagues from the Institute of Analysis and Numerics and from the Graduiertenkolleg for the fruitful exchanges of ideas, thoughts and problems. Special thanks belongs to Alina Bondarava, Andreas Hahn and Klim Kavaliou, who always found a minute to discuss upcoming difficulties and unexpected results.

I want to express deep gratitude to my parents, whose steady encouragement and continuous support brought me, where I am today, and to Martin Köhler, who aided me and backed me up at any time. I give thanks to the rest of my family and my friends to for their sympathetic ear and words of cheer.

Further, I am grateful to the Graduiertenkolleg *Micro-Macro-Interactions in structured Media and Particle Systems* for financial support during my doctoral studies.



## Zusammenfassung

Strömungen mit freien Oberflächen und Zwei-Phasen-Strömungen sind von großem Interesse auf dem Gebiet der Fluidodynamik. Die Strömung des Fluides kann dabei von so genannten Surfactants beeinflusst werden. Surfactants sind grenzflächenaktive Substanzen. Sie bezeichnen chemische Verbindungen, die sich an der Oberfläche anlagern und damit die Oberflächenspannung ändern können. Dies hat Einfluss auf das Strömungsverhalten des Fluides. Um den Einfluss dieser Stoffe auf die Strömung zu modellieren, werden Diffusions-Konvektions-Reaktions-Gleichungen im Fluid, dem Bulk, und auf dessen Oberfläche benötigt. Während Diffusions-Konvektions-Reaktions-Gleichungen im Bulk weitgehend untersucht sind, zählen Transportgleichungen auf Oberflächen  $\Gamma$

$$-\varepsilon \Delta_{\Gamma} u + \nabla_{\Gamma} \cdot (\mathbf{w}u) + cu = f$$

zu den aktuellen Forschungsgebieten.

In dieser Arbeit wird die obige Gleichung auf Oberflächen mit oder ohne Rand betrachtet. Das Finite-Elemente-Gitter wird durch Approximationen erster und höherer Ordnung der gekrümmten Oberfläche gegeben. Entsprechende Operatoren auf der glatten und der diskreten Oberfläche werden eingeführt. Die eindeutige Lösbarkeit des schwachen und des diskreten Problems werden aufgezeigt. Eine Fehleranalyse für Finite Elemente erster und höherer Ordnung wird durchgeführt. Dabei werden sowohl der Fall mit vorhandener  $L^2$ -Kontrolle ( $c > 0$ ) als auch der Fall mit fehlender  $L^2$ -Kontrolle ( $c = 0$ ) berücksichtigt. Speziellen Wert wird auf den konvektionsdominanten Fall, bei dem  $\varepsilon \ll 1$  gilt, gelegt. Alle Abschätzungen sind, so weit möglich, semi-robust bezüglich des Diffusionskoeffizientens. Das heißt, die Konstanten in den Fehlerabschätzungen hängen nicht von Termen ab, die für  $\varepsilon \rightarrow 0$  unbeschränkt wachsen. Dabei kann jedoch die verwendete Norm  $\varepsilon$ -abhängig sein.

Für konvektionsdominierte Transportgleichungen im Bulk ist bekannt, dass die Finite-Elemente-Methode zu unphysikalischen Oszillationen rund um Rand- und innere Grenzschichten führt. Dasselbe Verhalten kann auch für die Oberflächen-gleichung beobachtet werden. Mit der Lokalen Projektionsstabilisierung und der Streamline-Upwind-Petrov-Galerkin-Methode werden zwei für Bulk-Gleichungen übliche Stabilisierungstechniken auf Oberflächengleichungen erweitert.





## Abstract

The numerical simulation of free surface and two-phase flows is an area of high interest in fluid dynamics. Thereby, the fluid flow can be influenced by so called surfactants. Surfactant is an abbreviation for surface active agent and names a chemical compound, which can adsorb at the surface and change the surface tension. This influences the fluid motion. To model the influence of surfactants, diffusion-convection-reaction equations in the fluid phase, the bulk, and on the surface are required. Whereas diffusion-convection-reaction equations in the bulk are widely studied, transport equations on surfaces  $\Gamma$

$$-\varepsilon\Delta_{\Gamma}u + \nabla_{\Gamma} \cdot (\mathbf{w}u) + cu = f$$

are an area of recent research.

In this work the above equation on surfaces with and without boundary is studied. First and higher order approximations of the curved surface are used as finite element meshes. The corresponding operators on the smooth and the discrete surface are introduced. Unique solvability of the weak and the discretized problem are shown and an error analysis for first and higher order finite elements has been taken out. Thereby, the cases of provided  $L^2$ -control and missing  $L^2$ -control of the solution are considered. Special attention is paid to the convection dominated case, where  $\varepsilon \ll 1$ , and as far as possible estimates, that are semi-robust with reference to the diffusion coefficient  $\varepsilon$ , are obtained. That means, the constants in the error estimates does not depend on terms, that tend to infinity for  $\varepsilon \rightarrow 0$ . However, the norm used in the estimate can depend on  $\varepsilon$ .

It is well-known from convection dominated transport equations in the bulk, that finite element methods lead to non-physical oscillations at interior or boundary layers. The same behaviour can be observed for transport equations on surfaces. The Local Projection Stabilization and the Streamline-Upwind-Petrov-Galerkin method, two stabilization techniques common for bulk equations, are studied for surface diffusion-convection-reaction problems.



# Contents

<b>1</b>	<b>Introduction</b>	<b>1</b>
1.1	State of the Art . . . . .	2
1.2	Surface Description and Operators . . . . .	5
1.2.1	Surface Derivatives . . . . .	6
1.2.2	Surface Gauss Theorem . . . . .	7
1.3	Surface Sobolev Spaces . . . . .	8
<b>2</b>	<b>Surface Discretization</b>	<b>11</b>
2.1	Linear Approximation . . . . .	11
2.1.1	Projection Operator . . . . .	12
2.1.2	Exact Triangulation . . . . .	13
2.2	Higher Order Approximation . . . . .	13
2.2.1	Extension Operator . . . . .	19
2.2.2	Geometric Estimates . . . . .	19
2.3	Discrete Operators . . . . .	21
2.4	Integral Transformations . . . . .	26
2.5	Finite Element Spaces and Interpolation . . . . .	29
<b>3</b>	<b>Elliptic Equations on Surfaces</b>	<b>31</b>
3.1	Diffusion Convection Reaction Equation . . . . .	32
3.1.1	Weak Formulation . . . . .	32
3.1.2	Discretized Formulation . . . . .	34
3.1.3	Error Estimates . . . . .	35
3.2	Diffusion Convection Equation . . . . .	41
3.2.1	Problem Formulation . . . . .	42
3.2.2	Discretized Formulation . . . . .	43
3.2.3	Error Estimates . . . . .	45
<b>4</b>	<b>Stabilization Techniques on Surfaces</b>	<b>53</b>
4.1	Local Projection Stabilization . . . . .	54
4.1.1	Stabilized Formulation . . . . .	54
4.1.2	Error Estimates . . . . .	55
4.1.3	LPS for Diffusion-Convection Equations . . . . .	62

---

4.1.4	Choices for $X^r$ and $D^r$ . . . . .	63
4.2	Streamline-Upwind-Petrov-Galerkin Stabilization . . . . .	65
4.2.1	Stabilized Formulation . . . . .	66
4.2.2	Error Estimates . . . . .	68
4.2.3	SUPG for Diffusion-Convection Equations . . . . .	74
<b>5</b>	<b>Mixed Boundary Conditions</b>	<b>75</b>
5.1	Boundary Conditions for the Diffusion-Convection-Reaction Equation . . . . .	76
5.1.1	Discretized Formulation . . . . .	77
5.1.2	Error Estimates . . . . .	79
5.2	Boundary Conditions for the Diffusion-Convection Equation . . . . .	83
<b>6</b>	<b>Numerical Results</b>	<b>85</b>
6.1	Implementation . . . . .	85
6.2	Example 1: Code Validation . . . . .	88
6.3	Example 2: Non-smooth Right Hand Side . . . . .	96
6.4	Example 3: Circular Flow . . . . .	96
6.5	Example 4: Boundary layer . . . . .	102
<b>7</b>	<b>Conclusion</b>	<b>105</b>
	<b>Bibliography</b>	<b>107</b>

# List of Figures

1.1	Curved Surface with normal, conormal and surface gradient . . .	7
2.1	Smooth surface with linear approximation and exact triangulation in 2D and 3D . . . . .	14
2.2	Visualization of the sets $F_K(\Lambda_0)$ and $F_K(\Lambda_1)$ . . . . .	15
2.3	Smooth 2D surface with its linear and quadratic approximation .	18
6.1	Unstabilized solutions of Example 2 for different refinement levels	97
6.2	Comparison of unstabilized and stabilized solutions for Example 2	97
6.3	Smooth surface $\Gamma$ used in Examples 3 and 4. . . . .	99
6.4	Stabilized and unstabilized linear and quadratic solutions of Ex- ample 3 . . . . .	100
6.5	Stabilized and unstabilized linear solutions of Example 3 over in- tersection curve . . . . .	100
6.6	Stabilized and unstabilized quadratic solutions of Example 3 over intersection curve . . . . .	101
6.7	Stabilized and unstabilized linear solutions of Example 3 over out- flow boundary . . . . .	101
6.8	Stabilized and unstabilized quadratic solutions of Example 3 over outflow boundary . . . . .	101
6.9	Stabilized and unstabilized linear solutions of Example 4 on inter- section curve . . . . .	103
6.10	Stabilized and unstabilized quadratic solutions of Example 4 on intersection curve . . . . .	103



# List of Tables

6.1	Error and convergence order for unstabilized methods in 1D with $\varepsilon = 10^{-2}$ . . . . .	89
6.2	Error and convergence order for unstabilized methods in 1D with $\varepsilon = 10^{-6}$ . . . . .	89
6.3	Error and convergence order for stabilized methods in 1D with $\varepsilon = 10^{-2}$ . . . . .	90
6.4	Error and convergence order for stabilized methods in 1D with $\varepsilon = 10^{-6}$ . . . . .	91
6.5	Error and convergence order for unstabilized methods in 2D with $\varepsilon = 10^{-2}$ . . . . .	92
6.6	Error and convergence order for unstabilized methods in 2D with $\varepsilon = 10^{-6}$ . . . . .	92
6.7	Error and convergence order for stabilized methods in 2D with $\varepsilon = 10^{-2}$ . . . . .	93
6.8	Error and convergence order for stabilized methods in 2D with $\varepsilon = 10^{-6}$ . . . . .	94





# Chapter 1

## Introduction

Differential equations on surfaces play an important role in many different applications in mechanics, fluid dynamics, computer graphics [24], cell biology [32] and chemistry. In this thesis, convection-dominated transport equations on surfaces,

$$-\varepsilon\Delta_{\Gamma}u + \nabla_{\Gamma} \cdot (\mathbf{w}u) + cu = f \quad \text{on } \Gamma$$

with  $\varepsilon \ll 1$ , are studied. They are important, e.g. to model the distribution of surfactants in a fluid.

The first chapter provides an overview on existing techniques for surface differential equations in general and diffusion-convection-reaction equations on surfaces in particular. A description of the surface as a part of the zero level set of a function is introduced and essential notations and operators, based on this, are given. Important formulas and identities on surfaces are presented and surface Sobolev spaces are established.

In Chapter 2 the linear approximation of a given curved surface by a polyhedral surface is introduced. Based on this, an exact triangulation and higher order Lagrange interpolations of the surface are defined. Discrete surface operators are given and geometric error estimates are obtained. Surface Finite Element spaces are established.

The transport equation on closed surfaces is studied in Chapter 3. Thereby, we distinguish the case, where the energy norm provides  $L^2$ -control, and the case of missing  $L^2$ -control in the energy norm. The first one is called diffusion-convection-reaction problem and the second one diffusion-convection problem. A numerical analysis of the problems is shown, including the unique solvability of the weak and the discretized problem together with a detailed error analysis.

Stabilization techniques for surface equations are examined in Chapter 4. The Local Projection Stabilization and the Streamline-Upwind-Petrov-Galerkin stabilization are described for surface equations. It is shown, that for diffusion-convection-reaction equations an improved error estimate, compared to the standard Galerkin surface finite element method, can be obtained for the convection term.

In Chapter 5 surfaces with boundaries are taken into concern. The incorporation of mixed Dirichlet and Neumann boundary conditions is demonstrated for diffusion-convection-reaction equations. Error estimates are provided and compared to the case of a closed surface. Boundary conditions for diffusion-convection equations are shortly discussed.

Finally, Chapter 6 presents some numerical tests. Different numerical examples confirm the analytically determined convergence orders and show the potential of Local Projection Stabilization for surface equations.

## 1.1 State of the Art

A key ingredient in the solution of surface partial differential equations using the finite element method is the handling of the curved surface  $\Gamma$ . Several different approaches exist in the literature. An extensive overview is given by Dziuk and Elliott in [30].

One approach is to solve the equation without the requirement of a discretization of the surface. These methods are based on an extension of the equation into a higher dimensional domain containing the surface. This overcomes the difficulties introduced with surface equations at the costs of solving a higher dimensional problem. If the width of the higher dimensional domain is comparable with the element size one speaks of the Narrow Band method. The extension can be based on a level set or a phase field function [11]. Schemes using the level set approach are formulated in [20] for diffusion-reaction equations and in [29] for transport problems on surfaces. The phase field representative is used amongst others in [33] and [63].

An other idea, getting along without an explicit triangulation of the surface, is inspired by interfaces of two-phase problems on unfitted meshes. In CutFEM or TraceFEM the 1D or 2D interface has to be calculated from a level-set function defined on an underlying 2D or 3D mesh, respectively. The ansatz and test spaces are obtained as traces of a polynomial space defined on the underlying mesh. In general no shape-regularity can be assumed for the surface mesh. Therefore, the discretized problem is ill-conditioned and special stabilization terms are required. This method was introduced by Olshanskii, Reusken and Xu in [59] considering a first order method for the Laplace-Beltrami equation on closed surfaces. In [18] different stabilization methods are discussed. A space-time formulation of the CutFEM of lowest order is given in [60]. Higher order variants of the CutFEM are recently introduced in [40] and [41].

In [21] both techniques introduced above are combined to get an unfitted finite element method for parabolic equations on evolving domains.

In this work, the natural ansatz of a direct triangulation of the surface, also called fitted finite elements, is utilized. This approach goes back to the study of the Poisson problem for the Laplace-Beltrami operator using linear approximations

for the surface and the finite element space by Dziuk in [26]. In [23], this method is extended to surfaces with boundary. Homogeneous Dirichlet boundary conditions are studied, but the analysis is restricted to linear triangulations  $\Gamma_h$  such that  $\mathbf{p}(\partial\Gamma_h) = \partial\Gamma$ . In this case, the boundary is called *curvilinear*. Thereby,  $\mathbf{p}$  is the closest point projection onto  $\Gamma$ . Parabolic equations on surfaces with boundary have been investigated in [27]. Therein, the solution is assumed to be time-dependent, but the surface stays fixed over time. For the first time in [28], the surface was not assumed to be fixed. The technique is brought to the setting of evolving surfaces. Homogeneous Dirichlet and Neumann boundary conditions are considered but still one is restricted to linear approximations of the surface. The analysis of the method is extended to  $L^2$ -error estimates uniformly in time in [31].

To obtain higher order variants of the method, a better approximation of the surface is required. In [22], a piecewise Lagrangian interpolation of the surface combined with higher order Lagrangian finite elements is studied for the Laplace-Beltrami equation on closed surfaces. Thereby, the order of geometric approximation of the surface and the polynomial degree of the mapped finite element space are independent. Based on the higher order geometric approximation, a discontinuous finite element technique on closed surfaces is introduced in [2].

In this work, a higher order surface discretization based on [22] for fixed surfaces with Dirichlet and/or Neumann boundary conditions is introduced. Due to the same reasons as in [23], this is restricted to closed surfaces and surfaces with a *curvilinear* boundary.

Furthermore, the convection-dominated diffusion-convection-reaction equation with a variable velocity field  $\mathbf{w}$  and a variable reaction coefficients  $c$  is considered, compared to the pure Laplace-Beltrami or diffusion-reaction equations mainly studied above. Most of the previous studies have been performed for a fixed  $\varepsilon$ . Here, we are interested, how the error constants depend on the perturbation parameter  $\varepsilon$ . A crucial issue in the analysis of convection dominated problems is the quasi-uniformity of the error estimates with reference to  $\varepsilon$ . A negative power of  $\varepsilon$ , for example, would tend to infinity, if the diffusion coefficient tends to zero, and the constant in the estimates becomes unbounded. Additionally, the diffusion-convection problem is studied. The challenge here is the missing  $L^2$ -control.

An additional issue occurring in the case of convection-dominated problems is well known from bulk equations. The solution of such problems can contain inner or boundary layers. If the finite element mesh is not fine enough, non-physical oscillations around the layers can appear. Different stabilization techniques are introduced for bulk equations. A good overview is the monograph Roos et. al. [64].

One possibility is to add scaled residuals of the strong form of the differential equation to the weak formulation of the problem. Naturally, this methods are consistent and provide a high accuracy on sub-domains excluding the layer.

The idea of using the directional derivative in flow direction to scale the residual leads to the Streamline-Upwind-Petrov-Galerkin (SUPG) method introduced in [44] and analysed in [58] for convection-diffusion problems. It was extended to time-dependent convection-diffusion problems in [13], [46], and [47]. In [10] the idea was transferred to incompressible Navier-Stokes equations. A comprehensive error analysis for the SUPG method applied to Stokes and incompressible Navier-Stokes equations is given in [67]. The usage of upwind terms reduces the numerical diffusion in cross-wind direction and decreases the non-physical smear out.

Another possibility is to combine the advantages of the Galerkin and the least-squares method by adding the variational problem coming from the least-squares minimization problem element wise. This technique was introduced for diffusion-convection equations in [45]. An extension to diffusion-reaction equations is given by the so called Galerkin gradient least-square method presented in [35]. Subsequently, the method was studied for several different problems: amongst others elasticity equations [36], Helmholtz equations [66], Navier-Stokes equations [52], and viscoelastic flows [34].

The residual based methods described above require the evaluation of the residual, which needs for a higher regularity of the solution function and can get quite complex to implement. Additionally, the non-symmetric formulation of the stabilization terms may lead to problems, if the equations are used in optimal control. The following methods overcome these problems at the cost of introducing a consistency error. A non-consistent symmetric stabilization term is added providing additional control of  $H^1$ -type.

In the standard Galerkin approach the solution function is only considered to be continuous but not continuously differentiable over element boundaries. Hence, the gradient of the solution function can jump across the element faces or edges. In the continuous interior penalty method (CIP), a stabilization term penalizing jumps of the gradient over inner edges is added. Additionally, the same technique is used to incorporate Dirichlet boundary conditions weakly. This method was introduced in [25] and studied for diffusion-convection problems in [12] and [14]. Continuous interior penalty methods have also been applied to many other flow problems, as the Ossen problem [16], the Stokes problem [17], and the Navier-Stokes problem [15].

Another symmetric stabilization method is the Local Projection Stabilization (LPS). Having a closer look on where the stabilization in the SUPG method comes from, it turns out that only the convective part of the residuum is responsible for the increased stability. However, taking only the convective part of the residuum would lead to a high consistency error. The workaround used in the LPS method is the usage of only higher order modes of the gradient in the stabilization term. The stabilizing effect is preserved and the order of consistency error can be adjusted by the choice of a projection space. The LPS method was introduced by Becker and Braack in [4] and further studied in [1, 9, 37] for the

Stokes problem. It was extended to the Navier-Stokes problem in [3, 5] and to the Oseen problem in [8, 55]. Local Projection Stabilization for convection-diffusion problems is topic of [50, 56] and is transferred to Shishkin [54], layer-adapted [53] and overlapping [48] meshes. There are two main approaches for LPS: the one-level approach and the two-level approach. Whereas in the one-level approach the finite element space and the projection space are defined on the same mesh, the projection space is given on a coarser mesh in case of the two-level approach. In [49], both are applied to diffusion-convection-reaction equations and compared. Later it has been shown that, at least in the bulk case, the two-level approach can be interpreted as an enriched one-level approach on the coarser mesh. See [68] for the one-dimensional case and [43] for higher dimensions.

As wide-ranging as the stabilization techniques for bulk equations are, as limited is the literature for stabilization of surface equations. Until now, the author is only aware of [60] presenting a stabilization technique for diffusion-convection-reaction problems on surfaces. That paper considers a closed fixed surface discretized by a first order CutFEM approach. For stabilization a surface variant of the SUPG method is introduced.

In this work, on the one hand, the introduced SUPG method for surface equations is transferred to higher order approaches on fitted meshes. On the other hand, the LPS on surfaces is introduced. Due to the construction of higher order fitted approximations of the surface the refinement  $\Gamma_h$  of a discrete surface  $\Gamma_{2h}$  is not a subset of it:  $\Gamma_h \not\subseteq \Gamma_{2h}$ . Therefore, the usage of two-level LPS would entail additional difficulties and we restrict ourselves to the (extended) one-level approach. Here again, special attention is paid to the convection-dominated case. As far as possible, semi-robust error estimates with reference to the diffusion parameter are provided. Thereby, semi-robustness means, that the constant of the error estimates does not depend on  $\varepsilon$  in an unfavourable way. The constant is not allowed to tend to infinity if  $\varepsilon \rightarrow 0$ , especially it should not depend on negative powers of  $\varepsilon$ . Nevertheless, the constant can include for example positive powers of  $\varepsilon$ . The norm, the error estimate is obtained in, is allowed to depend on  $\varepsilon$  in any way.

## 1.2 Surface Description and Operators

To understand and to handle surface partial differential equations, surface derivatives have to be explained first. This needs foremost for a mathematical description of the given surface. Based on this the surface gradient can be introduced and well known formulas can be transferred from the bulk to the surface setting.

### 1.2.1 Surface Derivatives

Let  $\Gamma$  be a  $C^{k+1}$  ( $k \geq 1$ ) bounded, connected, not self-intersecting, orientable  $n$  dimensional hyper surface embedded in  $\mathbb{R}^{n+1}$ . At first  $\Gamma$  is assumed to be closed, i.e.  $\partial\Gamma = \emptyset$ . The domain enclosed by the surface  $\Gamma$  is called  $\Omega$ . The surface  $\Gamma$  is described as the zero level set of an oriented distance function:

$$d(\mathbf{x}) : \mathbb{R}^{n+1} \rightarrow \mathbb{R}, \quad d(\mathbf{x}) := \begin{cases} -\text{dist}(\mathbf{x}, \Gamma) & \text{if } \mathbf{x} \in \Omega \\ 0 & \text{if } \mathbf{x} \in \Gamma \\ \text{dist}(\mathbf{x}, \Gamma) & \text{if } \mathbf{x} \notin \Omega \end{cases}, \quad (1.1)$$

where  $\text{dist}(\mathbf{x}, \Gamma) := \min_{\mathbf{y} \in \Gamma} |\mathbf{x} - \mathbf{y}|$  is the distance of a point  $\mathbf{x}$  to the surface  $\Gamma$ . Hence,  $\Gamma = D_0 = \{\mathbf{x} \in \mathbb{R}^{n+1} \mid d(\mathbf{x}) = 0\}$ . We define the function  $\mathbf{n}$  by  $\mathbf{n}(\mathbf{x}) := \nabla d(\mathbf{x})$  with  $\nabla$  being the standard gradient in  $\mathbb{R}^{n+1}$ . It can easily be seen, that  $\mathbf{n}(\mathbf{x})$  for  $\mathbf{x} \in \Gamma$  is the unit outward normal on  $\Gamma$ .

The surface gradient  $\nabla_\Gamma$  of a function  $\phi : \Gamma \rightarrow \mathbb{R}$  can be defined as:

$$\nabla_\Gamma \phi := \nabla \tilde{\phi} - (\nabla \tilde{\phi} \cdot \mathbf{n}) \mathbf{n},$$

where  $\tilde{\phi} : U(\Gamma) \rightarrow \mathbb{R}$  is an arbitrary smooth extension of  $\phi$  into a neighbourhood  $U(\Gamma)$  of  $\Gamma$ . For a visualization of the surface gradient  $\nabla_\Gamma$  compare Figure 1.1. It can be shown, that on  $\Gamma$  the surface gradient does not depend on the choice of the extension  $\tilde{\phi}$  but on the values of  $\phi$  on  $\Gamma$  only, compare [30, Lemma 2.4]. Thus, the surface gradient is well defined and an explicit declaration of an extension is omitted in the following. The Hessian of  $d$  is denoted by  $H(\mathbf{x}) := \nabla^2 d(\mathbf{x})$ . The trace of  $H$  is the sum of principal curvatures of  $\Gamma$  and can be obtained as the surface divergence of the unit outward normal  $\mathbf{n}$ :  $\mathcal{H}(\mathbf{x}) := \text{tr}(H(\mathbf{x})) = \nabla_\Gamma \cdot \mathbf{n}(\mathbf{x})$  [62]. The Laplace-Beltrami operator  $\Delta_\Gamma$  is the surface analogue of the Laplace operator and defined equivalent to the bulk case as:

$$\Delta_\Gamma \phi = \nabla_\Gamma \cdot \nabla_\Gamma \phi.$$

Considering an open  $C^{k+1}$  surface  $\Gamma$  with a boundary  $\partial\Gamma$ , the boundary is assumed to be (piecewise)  $C^{k+1}$ , too. Such surfaces can be extended to closed  $C^{k+1}$  surfaces and can be described as a part of the zero level set of the signed distance function (1.1) obtained for the closed extended surface. The conormal onto  $\partial\Gamma$  in a point  $\mathbf{x} \in \partial\Gamma$  is a unit vector lying in the tangential plane on  $\Gamma$  in  $\mathbf{x}$ , being perpendicular to the boundary  $\partial\Gamma$  and pointing outside of  $\Gamma$ . It is denoted by  $\boldsymbol{\nu}(\mathbf{x})$ . For an example see Figure 1.1 again. All definitions of surface operators given above for the closed surface are extended directly to surfaces with boundaries.

In the following it is shortly written  $a \lesssim b$  or  $a \gtrsim b$  if it exists a positive constant  $C$  independent of  $\varepsilon$  and the later introduced mesh size  $h$ , such that  $a(\mathbf{x}) \leq Cb(\mathbf{x})$  or  $a(\mathbf{x}) \geq Cb(\mathbf{x})$  for all  $\mathbf{x}$ , respectively. If  $a \lesssim b$  and  $a \gtrsim b$ , then this is condensed to  $a \sim b$ .

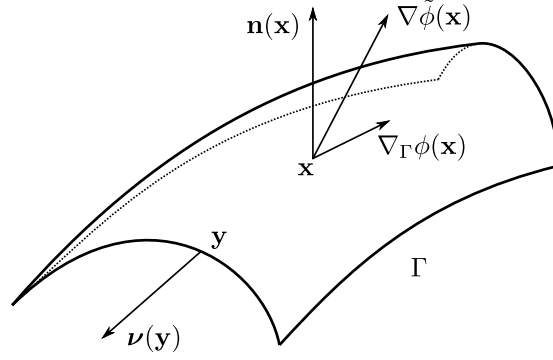


Figure 1.1: Example for a curved surface  $\Gamma$  visualizing the normal  $\mathbf{n}$ , the conormal  $\boldsymbol{\nu}$  and the surface gradient  $\nabla_{\Gamma}\phi$  of a function  $\phi$ .

### 1.2.2 Surface Gauss Theorem

In the following, a formula for partial integration over surfaces  $\Gamma$  with boundary  $\partial\Gamma$  is presented. This formula and the ones derived from it below provide the tools to obtain the weak formulation of a surface partial differential equation.

An analogon to the Gauss theorem in the bulk for a scalar surface function  $\phi \in C^1(\bar{\Gamma})$  is given in [30, Theorem 2.10] by:

$$\int_{\Gamma} \nabla_{\Gamma}\phi \, ds = \int_{\Gamma} \phi \mathcal{H} \mathbf{n} \, ds + \int_{\partial\Gamma} \phi \boldsymbol{\nu} \, d\mathbf{b}.$$

Setting  $\phi = uv$  with  $u, v \in C^1(\bar{\Gamma})$  and using the product rule, a formula for partial integration on surfaces can be concluded:

$$\int_{\Gamma} u \nabla_{\Gamma} v \, ds = - \int_{\Gamma} v \nabla_{\Gamma} u \, ds + \int_{\Gamma} uv \mathcal{H} \mathbf{n} \, ds + \int_{\partial\Gamma} uv \boldsymbol{\nu} \, d\mathbf{b}. \quad (1.2)$$

Choosing  $v = (\nabla_{\Gamma} w)_i$ ,  $i = 1, \dots, n+1$ , for a  $w \in C^2(\bar{\Gamma})$  and taking the sum over  $i$  leads to:

$$\int_{\Gamma} u \Delta_{\Gamma} w \, ds = - \int_{\Gamma} \nabla_{\Gamma} w \cdot \nabla_{\Gamma} u \, ds + \int_{\Gamma} u \mathcal{H} \nabla_{\Gamma} w \cdot \mathbf{n} \, ds + \int_{\partial\Gamma} u \nabla_{\Gamma} v \cdot \boldsymbol{\nu} \, d\mathbf{b}.$$

Due to the normal  $\mathbf{n}$  being perpendicular to the surface gradient the second term on the right hand side vanishes:

$$\int_{\Gamma} u \Delta_{\Gamma} w \, ds = - \int_{\Gamma} \nabla_{\Gamma} w \cdot \nabla_{\Gamma} u \, ds + \int_{\partial\Gamma} u \nabla_{\Gamma} v \cdot \boldsymbol{\nu} \, d\mathbf{b}. \quad (1.3)$$

For vector valued functions  $\boldsymbol{\phi} \in (C^1(\overline{\Gamma}))^{n+1}$  an other kind of partial integration formula can be obtained from (1.2):

$$\int_{\Gamma} \boldsymbol{\phi} \cdot \nabla_{\Gamma} u \, ds = - \int_{\Gamma} u \nabla_{\Gamma} \cdot \boldsymbol{\phi} \, ds + \int_{\Gamma} u \mathcal{H} \boldsymbol{\phi} \cdot \mathbf{n} \, ds + \int_{\partial\Gamma} u \boldsymbol{\phi} \cdot \boldsymbol{\nu} \, d\mathbf{b}. \quad (1.4)$$

### 1.3 Surface Sobolev Spaces

The presented formula of integration by parts on surfaces enables the definition of weak derivatives and hence the introduction of surface Sobolev and Hilbert spaces.

The surface Lebesgue spaces  $L^p(\Gamma)$ ,  $p \in [1, \infty)$ , are defined as the spaces of functions  $\phi : \Gamma \rightarrow \mathbb{R}$  for which the  $p$ -th power of their absolute value is Lebesgue integrable, i.e.  $\int_{\Gamma} |\phi|^p \, ds < \infty$ . The  $L^p$ -norm is defined as:

$$\|\phi\|_{L^p(\Gamma)} := \left( \int_{\Gamma} |\phi|^p \, ds \right)^{\frac{1}{p}} \quad \text{for } 1 \leq p < \infty.$$

For  $p = \infty$  the  $L^p$  norm is set to  $\|\phi\|_{L^\infty(\Gamma)} := \text{ess sup}_{\mathbf{x} \in \Gamma} |\phi(\mathbf{x})|$  and the Lebesgue space  $L^\infty(\Gamma)$  is given by all functions  $\phi$  with  $\|\phi\|_{L^\infty(\Gamma)} < \infty$ . The space  $L^p_{\text{loc}}(\Gamma)$  contains all functions which are in  $L^p(\Gamma_c)$  for all compact subsets  $\Gamma_c \subset \Gamma$ . If  $\Gamma$  is closed,  $L^p_{\text{loc}}(\Gamma) = L^p(\Gamma)$ . Further let  $\underline{D}_j$ ,  $j = 1 \dots n+1$ , denote the components of  $\nabla_{\Gamma} \phi =: (\underline{D}_1 \phi, \dots, \underline{D}_{n+1} \phi)$  and  $n_i$  the components of the unit outward vector on  $\Gamma$ :  $\mathbf{n} = (n_1, \dots, n_{n+1})$ .

On top of (1.2) weak surface derivatives are introduced:

#### Definition 1.1

A function  $\phi \in L^1_{\text{loc}}(\Gamma)$  is called weakly differentiable w.r.t.  $x_i$  on  $\Gamma$  if there exists a function  $\xi \in (L^1_{\text{loc}}(\Gamma))$  such that for all  $\eta \in C^1(\Gamma)$  with compact support:

$$\int_{\Gamma} \phi \underline{D}_i \eta \, ds = - \int_{\Gamma} \xi \eta \, ds + \int_{\Gamma} \phi \eta \mathcal{H} n_i \, ds$$

holds.

$\xi = \underline{D}_i \phi$  is called weak surface derivative of  $\phi$  w.r.t.  $x_i$ .

All weak derivatives of  $\phi$  of order  $l$  are denoted by  $\phi^{(l)}$ . For bulk equations one would introduce a multi-index  $\boldsymbol{\alpha} = (\alpha_1, \dots, \alpha_{n+1})$ . Then all weak derivatives of order  $l$  are given by  $\underline{D}^{\boldsymbol{\alpha}}$  with  $|\boldsymbol{\alpha}| = \alpha_1 + \dots + \alpha_{n+1} = l$ . But this is based on the commutativity of the derivatives in the bulk. On surfaces, derivatives are not longer commutative, compare [30, Lemma 2.6].

Thus, surface Sobolev spaces are defined recursively in the following way:



**Definition 1.2**

The surface Sobolev spaces  $W^{s,p}(\Gamma)$  for  $s \in \mathbb{N}$  and  $1 \leq p \leq \infty$  are defined as:

$$W^{0,p}(\Gamma) := L^p(\Gamma),$$

$$W^{s,p}(\Gamma) := \left\{ \phi \in W^{s-1,p}(\Gamma) \mid \underline{D}_j \phi^{(s-1)} \in L^p(\Gamma) \text{ for all } j = 1, \dots, n+1 \right\}.$$

For  $p = 2$  the notation  $H^s(\Gamma) := W^{s,2}(\Gamma)$  is used.

The norms  $\|\cdot\|_{s,p,\Gamma}$  and the semi-norms  $|\cdot|_{s,p,\Gamma}$  on  $W^{s,p}(\Gamma)$  for  $1 \leq p < \infty$  are defined via:

$$\|\phi\|_{s,p,\Gamma} := \left( \sum_{l=0}^s \|\phi^{(l)}\|_{L^p(\Gamma)}^p \right)^{\frac{1}{p}} \quad \text{and} \quad |\phi|_{s,p,\Gamma} := \left( \sum_{l=s}^s \|\phi^{(l)}\|_{L^p(\Gamma)}^p \right)^{\frac{1}{p}}.$$

For  $p = \infty$  the corresponding norm and semi norm are set to:

$$\|\phi\|_{s,\infty,\Gamma} := \max_{l \leq s} \left\{ \text{ess sup}_{\mathbf{x} \in \Gamma} |\phi^{(l)}(\mathbf{x})| \right\} \quad \text{and}$$

$$|\phi|_{s,\infty,\Gamma} := \max_{l=s} \left\{ \text{ess sup}_{\mathbf{x} \in \Gamma} |\phi^{(l)}(\mathbf{x})| \right\},$$

respectively.

**Lemma 1.1**

Let  $s \in \mathbb{N}$  and  $1 \leq p \leq \infty$ .

Then  $W^{s,p}(\Gamma)$  with the norm  $\|\phi\|_{s,p,\Gamma}$  is a Banach space and  $H^s(\Gamma)$  is a Hilbert space with the inner product

$$\langle \phi, \eta \rangle_{s,\Gamma} := \int_{\Gamma} \sum_{l=0}^s \phi^{(l)} \eta^{(l)} ds$$

and the corresponding norm  $\|\phi\|_{s,\Gamma} := \|\phi\|_{s,2,\Gamma}$ .

In the following, the index  $s$  of the inner product is skipped, if  $s = 0$ .

For the convenience of the reader, two important theorems for Sobolev spaces on surfaces are presented next:

**Lemma 1.2 (Trace Theorem)**

Let  $\Gamma$  be a bounded surface,  $\partial\Gamma$  be  $C^{k+1}$  and  $1/2 < s \leq k+1$ . Then there exists a bounded linear operator, called the trace operator,

$$\gamma : H^s(\Gamma) \rightarrow H^{s-1/2}(\partial\Gamma),$$

such that  $\gamma\phi = \phi|_{\partial\Gamma}$ , if  $\phi \in H^s(\Gamma) \cap C(\bar{\Gamma})$ , and

$$\|\gamma\phi\|_{s-1/2,\partial\Gamma} \lesssim \|\phi\|_{s,\Gamma} \quad \forall \phi \in H^s(\Gamma).$$

Additional, to every function  $\psi \in H^{s-1/2}(\partial\Gamma)$  there exists a  $\phi \in H^s(\Gamma)$  such that  $\gamma\phi = \psi$  and

$$\|\phi\|_{s,\Gamma} \lesssim \|\psi\|_{s-1/2,\partial\Gamma}$$

holds.

**Proof.**

The proof is equivalent to the proof in the bulk case and can be found in [42, Satz 6.2.40].  
□

**Lemma 1.3 (Poincare Type Inequalities)**

Let  $\Gamma$  be a  $C^3$  bounded surface and  $1 \leq p < \infty$ . Then, for all  $\phi \in H^1(\Gamma)$  with either

- a)  $\langle \phi, 1 \rangle = 0$  or
- b)  $\phi = 0$  on a Dirichlet boundary part  $B_D \subset \partial\Gamma$  with  $|B_D| > 0$ ,

the following inequality holds true:

$$\|\phi\|_{0,p,\Gamma} \lesssim |\phi|_{1,p,\Gamma}.$$

**Proof.**

The proof of case a) is given in [30, Theorem 2.12]. The result can be proven for assumption b) in the same manner. Following the definitions and ideas of [30, Theorem 2.12], it is used, that  $\bar{f}(\mathbf{x}) = f(p(\mathbf{x}))$  has zero boundary values on the extension of  $B_D$ . Thus, it follows from the standard Poincare-Friedrichs inequality:

$$\int_{U_\varepsilon} |\bar{f}(\mathbf{x})| d\mathbf{x} \lesssim \int_{U_\varepsilon} |\nabla \bar{f}(\mathbf{x})| d\mathbf{x}.$$

Using this formula, the conclusions of the proof in [30] can be transferred directly to case b).  
□

## Chapter 2

# Surface Discretization

Finite element methods are based on a triangulation of the given domain. In the case of surface equations, this triangulation is in general not a partition, as known from bulk equations, but only an approximation of the curved domain  $\Gamma$ . Additional geometric errors occur. First, a linear approximation  $\Gamma_h$  of  $\Gamma$  is introduced. Based on  $\Gamma_h$ , an exact triangulation of the surface is provided and higher order surface approximations  $\Gamma_h^k$  are obtained. Geometric estimates, surface operators on the discrete surface and integral transformation formulas are presented. Mapped finite elements on  $\Gamma_h^k$  are introduced and trace and inverse inequalities as well as an interpolation estimate for finite element functions are given.

In this and the following chapters, we restrict ourselves to the case  $n = 2$ , i.e. a 2D curved surface embedded in  $\mathbb{R}^3$ , to improve the readability. Nevertheless, similar results are obtained for  $n = 1$ .

### 2.1 Linear Approximation

For a linear approximation  $\Gamma_h$  of  $\Gamma$ , a polyhedral mesh consisting of simplices  $K$  (triangles in 3D) is utilized. The vertices of all elements are located at the surface  $\Gamma$ . Naturally, this construction provides a linear approximation of the curved surface. The diameter of element  $K$  is named  $h_K$ , the mesh size  $h$  is set to  $h := \max_K h_K$  and the mesh is assumed to be shape regular and quasi-uniform. The discrete unit normal on  $\Gamma_h$  in  $\mathbf{x}$  is named  $\mathbf{n}_h(\mathbf{x})$ . Due to the mesh being polyhedral, the discrete normal is element-wise constant.  $\mathcal{T}_h$  and  $\mathcal{E}_h$  describe the set of all elements and the set of all edges of the mesh, respectively. For not closed surfaces  $\Gamma$ , a distinction is drawn between inner elements  $K \in \mathcal{T}_{h,I}$  and edges  $E \in \mathcal{E}_{h,I}$ , with at most one vertex located at the boundary  $\partial\Gamma$ , and boundary elements  $K \in \mathcal{T}_{h,B} = \mathcal{T}_h \setminus \mathcal{T}_{h,I}$  and edges  $E \in \mathcal{E}_{h,B} = \mathcal{E}_h \setminus \mathcal{E}_{h,I}$ . It is assumed that  $\Gamma$  is triangulated in such a way that all elements have at least one vertex located in  $\Gamma = \bar{\Gamma} \setminus \partial\Gamma$ .

### 2.1.1 Projection Operator

The description of  $\Gamma$  as a bounded zero level set of a distance function  $d$ , compare Section 1.2.1, is recalled. The distance function provides the definition of a projection operator  $\mathbf{p}$  from a neighbourhood  $U(D_0)$  of the zero level set  $D_0$  onto  $D_0$  via:

$$\mathbf{p}(\mathbf{x}) := \mathbf{x} - d(\mathbf{x}) \mathbf{n}(\mathbf{p}(\mathbf{x})) = \mathbf{x} - d(\mathbf{x}) \nabla d(\mathbf{x}) \quad \text{for } \mathbf{x} \in U(D_0). \quad (2.1)$$

Thereby, every point  $\mathbf{x}$  from the neighbourhood is mapped onto its closest point  $\mathbf{p}(\mathbf{x})$  on the level set. This projection is well defined if  $U(D_0)$  is small enough, such that  $\alpha_1 \mathbf{n}(\mathbf{x}_1)$  and  $\alpha_2 \mathbf{n}(\mathbf{x}_2)$ ,  $\alpha_i \in \mathbb{R}$ , do not intersect in  $U(D_0)$  for all  $\mathbf{x}_1, \mathbf{x}_2 \in D_0$  with  $\mathbf{x}_1 \neq \mathbf{x}_2$ .

#### Definition 2.1

A neighbourhood

$$U(D_0) = \{\mathbf{x} + \delta \mathbf{n}(\mathbf{x}) \mid d(\mathbf{x}) = 0 \text{ and } -\delta_0(\mathbf{x}) \leq \delta \leq \delta_0(\mathbf{x})\}$$

is called valid if

$$\bigcap_{i=1,2} \{\mathbf{x}_i + \delta \mathbf{n}(\mathbf{x}_i) \mid -\delta_0(\mathbf{x}_i) \leq \delta \leq \delta_0(\mathbf{x}_i)\} = \emptyset$$

for all  $\mathbf{x}_1, \mathbf{x}_2 \in D_0$ ,  $\mathbf{x}_1 \neq \mathbf{x}_2$ .

From now on  $U(D_0)$  is assumed to be valid.

#### Notice 2.1.1

To characterize a set of valid neighbourhoods of  $\Gamma$  two points have to be considered.

To ensure that there is no intersection of two non-equal normals of  $\Gamma$  in  $U$ , the width  $\delta_0(\mathbf{x})$  of  $U$  has to be set smaller than all local radii of curvature in every point  $\mathbf{x} \in \Gamma$ :

$$\delta_0(\mathbf{x}) < \kappa_{\min}^{-1}(\mathbf{x}) = \min_{1 \leq i \leq 3} \{\kappa_i(\mathbf{x})^{-1}\}.$$

Additionally, it has to be taken care of such settings where the surface comes close to itself. Mathematically, the minimal distance  $\gamma(\mathbf{x})$  of a surface to itself in the point  $\mathbf{x} \in \Gamma$  can be given by:

$$\gamma(\mathbf{x}) := \min \gamma \quad \text{s.t. } \exists \mathbf{y} \in \Gamma : \mathbf{y} \in B_\gamma(\mathbf{x}) \text{ and } B_{\frac{2}{3}\gamma}(\mathbf{x}) \cap B_{\frac{2}{3}\gamma}(\mathbf{y}) \cap \Gamma = \emptyset.$$

For not self-intersecting surfaces  $\gamma(\mathbf{x})$  stays greater than zero in every point  $\mathbf{x}$ . Therefore, a valid neighbourhood for every  $C^2$ , bounded, connected, not self-

intersecting, orientable hyper-surface can be obtained by setting:

$$\delta_0(\mathbf{x}) < \min\{\kappa_{min}^{-1}(\mathbf{x}), \frac{1}{2}\gamma(\mathbf{x})\} \quad \text{for } \mathbf{x} \in \Gamma.$$

Obviously, for surfaces with boundary  $\mathbf{p}(\mathbf{x}) \in D_0$  holds for all  $\mathbf{x} \in \Gamma_h$ . But, it cannot be assumed that  $\mathbf{p}(\mathbf{x}) \in \Gamma$ . However,  $\mathbf{p}(\mathbf{x}) \in \Gamma$  is essential because the projection operator  $\mathbf{p}$  shall later on be used to extend the given data from  $\Gamma$  onto the discretized surface. Therefore, the set of curvilinear surfaces is defined:

### **Definition 2.2**

An open surface  $\Gamma \in \mathbb{R}^3$  with boundary  $\partial\Gamma$  is called *curvilinear*, if there exists a linear triangulation  $\Gamma_h$  of  $\Gamma$ , as described above, such that for the projection operator  $\mathbf{p}$  given in (2.1) it holds:  $\mathbf{p}(\partial\Gamma_h) = \partial\Gamma$ .

From now on, the surface  $\Gamma$  is assumed to be curvilinear and  $\Gamma_h$  to be a linear triangulation as referred to in the definition above.

### **Notice 2.1.2**

In case of a 1D surface, the boundary consists only of two separated points. For the construction of a linear surface approximation  $\Gamma_h$  these boundary points are chosen as boundary points of the mesh. Then,  $\mathbf{p}(\partial\Gamma_h) = \partial\Gamma$ . Hence, 1D surfaces are naturally curvilinear.

## **2.1.2 Exact Triangulation**

Based on the linear surface approximation, an exact triangulation of the curved surface  $\Gamma$  by curved triangles  $\tilde{K}$  is introduced, see Figure 2.1. In the case of a closed surface, an exact triangulation is given by the set of images  $\tilde{K} = \mathbf{p}(K)$  of elements  $K \in \mathcal{T}_h$ , compare [26]. This can be transferred to curvilinear surfaces because  $\mathbf{p}(\partial\Gamma_h) = \partial\Gamma$  and hence  $\mathbf{p}(\Gamma_h) = \Gamma$ . The exact triangulation and the set of edges of this triangulation are given by:

$$\begin{aligned} \tilde{\mathcal{T}}_h &:= \{\tilde{K} = \mathbf{p}(K) \mid K \in \mathcal{T}_h\} \text{ and} \\ \tilde{\mathcal{E}}_h &:= \{\tilde{E} = \mathbf{p}(E) \mid E \in \mathcal{E}_h\}. \end{aligned}$$

## **2.2 Higher Order Approximation**

The polygonal triangulation introduced above provides only lowest order geometric estimates. To improve the surface approximation, higher order triangulations are used. These are related to the isoparametric methods used for the

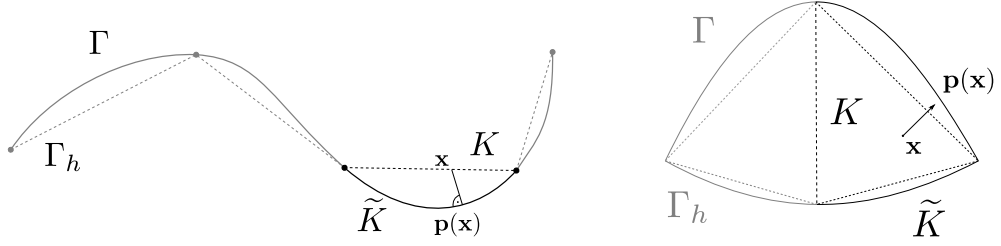


Figure 2.1: Picture of the continuous surface  $\Gamma$ , a linear approximation  $\Gamma_h$  consisting of simplices  $K$ , and an exact triangulation of  $\Gamma$  by the curved triangles  $\tilde{K} = \mathbf{p}(K)$  in 2D (left) and 3D (right).

surface approximation in bulk problems and based on the piecewise linear approximation  $\Gamma_h$ . For each element  $K \in \mathcal{T}_h$  the associated curved surface  $\tilde{K}$  is approximated by a Lagrange interpolation of order  $k$ .

Due to  $K \in \mathcal{T}_h$  being flat triangles, affine mappings  $F_K = B_K \hat{\mathbf{x}} + b_K$  from the reference element  $\hat{K} \in \mathbb{R}^2$  to  $K$  exist. Thereby,  $F_K$  is a parametrization of a flat hyper surface in  $\mathbb{R}^3$  over the reference element in  $\mathbb{R}^2$ . Thus,  $B_K \in \mathbb{R}^{3 \times 2}$ . Let  $\hat{\mathbf{x}}_1, \dots, \hat{\mathbf{x}}_{n_k}$  be the interpolation points and  $\hat{\psi}_1(\hat{\mathbf{x}}), \dots, \hat{\psi}_{n_k}(\hat{\mathbf{x}})$  the corresponding Lagrange basis functions on the reference element. Then, for all  $\hat{\mathbf{x}} \in \hat{K}$  the approximation  $\mathbf{a}_K^k(\cdot)$  of  $\mathbf{p}(F_K(\cdot))$  is defined by:

$$\mathbf{a}_K^k(\hat{\mathbf{x}}) := \sum_{i=1}^{n_k} \mathbf{p}(F_K(\hat{\mathbf{x}}_i)) \hat{\psi}_i(\hat{\mathbf{x}}). \quad (2.2)$$

Applying this definition to all elements  $K \in \mathcal{T}_h$  leads to a continuous piecewise polynomial approximation of  $\Gamma$ , if the approximation  $\mathbf{a}_K^k$  on an edge of the reference element is uniquely defined by the function values in the interpolation points on the edge.

Unfortunately, this approximation suffers from the same problem as detected for linear approximations of  $\Gamma$ , namely that in general  $\mathbf{p}(\mathbf{a}_K^k(\hat{\mathbf{x}}))$  does not lie in  $\Gamma$ , if  $\Gamma$  is not closed. Therefore, the standard interpolation  $\mathbf{a}_K^k$  is perturbed with a special mapping  $\Phi_K^k : \hat{K} \rightarrow \mathbb{R}^{n+1}$ :

$$G_K^k := \mathbf{a}_K^k + \Phi_K^k.$$

In the following a possible choice for  $\Phi_K^k$ , ensuring  $\mathbf{p}(G_K^k(\hat{\mathbf{x}})) \in \Gamma$ , is obtained. For inner elements  $K \in \mathcal{T}_{h,I}$  the perturbation is set to zero and  $G_K^k = \mathbf{a}_K^k$ . Now, the construction of  $\Phi_K^k$  for an arbitrary but fixed element  $K \in \mathcal{T}_{h,B}$  is described. Let  $\lambda_1, \dots, \lambda_n$  name the barycentric coordinates on  $\hat{K}$  and the points  $\hat{\mathbf{x}} \in \hat{K}$  be identified with their barycentric coordinates  $\hat{\mathbf{x}} = (\lambda_1, \dots, \lambda_n)$ . The number of vertices of  $K$  located at the boundary is denoted by  $l$  and the vertices of  $K$ ,  $V_1, \dots, V_{n+1}$ , are numbered such that  $V_1, \dots, V_l$  lie on  $\partial\Gamma_h$ . The set of points

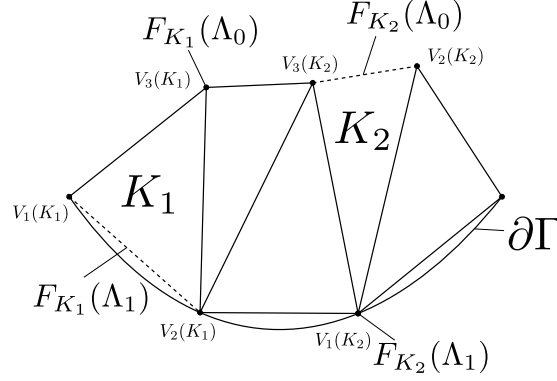


Figure 2.2: Figure of the sets  $F_K(\Lambda_0)$  and  $F_K(\Lambda_1)$  for different cases of boundary elements  $K$ .

$\widehat{\mathbf{x}} \in \widehat{K}$ , where  $\lambda_i = 0$  for all  $i = 1, \dots, l$ , is given by:

$$\Lambda_0 := \{\widehat{\mathbf{x}} \in \widehat{K} \mid \lambda^*(\widehat{\mathbf{x}}) = 0\} \quad \text{with} \quad \lambda^*(\widehat{\mathbf{x}}) := \sum_{i=1}^l \lambda_i.$$

The set of all points  $\widehat{\mathbf{x}} \in \widehat{K}$ , where  $\lambda_i = 0$  for all  $i = l + 1, \dots, n + 1$  is defined similarly:

$$\Lambda_1 := \{\widehat{\mathbf{x}} \in \widehat{K} \mid \lambda^*(\widehat{\mathbf{x}}) = 1\}.$$

This definition provides, that  $F_K(\Lambda_1) = K \cap \partial\Gamma_h$ .

### Notice 2.2.1

For an 1D surface, an element contains at most one vertex at the surface. The only exception is a domain  $\Gamma_h$  consisting of only one element. In this case a refinement is used to obtain the assumed setting. If there is no boundary vertex in  $K$ , then  $\lambda^*$  is an empty sum,  $\lambda^* = 0$ , and  $F_K(\Lambda_0) = K$ . Now, the existence of one boundary vertex is considered. Following the naming conventions from above the vertex on the boundary is  $V_1$  and  $\Lambda_0 = \{\widehat{\mathbf{x}} \in \widehat{K} \mid \lambda_1 = 0\}$ . It follows that  $F_K(\Lambda_0) = V_2$ .

On a 2D surface, there can be up to two boundary vertices (after suitable refinement if necessary). Looking at two boundary vertices  $V_1$  and  $V_2$ , we get  $\Lambda_0 = \{\mathbf{x} \in K \mid \lambda^* = \lambda_1 + \lambda_2 = 0\}$  and  $F_K(\Lambda_0) = V_3$ . The other cases are equivalent to the 1D case. One gets  $F_K(\Lambda_0) = K$  in the case of no boundary vertex at all. For one boundary vertex it follows that  $\Lambda_0 = \{\mathbf{x} \in K \mid \lambda_1 = 0\}$  and  $F_K(\Lambda_0)$  is the edge  $V_2V_3$ . For a visualization compare Figure 2.2.

At first, the displacement  $\Phi_K^k$  for all points  $\widehat{\mathbf{x}} \in \Lambda_1$  is determined, such that  $\mathbf{p}(G_K^k(\Lambda_1)) \in \partial\Gamma$ . Then, this displacement is smoothly extended to  $\widehat{K}$ . Therefore, on  $\Lambda_1$  the mapping  $G_K^k(\widehat{\mathbf{x}})$  is set to  $\mathbf{p}(F_K(\widehat{\mathbf{x}}))$ . Remember that  $\Gamma$  is assumed

to be curvilinear and thus  $\mathbf{p}(\partial\Gamma_h) = \partial\Gamma$ . Thereby it follows for all  $\widehat{\mathbf{x}} \in \Lambda_1$ :

$$\Phi_K^k = \mathbf{p}(F_K(\widehat{\mathbf{x}})) - \mathbf{a}_K^k(\widehat{\mathbf{x}}).$$

This mapping shall be extended continuously to the whole reference element  $\widehat{K}$ . Therefore, for all points  $\widehat{\mathbf{x}} \in \widehat{K} \setminus \Lambda_0$  a projection onto  $\Lambda_1$  is defined via:

$$\widehat{\mathbf{y}}(\widehat{\mathbf{x}}) = (y_1, \dots, y_l, 0, \dots, 0) \quad \text{with } y_i = \frac{\lambda_i}{\lambda^*} \text{ for } 1 \leq i \leq l.$$

The position of  $\mathbf{a}_K^k(\widehat{\mathbf{x}})$  for  $\widehat{\mathbf{x}} \in \Lambda_0$  is independent of a displacement of the points  $V_1, \dots, V_l$ . Hence,  $\Phi_K^k$  can be set to zero on  $\Lambda_0$ . Then, the perturbation is given on  $\widehat{K}$  via:

$$\Phi_K^k(\widehat{\mathbf{x}}) = \begin{cases} (\lambda^*)^{r+2} (\mathbf{p}(F_K(\widehat{\mathbf{y}}(\widehat{\mathbf{x}}))) - \mathbf{a}_K^k(\widehat{\mathbf{y}}(\widehat{\mathbf{x}}))), & \text{for } \lambda^* \neq 0 \\ 0, & \text{for } \lambda^* = 0 \end{cases}. \quad (2.3)$$

This perturbation  $\Phi_K^k(\widehat{\mathbf{x}})$  ensures  $\mathbf{p}(G_K^k(\widehat{\mathbf{x}})) \in \Gamma$  by construction.

**Notice 2.2.2**

*For elements with only one vertex on the boundary, the mapping  $\Phi_K^k(\widehat{\mathbf{x}})$  for  $\widehat{\mathbf{x}} \in \Lambda_1$  can be easily given. By construction,  $F_K(\Lambda_1) = V_1 \in \Gamma$  and hence  $\Phi_K^k(\Lambda_1) = \mathbf{p}(V_1) - V_1 = 0$ . This leads to  $G_K^k = \mathbf{a}_K^k$ , which coincides with the definition of these elements as inner elements.*

*For a 2D element with the boundary edge  $V_1V_2$  the mapping  $\Phi_K^k(\mathbf{x})$  on  $\Lambda_1$  is given as the difference of  $\mathbf{p}(F_K(\Lambda_1)) = \mathbf{p}(V_1V_2)$  and its  $k$ -th order approximation  $\mathbf{a}_K^k(\Lambda_1)$ .*

The image of  $\widehat{K}$  is named by  $K^k = G_K^k(\widehat{K})$  and the discrete surface is set to:

$$\Gamma_h^k := \bigcup_{K \in \mathcal{T}_h} G_K^k(\widehat{K}).$$

The sets of all higher order elements  $K^k$  and edges  $E^k$  are given by:

$$\mathcal{T}_h^k := \{G_K^k(\widehat{K}) \mid K \in \mathcal{T}_h\} \quad \text{and} \quad \mathcal{E}_h^k := \{G_K^k(\widehat{E}) \mid \widehat{E} \text{ edge of } \widehat{K}, K \in \mathcal{T}_h\}.$$

The sets of boundary and inner elements are defined from the sets of boundary and inner elements of the linear approximation:

$$\mathcal{T}_{h,B}^k := \{G_K^k(\widehat{K}) \mid K \in \mathcal{T}_{h,I}\} \quad \text{and} \quad \mathcal{T}_{h,I}^k := \{G_K^k(\widehat{K}) \mid K \in \mathcal{T}_{h,B}\}.$$

The sets of boundary and inner edges are given by:

$$\mathcal{E}_{h,B}^k := \{E^k \in \mathcal{E}_h^k \mid E^k \cap \partial\Gamma_h^k = E^k\} \quad \text{and} \quad \mathcal{E}_{h,I}^k := \{E^k \in \mathcal{E}_h^k \mid E^k \cap \partial\Gamma_h^k = \emptyset\}.$$



The unit outward normal on  $\Gamma_h^k$  is defined element-wise and is named  $\mathbf{n}_h^k$ . In the following it is shown that  $\Phi_K^k$  is a  $C^{k+1}$  mapping and  $\|\Phi_K^k\|_{m,\infty,\widehat{K}} \lesssim h^k$  for all  $1 \leq m \leq k+1$ . This result is afterwards used to get bijective mappings between the reference element and the higher order elements. These mappings are required to define finite element spaces on the higher order surface approximations. To obtain this result we are following the ideas from [62].

**Lemma 2.1**

The projection  $\widehat{\mathbf{y}} : \widehat{K} \setminus \Lambda_0 \rightarrow \Lambda_1$  is  $C^{k+1}$  and for all  $1 \leq m \leq k+1$  it holds:

$$\|F_K \circ \widehat{\mathbf{y}}\|_{m,\infty,\widehat{K} \setminus \Lambda_0} \lesssim \frac{h_K}{(\lambda^*)^m}.$$

**Proof.**

The proof is given in [6, Lemma 6.2]. □

**Lemma 2.2**

The mapping  $\mathbf{p}(F_K(\widehat{\mathbf{y}}))$  is  $C^{k+1}$  and for  $1 \leq m \leq k+1$  it holds:

$$\|\mathbf{p}(F_K(\widehat{\mathbf{y}})) - \mathbf{a}_K^k(\widehat{\mathbf{y}})\|_{m,\infty,\widehat{K} \setminus \Lambda_0} \lesssim \frac{h_K^k}{(\lambda^*)^m}.$$

**Proof.**

At first it should be recognized that by construction  $\mathbf{p}(F_K(\cdot))$  over  $\Lambda_1$  is a parametrization of a  $C^{k+1}$  boundary part of  $\Gamma$ . Hence,  $\mathbf{p}(F_K(\cdot))$  on  $\Lambda_1$  is a  $C^{k+1}$  mapping. The estimate is obtained following the proof of [62, Lemma 2.3.4]. It is used that  $\mathbf{a}_K^k$  is a Lagrange interpolation of order  $k$  of  $\mathbf{p}(F_K)$  over  $\Lambda_1$  and hence

$$\|\mathbf{p} \circ F_K - \mathbf{a}_K^k\|_{m,\infty,\Lambda_1} \lesssim h^{k+1-m}.$$

□

**Lemma 2.3**

The mapping  $\Phi_K^k$  is  $C^{k+1}$  on  $\widehat{K}$  and for all  $1 \leq m \leq k+1$  it holds:

$$\|\Phi_K^k\|_{m,\infty,\widehat{K}} \lesssim h_K^k.$$

**Proof.**

This directly follows from [62, Proposition 2.3.5]. □

Now the question occurs, whether the mapping  $G_K^k : \widehat{K} \rightarrow K^k$  is bijective or not. The answer strongly depends on the Lagrange interpolation of the surface.

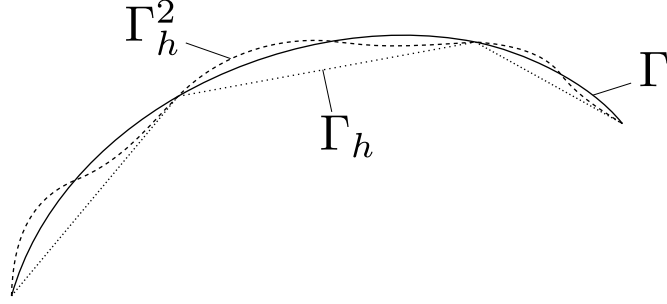


Figure 2.3: A 2D example for a surface  $\Gamma$ , its linear approximation  $\Gamma_h$  and its quadratic approximation  $\Gamma_h^2$ .

It is known from isoparametric approaches for bulk equations that Lagrange interpolations of smooth surfaces are not unconditionally one-to-one. Therefore, for bulk equations the distortion parameter of the Lagrange interpolation usually is defined as:

$$\|D(a_K^k - F_K)B_K^{-1}\|_{0,\infty,\hat{K}} = \gamma_K$$

and assumed to be less than one uniformly over all elements  $\gamma_K \leq \gamma < 1$ . This assumption guarantees the bijectivity of the Lagrange interpolation of the surface, see [6, Lemma 2.1]. In the case of surface equations  $B_K \in \mathbb{R}^{3 \times 2}$  and therefore not invertible. Nevertheless, we can introduce the Moore-Penrose pseudoinverse  $B_K^+ := (B_K^T B_K)^{-1} B_K^T$  and assume:

$$\|D(a_K^k - F_K)B_K^+\|_{0,\infty,\hat{K}} = \gamma_K \leq \gamma < 1.$$

Having in mind that  $\|F_K\|_{1,\infty,\hat{K}} = \|B_K\|_{0,\infty,\hat{K}} \leq h_K$ , the estimation obtained in Lemma 2.3 directly yields in:

$$\begin{aligned} \|D(G_K^k - F_K)B_K^+\|_{0,\infty,\hat{K}} &\leq \|D(a_K^k - F_K)B_K^+\|_{0,\infty,\hat{K}} + \|D\Phi_K^k B_K^+\|_{0,\infty,\hat{K}} \\ &\lesssim \gamma_K + h_K. \end{aligned}$$

Thus, for a fixed  $k$  there exists an  $h_0$ , such that for all triangulation with  $h \leq h_0$  and for all  $K \in \mathcal{T}_h$  it follows:

$$\|D(G_K^k - F_K)B_K^+\|_{0,\infty,\hat{K}} \leq c_K < 1$$

with  $c_K$  being a constant. As in [57, Lemma 2] the following lemma can be concluded:

**Lemma 2.4**

$G_K^k$  is a bijective  $C^1$ -mapping from  $\widehat{K}$  to  $K^k$  satisfying

$$\begin{aligned} \|DG_K^k\|_{0,\infty,\widehat{K}} &\leq (1 + c_K) \|B_K\|_{0,\infty,\widehat{K}} \\ \|(DG_K^k)^+\|_{0,\infty,\widehat{K}} &\leq (1 - c_K)^{-1} \|(B_K)^+\|_{0,\infty,\widehat{K}} \\ |K|n!(1 - c_K)^n &\leq |\sqrt{\det((DG_K^k)^T DG_K^k)}| \leq |K|n!(1 + c_K)^n. \end{aligned}$$

For the defined pseudoinverse it holds for  $\phi : K^k \rightarrow \mathbb{R}$  and  $\widehat{\phi} = \phi \circ G_K^k$ :

$$\nabla_{\Gamma_h^k} \phi(G_K^k(\widehat{x})) = \left( (DG_K^k)^+ \right)^T \widehat{\nabla} \widehat{\phi}(\widehat{x}).$$

Hence, the results from Lemma 2.4 above enable the definition of a mapped finite element space on  $\Gamma_h^k$ . Further, the estimations given in Lemma 2.4 provide standard estimates for functions in this finite element space. This topic is elaborated in Section 2.5.

**2.2.1 Extension Operator**

After the construction of an exact triangulation and a discrete surface  $\Gamma_h^k$  it is necessary to provide an operator which extends the data given on  $\Gamma$  to  $\Gamma_h^k$ . Recalling the projection operator  $\mathbf{p} : U(D_0) \rightarrow D_0$  defined in 2.1 and  $\mathbf{p}(\Gamma_h^k) = \Gamma$ , it can easily be concluded, that  $\mathbf{p}|_{\Gamma_h^k} : \Gamma_h^k \rightarrow \Gamma$  is bijective. The extension operator for a function  $\phi$  defined on  $\Gamma$  onto  $\Gamma_h^k$  and its inverse, the lift operator for a function  $\phi_h$  defined on  $\Gamma_h^k$ , are given by:

$$\phi^E(\mathbf{x}) := \phi(\mathbf{p}(\mathbf{x})) \quad \text{for } \mathbf{x} \in \Gamma_h^k, \quad (2.4)$$

$$\phi_h^L(\mathbf{x}) := \phi_h((\mathbf{p})^{-1}(\mathbf{x})) \quad \text{for } \mathbf{x} \in \Gamma. \quad (2.5)$$

**2.2.2 Geometric Estimates**

In this section, a geometric estimate of the distance between the smooth surface  $\Gamma$  and its higher order approximation  $\Gamma_h^k$  is given. Additionally, the differences between geometric surface quantities on the smooth surface and their discrete versions are bounded. These estimates are the basis of the analysis of the error terms occurring due to the surface approximation.

Estimates comparable to the approximation properties of the Lagrange approximation  $\mathbf{a}_K^k$  are developed for  $G_K^k$ :

**Lemma 2.5**

For  $h$  being small enough, it holds for all  $K \in \mathcal{T}_h$  and  $0 \leq m \leq k$  that

$$\|\mathbf{p}(F_K) - G_K^k\|_{m,\infty,\widehat{K}} \lesssim h_K^{k+1-m}.$$

**Proof.**

To prove this proposition, the interpolation properties of  $\mathbf{a}_K^k$  are used:

$$\|\mathbf{p}(F_K) - \mathbf{a}_K^k\|_{m,\infty,\widehat{K}} \lesssim h_K^{k+1-m}.$$

It follows from Lemma 2.2 for  $1 \leq m \leq k$ :

$$\begin{aligned} \|\mathbf{p}(F_K) - G_K^k\|_{m,\infty,\widehat{K}} &= \|\mathbf{p}(F_K) - \mathbf{a}_K^k - (\lambda^*)^{k+2} (\mathbf{p}(F_K(\widehat{\mathbf{y}})) - \mathbf{a}_K^k(\widehat{\mathbf{y}}))\|_{m,\infty,\widehat{K}} \\ &\leq \|\mathbf{p}(F_K) - \mathbf{a}_K^k\|_{m,\infty,\widehat{K}} \\ &\quad + \|(\lambda^*)^{k+2} (\mathbf{p}(F_K(\widehat{\mathbf{y}})) - \mathbf{a}_K^k(\widehat{\mathbf{y}}))\|_{m,\infty,\widehat{K}} \\ &\lesssim h_K^{k+1-m} + h_K^k \lesssim h_K^{k+1-m}. \end{aligned}$$

In the case of  $m = 0$ , it can be directly concluded that

$$\begin{aligned} \|\mathbf{p}(F_K) - G_K^k\|_{0,\infty,\widehat{K}} &\leq \|\mathbf{p}(F_K) - \mathbf{a}_K^k\|_{0,\infty,\widehat{K}} + \|(\mathbf{p}(F_K(\widehat{\mathbf{y}})) - \mathbf{a}_K^k(\widehat{\mathbf{y}}))\|_{0,\infty,\widehat{K}} \\ &\lesssim h_K^{k+1}. \end{aligned}$$

□

From this estimate it directly follows for the distance function  $d$ , the normal  $\mathbf{n}$  and conormal  $\boldsymbol{\nu}$  on  $\Gamma$ , and the normal  $\mathbf{n}_h^k$  and conormal  $\boldsymbol{\nu}_h^k$  on  $\Gamma_h^k$ :

**Lemma 2.6**

For  $h$  being small enough and  $K^k = G_K^k \widehat{K} \in \mathcal{T}_h^k$ , it holds

$$\|d\|_{0,\infty,K^k} \lesssim h_K^{k+1}, \quad (2.6)$$

$$\|\mathbf{n}^E - \mathbf{n}_h^k\|_{0,\infty,K^k} \lesssim h_K^k, \quad (2.7)$$

$$\|\boldsymbol{\nu}^E - \boldsymbol{\nu}_h^k\|_{0,\infty,K^k} \lesssim h_K^k. \quad (2.8)$$

**Proof.**

This is a direct consequence of Lemma 2.5 following [22, Proposition 2.3]. □

In the following, also orthogonal projection operators  $P$  and  $P_h^k$  onto the given surface and the approximating surface, respectively, are required:

$$\begin{aligned} P(\mathbf{x}) &:= I - \mathbf{n}(\mathbf{x}) \mathbf{n}(\mathbf{x})^T \quad \text{for } \mathbf{x} \in U(D_0), \\ P_h^k(\mathbf{x}) &:= I - \mathbf{n}_h^k(\mathbf{x}) \mathbf{n}_h^k(\mathbf{x})^T \quad \text{for } \mathbf{x} \in \Gamma_h^k. \end{aligned}$$

From Lemma 2.6 it directly follows that:

$$\|P_h^k - P\|_{\infty, \Gamma_h^k} \lesssim h^k, \quad (2.9)$$

$$\|dP_h^k H\|_{\infty, \Gamma_h^k} \lesssim h^{k+1}. \quad (2.10)$$

## 2.3 Discrete Operators

After defining the discrete surfaces  $\Gamma_h^k$ , the corresponding surface operators are introduced.

The surface gradient  $\nabla_{\Gamma_h^k}$  of a function  $\phi$  given on  $\Gamma_h^k$  is defined element-wise using the element-wise defined normal  $\mathbf{n}_h^k$  via:

$$\nabla_{\Gamma_h^k} \phi := \nabla \tilde{\phi} - \left( \mathbf{n}_h^k \cdot \nabla \tilde{\phi} \right) \mathbf{n}_h^k,$$

where  $\tilde{\phi}$  is a smooth extension of  $\phi$ . In the same way as for  $\nabla_{\Gamma}$ , independence of  $\nabla_{\Gamma_h^k}$  from the choice of the extension can be proven, see [30, Lemma 2.4], and the surface gradient is well defined.

Having in mind the extension operator given in (2.4), the identity:

$$\nabla u^E(\mathbf{x}) = \left( \frac{\partial \mathbf{p}}{\partial \mathbf{x}} \right)^T \nabla u(\mathbf{p}(\mathbf{x}))$$

can be obtained by chain rule for all  $\mathbf{x} \in U(D_0)$ . Recalling the definition of  $\mathbf{p}$ , it follows:

$$\frac{\partial \mathbf{p}}{\partial \mathbf{x}} = P(\mathbf{x}) - d(\mathbf{x}) H(\mathbf{x}).$$

Using  $HP = H$  it follows:

$$\nabla u^E(\mathbf{x}) = (I - dH)(\mathbf{x}) \nabla_{\Gamma} u(\mathbf{p}(\mathbf{x}))$$

and hence for  $\mathbf{x} \in \Gamma_h^k$ :

$$\nabla_{\Gamma_h^k} u^E(\mathbf{x}) = P_h^k(\mathbf{x}) (I - dH)(\mathbf{x}) \nabla_{\Gamma} u(\mathbf{p}(\mathbf{x})). \quad (2.11)$$

With (2.11) a way to represent  $\nabla_{\Gamma_h^k}$  in terms of  $\nabla_{\Gamma}$  is given. But, to transform an integral over  $\Gamma$  into the according integral over  $\Gamma_h^k$ , the opposite expression is necessary. Introducing  $\tilde{P}_h^k(\mathbf{x}) := I - \mathbf{n}_h^k(\mathbf{x}) (\mathbf{n}^T(\mathbf{x}) / (\mathbf{n}_h^k(\mathbf{x}) \cdot \mathbf{n}(\mathbf{x})))$  and noting that  $\tilde{P}_h^k P_h^k = P_h^k$ ,  $\nabla_{\Gamma} u$  can be written as:

$$\nabla_{\Gamma} u(\mathbf{p}(\mathbf{x})) = (I - dH)^{-1}(\mathbf{x}) \tilde{P}_h^k(\mathbf{x}) \nabla_{\Gamma_h^k} u^E(\mathbf{x}). \quad (2.12)$$

Following this approach, a formula for the second derivatives on  $\Gamma_h^k$  can be given:

$$\begin{aligned} \nabla^2 u^E(\mathbf{x}) &= (P - dH) \nabla^2 u^E(\mathbf{p}(\mathbf{x})) (P - dH) - \mathbf{n}^T \nabla u^E(\mathbf{p}(\mathbf{x})) H \\ &\quad - (H \nabla u^E(\mathbf{p}(\mathbf{x}))) \mathbf{n}^T - \mathbf{n} (H \nabla u^E(\mathbf{p}(\mathbf{x})))^T \\ &\quad - d \nabla H : \nabla u^E(\mathbf{p}(\mathbf{x})), \end{aligned} \quad (2.13)$$

where the dependency of  $d$ ,  $P$  and  $H$  on  $\mathbf{x}$  is skipped to increase the readability. An estimation for the geometric errors, occurring from the transformation of the surface divergence and the Laplace-Beltrami operator, is needed in the later analysis.

### Lemma 2.7

For  $\Gamma_h^k$  being an approximation of  $\Gamma$  as described in Section 2.2, the following estimate holds for all  $\mathbf{w} \in (W^{1,\infty}(\Gamma))^{n+1}$ :

$$\|\nabla_{\Gamma_h^k} \cdot \mathbf{w}^E - (\nabla_{\Gamma} \cdot \mathbf{w})^E\|_{0,\infty,\Gamma_h^k} \lesssim h^k |\mathbf{w}|_{1,\infty,\Gamma}.$$

### Proof.

The surface divergence can be written as:

$$\begin{aligned} \nabla_{\Gamma_h^k} \cdot \mathbf{w}^E &= \text{tr} \left( \nabla_{\Gamma_h^k} \mathbf{w}^E \right) = \text{tr} \left( P_h^k \nabla \mathbf{w}^E \right) \\ \nabla_{\Gamma} \cdot \mathbf{w} &= \text{tr} \left( \nabla_{\Gamma} \mathbf{w} \right) = \text{tr} \left( P \nabla \mathbf{w} \right). \end{aligned}$$

Taking  $\mathbf{x} \in \Gamma_h^k$  arbitrary but fixed (excluding the edges of  $\Gamma_h^k$ ) and using equation (2.11) we get:

$$\begin{aligned} \nabla_{\Gamma_h^k} \cdot \mathbf{w}^E &= \text{tr} \left( P_h^k (I - dH) (\nabla_{\Gamma} \mathbf{w})^E \right) \\ &= \text{tr} \left( P_h^k (\nabla_{\Gamma} \mathbf{w})^E \right) + \text{tr} \left( P_h^k dH (\nabla_{\Gamma} \mathbf{w})^E \right) \\ &= \text{tr} \left( (P_h^k - P) (\nabla_{\Gamma} \mathbf{w})^E \right) + \text{tr} \left( P (\nabla_{\Gamma} \mathbf{w})^E \right) + d \text{tr} \left( P_h^k H (\nabla_{\Gamma} \mathbf{w})^E \right). \end{aligned}$$

Using (2.6) and (2.9) leads to the estimate

$$\begin{aligned} \|\nabla_{\Gamma_h^k} \cdot \mathbf{w}^E - (\nabla_{\Gamma} \cdot \mathbf{w})^E\|_{0,\infty,\Gamma_h^k} &= \left\| \text{tr} \left( (P_h^k - P) (\nabla_{\Gamma} \mathbf{w})^E \right) + d \text{tr} \left( P_h^k H (\nabla_{\Gamma} \mathbf{w})^E \right) \right\|_{0,\infty,\Gamma_h^k} \\ &= \left( \|P_h^k - P\|_{0,\infty,\Gamma_h^k} + \|dP_h^k H\|_{0,\infty,\Gamma_h^k} \right) \|(\nabla_{\Gamma} \mathbf{w})^E\|_{0,\infty,\Gamma_h^k} \\ &\lesssim h^k \|\nabla_{\Gamma} \mathbf{w}\|_{0,\infty,\Gamma}. \end{aligned}$$

□

**Lemma 2.8**

Let  $\Gamma_h^k$  be an approximation of  $\Gamma$  as described in Section 2.2, then for  $u \in H^2(\Gamma)$  it holds:

$$\|\Delta_{\Gamma_h^k} u^E - (\Delta_{\Gamma} u)^E\|_{0, \Gamma_h^k} \lesssim h^k \|u\|_{2, \Gamma}.$$

**Proof.**

Making use of the identity:

$$\Delta_{\Gamma} u(\mathbf{x}) = \nabla_{\Gamma} \cdot (\nabla_{\Gamma} u(\mathbf{x})) = \text{tr} \left( P \nabla (P \nabla u^E(\mathbf{p}(\mathbf{x})))^T \right) = \text{tr} (P \nabla^2 u^E(\mathbf{p}(\mathbf{x})) P)$$

and equivalent for  $\mathbf{x} \in \Gamma_h^k$ :

$$\Delta_{\Gamma_h^k} u^E(\mathbf{x}) = \text{tr} \left( P_h^k \nabla^2 u^E(\mathbf{x}) P_h^k \right),$$

the term can be rewritten as:

$$\Delta_{\Gamma_h^k} u^E - (\Delta_{\Gamma} u)^E = \text{tr} \left( P_h^k \nabla^2 u^E(\mathbf{x}) P_h^k - P \nabla^2 u^E(\mathbf{p}(\mathbf{x})) P \right).$$

A clever addition of zero and a triangle inequality yield:

$$\begin{aligned} & |P_h^k \nabla^2 u^E(\mathbf{x}) P_h^k - P \nabla^2 u^E(\mathbf{p}(\mathbf{x})) P| \\ & \leq \left| (P_h^k - P) \nabla^2 u^E(\mathbf{x}) P_h^k \right| + \left| P \nabla^2 u^E(\mathbf{x}) (P_h^k - P) \right| \\ & \quad + \left| P (\nabla^2 u^E(\mathbf{x}) - \nabla^2 u^E(\mathbf{p}(\mathbf{x}))) P \right| \\ & \lesssim h^k |\nabla^2 u^E(\mathbf{x})| + |P (\nabla^2 u^E(\mathbf{x}) - \nabla^2 u^E(\mathbf{p}(\mathbf{x}))) P|. \end{aligned}$$

Here, estimate (2.9) and  $|P|, |P_h^k| \leq 1$  have been used.

The term  $|\nabla^2 u^E(\mathbf{x})|$  is bounded using formula (2.13) and  $|P|, |H|, |\nabla H| \leq 1$  and  $|d| \lesssim h^{k+1}$  on  $\Gamma_h^k$ :

$$|\nabla^2 u^E(\mathbf{x})| \lesssim |\nabla^2 u^E(\mathbf{p}(\mathbf{x}))| + |\nabla u^E(\mathbf{p}(\mathbf{x}))|.$$

The last summand is evaluated plugging (2.13) in and estimating the result term by term:

$$\begin{aligned} & P(\nabla^2 u^E(\mathbf{x}) - \nabla^2 u^E(\mathbf{p}(\mathbf{x}))) P \\ & \leq P(P - dH) \nabla^2 u^E(\mathbf{p}(\mathbf{x})) (P - dH) P - P \nabla^2 u^E(\mathbf{p}(\mathbf{x})) P \\ & \quad - P \mathbf{n}^T \nabla u^E(\mathbf{p}(\mathbf{x})) H P \\ & \quad - P (H \nabla u^E(\mathbf{p}(\mathbf{x}))) \mathbf{n}^T P - P \mathbf{n} (H \nabla u^E(\mathbf{p}(\mathbf{x})))^T P \\ & \quad - P d \nabla H : \nabla u^E(\mathbf{p}(\mathbf{x})) P \\ & =: T_1 + T_2 + T_3 + T_4. \end{aligned}$$

The term  $T_1$  is bounded using  $|d| \leq h^{k+1}$  and the idempotence of  $P$ :

$$\begin{aligned} |T_1| &= |P(P - dH) \nabla^2 u^E(\mathbf{p}(\mathbf{x})) (P - dH) P - P \nabla^2 u^E(\mathbf{p}(\mathbf{x})) P| \\ &\leq (h^{k+1} + h^{2k+2}) |\nabla^2 u^E(\mathbf{p}(\mathbf{x}))|. \end{aligned}$$

For the term  $T_2$  it is utilized that  $\mathbf{n}^T \nabla u^E(\mathbf{p}(\mathbf{x}))$  is the directional derivative of  $u^E$  in direction of the normal  $\mathbf{n}$ . By construction,  $u^E$  is constant along the normal and hence  $\mathbf{n}^T \nabla u^E(\mathbf{p}(\mathbf{x})) = 0$ :

$$|T_2| = |P \mathbf{n}^T \nabla u^E(\mathbf{p}(\mathbf{x})) H P| = 0.$$

The next line is estimated making use of  $P \mathbf{n} = 0$  and  $\mathbf{n}^T P = 0$ :

$$|T_3| = \left| P (H \nabla u^E(\mathbf{p}(\mathbf{x}))) \mathbf{n}^T P - P \mathbf{n} (H \nabla u^E(\mathbf{p}(\mathbf{x})))^T P \right| = 0.$$

The expression  $T_4$  is bounded using  $|d| \leq h^{k+1}$  and  $|P|, |H| \leq 1$  again:

$$|T_4| = |P d \nabla H : \nabla u^E(\mathbf{p}(\mathbf{x})) P| \leq h^{k+1} |\nabla u^E(\mathbf{p}(\mathbf{x}))|.$$

Combining the obtained estimates and having in mind that  $\mathbf{n} \cdot \nabla u^E = 0$  one gets

$$\begin{aligned} \|\Delta_{\Gamma_h^k} u^E - (\Delta_{\Gamma} u)^E\|_{0, \Gamma_h^k} &\lesssim h^k \left( \|\nabla^2 u^E(\mathbf{p}(\mathbf{x}))\|_{0, \Gamma_h^k} + \|\nabla u^E(\mathbf{p}(\mathbf{x}))\|_{0, \Gamma_h^k} \right) \\ &\lesssim h^k (\|\nabla^2 u^E\|_{0, \Gamma} + \|\nabla u^E\|_{0, \Gamma}) \\ &= h^k \|u\|_{2, \Gamma}. \end{aligned}$$

□

Due to  $\Gamma_h^k$  being a non-smooth surface, integrals over the mesh edges occur by partial integration. Geometric values, for example the discrete normal  $\mathbf{n}_h^k$ , can jump over edges. Particularly, the jump of co-normals over an edge will occur later in the numerical analysis and, therefore, is investigated here:

**Lemma 2.9**

Let  $K_1 \in \mathcal{T}_h^k$  and  $K_2 \in \mathcal{T}_h^k$  be two neighbouring elements with common edge  $E$ .  $\boldsymbol{\nu}_1$  and  $\boldsymbol{\nu}_2$  name the discrete co-normals at  $E$  belonging to  $K_1$  and  $K_2$ , respectively. Then

$$|P(\boldsymbol{\nu}_1 + \boldsymbol{\nu}_2)| \lesssim h_K^{2k}.$$

**Proof.**

The proof is following the ideas of Lemma 3.6 in [61] but is extended to the higher order setting here.

The unit tangential vector along the edge  $E$  at point  $\mathbf{x}$  is denoted by  $\boldsymbol{\xi}(\mathbf{x})$ . Because  $\boldsymbol{\xi}(\mathbf{x})$  is orthogonal to the vectors  $\mathbf{n}_h^k|_{K_i}(\mathbf{x})$  and  $\boldsymbol{\nu}_i$ ,  $i = 1, 2$ , the tangential vector can



be expressed as the cross product of  $\mathbf{n}_h^k|_{K_i}$  and  $\boldsymbol{\nu}_i$  for  $i = 1, 2$ . The sign of  $\boldsymbol{\xi}(\mathbf{x})$  is chosen such that  $\boldsymbol{\xi}(\mathbf{x}) = \mathbf{n}_h^k|_{K_1}(\mathbf{x}) \times \boldsymbol{\nu}_1(\mathbf{x}) = \boldsymbol{\nu}_2(\mathbf{x}) \times \mathbf{n}_h^k|_{K_2}(\mathbf{x})$ . Then,  $\boldsymbol{\nu}_i$ ,  $\mathbf{n}_h^k|_{K_i}$  and  $\boldsymbol{\xi}$  set up an orthonormal system at  $\mathbf{x}$ ,  $i = 1, 2$ , and it follows

$$\boldsymbol{\nu}_1 + \boldsymbol{\nu}_2 = \boldsymbol{\xi} \times \mathbf{n}_h^k|_{K_1} + \mathbf{n}_h^k|_{K_2} \times \boldsymbol{\xi} = \boldsymbol{\xi} \times \left( \mathbf{n}_h^k|_{K_1} - \mathbf{n}_h^k|_{K_2} \right).$$

The discrete normals  $\mathbf{n}_h^k$  are written as a direct sum of  $\boldsymbol{\tau}^i \perp \mathbf{n}$  and  $\beta^i \mathbf{n}$  and the following expression for  $\beta^i$  is obtained:

$$\begin{aligned} 1 &= |\mathbf{n}_h^k|_{K_i}|^2 = |\boldsymbol{\tau}^i|^2 + (\beta^i)^2 |\mathbf{n}|^2 \\ &= |\boldsymbol{\tau}^i|^2 + (\beta^i)^2 \\ \Rightarrow \beta^i &= \sqrt{1 - |\boldsymbol{\tau}^i|^2}. \end{aligned}$$

From Lemma 2.6 it follows that:

$$\begin{aligned} h_K^{2k} &\gtrsim \left| \mathbf{n} - \mathbf{n}_h^k|_{K_i} \right|^2 \\ &= \left| \mathbf{n} - \beta^i \mathbf{n} - \boldsymbol{\tau}^i \right|^2 \\ &= (1 - \beta^i)^2 |\mathbf{n}|^2 + |\boldsymbol{\tau}^i|^2 \\ &= 1 - 2\beta^i + 1 - |\boldsymbol{\tau}^i|^2 + |\boldsymbol{\tau}^i|^2 \\ &= 2 - 2\beta^i \Rightarrow 1 - \beta^i \lesssim h_K^{2k}. \end{aligned}$$

Therefore, the jump of the discrete normals can be written in the following way:

$$\begin{aligned} \mathbf{n}_h^k|_{K_2} - \mathbf{n}_h^k|_{K_1} &= \left( \mathbf{n} - \mathbf{n}_h^k|_{K_1} \right) - \left( \mathbf{n} - \mathbf{n}_h^k|_{K_2} \right) \\ &= \mathbf{n} - \boldsymbol{\tau}^1 - \beta^1 \mathbf{n} - \mathbf{n} + \boldsymbol{\tau}^2 + \beta^2 \mathbf{n} \\ &= ((1 - \beta^1) - (1 - \beta^2)) \mathbf{n} + \boldsymbol{\tau}^2 - \boldsymbol{\tau}^1 \\ &= \beta \mathbf{n} + \boldsymbol{\tau} \end{aligned}$$

with  $\beta \lesssim h_K^{2k}$  and  $\boldsymbol{\tau} \perp \mathbf{n}$ . Additionally, Lemma 2.6 and the orthogonality of  $\mathbf{n}$  and  $\boldsymbol{\tau}$  lead to:

$$\left| \mathbf{n}_h^k|_{K_1} - \mathbf{n}_h^k|_{K_2} \right| \leq \left| \mathbf{n}_h^k|_{K_1} - \mathbf{n} \right| + \left| \mathbf{n}_h^k|_{K_2} - \mathbf{n} \right| \lesssim h^k \Rightarrow |\boldsymbol{\tau}| \lesssim h_K^k.$$

By construction, the term  $\boldsymbol{\xi}$  can be written as:

$$\boldsymbol{\xi} = \mathbf{n}_h^k|_{K_1} \times \boldsymbol{\nu}_1 = \left( \mathbf{n} + \left( \mathbf{n}_h^k|_{K_1} - \mathbf{n} \right) \right) \times \boldsymbol{\nu}_1 = \mathbf{n} \times \boldsymbol{\nu}_1 + \tilde{\boldsymbol{\xi}},$$

where  $|\tilde{\boldsymbol{\xi}}| = |(\mathbf{n}_h^k|_{K_1} - \mathbf{n}) \times \boldsymbol{\nu}_1| \lesssim h_K^k$  due to Lemma 2.6 and  $|\boldsymbol{\nu}_1| = 1$ . Now,  $|P(\boldsymbol{\nu}_1 + \boldsymbol{\nu}_2)|$  can be estimated by:

$$\begin{aligned} |P(\boldsymbol{\nu}_1 + \boldsymbol{\nu}_2)| &= |P\left(\left(\mathbf{n} \times \boldsymbol{\nu}_1 + \tilde{\boldsymbol{\xi}}\right) \times (\beta \mathbf{n} + \boldsymbol{\tau})\right)| \\ &= |P((\mathbf{n} \times \boldsymbol{\nu}_1) \times \boldsymbol{\tau}) + P(\tilde{\boldsymbol{\xi}} \times \boldsymbol{\tau}) + P\left(\left(\mathbf{n} \times \boldsymbol{\nu}_1 + \tilde{\boldsymbol{\xi}}\right) \times (\beta \mathbf{n})\right)| \\ &\lesssim |P|\left(|\tilde{\boldsymbol{\xi}}| |\boldsymbol{\tau}| + h^{2k}\right) \lesssim h^{2k}. \end{aligned}$$

Here it was used, that  $\boldsymbol{\tau} \perp \mathbf{n}$ . Hence  $(\mathbf{n} \times \boldsymbol{\nu}_1) \times \boldsymbol{\tau} \parallel \mathbf{n}$  and thus  $P((\mathbf{n} \times \boldsymbol{\nu}_1) \times \boldsymbol{\tau}) = 0$ .  $\square$

## 2.4 Integral Transformations

To transfer integrals from the given surface  $\Gamma$  to the approximating surface  $\Gamma_h^k$ , formulas are required, that relate the surface measures  $ds$  and  $ds_h^k$  and the boundary measures  $d\mathbf{b}$  and  $d\mathbf{b}_h^k$ .

First, the surface measure  $ds$  and the boundary measure  $d\mathbf{b}$  on  $\Gamma$  are related to the surface measure  $ds_h$  and boundary measure  $d\mathbf{b}_h$  on the linear surface  $\Gamma_h$ . Setting  $\mu_h$  and  $\theta_h$  to the quotients of the surface and boundary measure, such that:

$$\mu_h(\mathbf{x}) ds_h = ds \quad \text{and} \quad \theta_h(\mathbf{x}) d\mathbf{b}_h = d\mathbf{b}, \quad (2.14)$$

the integral transformation formulas for the product of two functions  $\phi : \Gamma \rightarrow \mathbb{R}$  and  $\psi : \Gamma \rightarrow \mathbb{R}$  are given by:

$$\int_{\Gamma} \phi(\mathbf{x}) \psi(\mathbf{x}) ds = \int_{\Gamma_h} \phi^E(\mathbf{x}) \psi^E(\mathbf{x}) \mu_h(\mathbf{x}) ds_h$$

and

$$\int_{\partial\Gamma} \phi(\mathbf{x}) \psi(\mathbf{x}) d\mathbf{b} = \int_{\partial\Gamma_h} \phi(\mathbf{p}(\mathbf{x})) \psi(\mathbf{p}(\mathbf{x})) \theta_h(\mathbf{x}) d\mathbf{b}_h.$$

The following estimates for  $\mu_h$  and  $\theta_h$  can be obtained:

**Lemma 2.10**

Let  $\mu_h$  and  $\theta_h$  be the quotient of the surface and the boundary measure for a curved surface  $\Gamma$  and its linear triangulation  $\Gamma_h$ , compare (2.14). Then, it holds

$$\begin{aligned} \|1 - \mu_h\|_{0,\infty,\Gamma_h} &\lesssim h^2, \\ \|1 - \theta_h\|_{0,\infty,\partial\Gamma_h} &\lesssim h^2. \end{aligned}$$

**Proof.**

The proof is given in [30, Lemma 4.1.] and can directly be extended to the case of non-closed surfaces and boundary measures.  $\square$

A similar result also holds true for the  $k$ -th order approximation using the standard interpolation estimates. To relate the surface and boundary measure of the given surface  $\Gamma$  and the higher order approximation  $\Gamma_h^k$ , the quotients  $\mu_h^k$  and  $\theta_h^k$  are introduced such that

$$ds = \mu_h^k ds_h^k \quad \text{and} \quad d\mathbf{b} = \theta_h^k d\mathbf{b}_h^k.$$

**Lemma 2.11**

For  $\mu_h^k$  and  $\theta_h^k$  being the quotient of the surface and the boundary measure for a given surface  $\Gamma$  and its higher order approximation  $\Gamma_h^k$ , it can be obtained that

$$\begin{aligned} \|1 - \mu_h^k\|_{0,\infty,\Gamma_h^k} &\lesssim h^{k+1}, \\ \|1 - \theta_h^k\|_{0,\infty,\partial\Gamma_h^k} &\lesssim h^{k+1}. \end{aligned}$$

**Proof.**

Compare [30, Lemma 4.4]. □

The integral transformation formulas for the product of two functions  $\phi : \Gamma \rightarrow \mathbb{R}$  and  $\psi : \Gamma \rightarrow \mathbb{R}$  are then given by:

$$\int_{\Gamma} \phi(\mathbf{x}) \psi(\mathbf{x}) ds = \int_{\Gamma_h^k} \phi^E(\mathbf{x}) \psi^E(\mathbf{x}) \mu_h^k(\mathbf{x}) ds_h^k \quad \text{and} \quad (2.15)$$

$$\int_{\partial\Gamma} \phi(\mathbf{x}) \psi(\mathbf{x}) d\mathbf{b} = \int_{\partial\Gamma_h^k} \phi^E(\mathbf{x}) \psi^E(\mathbf{x}) \theta_h^k(\mathbf{x}) d\mathbf{b}_h^k. \quad (2.16)$$

The problem becomes more complex if the product of the surface gradients of  $\phi$  and  $\psi$  or the product of a surface gradient with a given vector  $\mathbf{w} : \Gamma \rightarrow \mathbb{R}^n$  shall be integrated. Due to (2.12) it follows:

$$\begin{aligned} &\int_{\Gamma} \nabla_{\Gamma} \phi(\mathbf{x}) \cdot \nabla_{\Gamma} \psi(\mathbf{x}) ds \\ &= \int_{\Gamma_h^k} (I - dH)^{-1} \tilde{P}_h^k \nabla_{\Gamma_h^k} \phi^E(\mathbf{x}) \cdot (I - dH)^{-1} \tilde{P}_h^k \nabla_{\Gamma_h^k} \psi^E(\mathbf{x}) \mu_h^k(\mathbf{x}) ds_h^k \\ &= \int_{\Gamma_h^k} A_h^k \nabla_{\Gamma_h^k} \phi^E(\mathbf{x}) \cdot \nabla_{\Gamma_h^k} \psi^E(\mathbf{x}) ds_h^k, \end{aligned} \quad (2.17)$$

with  $A_h^k := \mu_h^k \left( \tilde{P}_h^k \right)^T (I - dH)^{-2} \tilde{P}_h^k$ . Using  $\mathbf{n} \cdot \mathbf{w} = 0$  on  $\Gamma$  it can be concluded that  $\mathbf{n}(\mathbf{x}) \cdot \mathbf{w}^E(\mathbf{x}) = 0$  for all  $\mathbf{x} \in \Gamma_h^k$ . It follows that  $\mathbf{w}^E(\mathbf{x}) = \tilde{P}_h^k \mathbf{w}^E(\mathbf{x})$  and hence:

$$\begin{aligned}
& \int_{\Gamma} \mathbf{w}(\mathbf{x}) \cdot \nabla_{\Gamma} \phi(\mathbf{x}) \, ds \\
&= \int_{\Gamma_h^k} \left( \tilde{P}_h^k \mathbf{w}^E(\mathbf{x}) \right) (I - dH)^{-1} \tilde{P}_h^k \nabla_{\Gamma_h^k} \phi^E(\mathbf{x}) \mu_h^k(\mathbf{x}) \, ds_h^k \\
&= \int_{\Gamma_h^k} B_h^k \nabla_{\Gamma_h^k} \phi^E(\mathbf{x}) \cdot \mathbf{w}^E(\mathbf{x}) \, ds_h^k, \tag{2.18}
\end{aligned}$$

with  $B_h^k := \mu_h^k \left( \tilde{P}_h^k \right)^T (I - dH)^{-1} \tilde{P}_h^k$ . The following estimates are presented in [59] for linear approximations of closed surfaces, but can be transferred to the more general setting studied here.

**Lemma 2.12**

For  $A_h^k$  and  $B_h^k$  given by (2.17) and (2.18) the following estimates hold true:

$$\begin{aligned}
\|A_h^k - P_h^k\|_{0,\infty,\Gamma_h^k} &\lesssim h^{k+1}, \\
\|B_h^k - P_h^k\|_{0,\infty,\Gamma_h^k} &\lesssim h^{k+1}.
\end{aligned}$$

**Proof.**

To estimate the term  $\|B_h^k - P_h^k\|_{0,\infty,\Gamma_h^k}$  it is used that  $(I - dH) = I + \mathcal{O}(h^{k+1})$  and hence:

$$\|B_h^k - P_h^k\|_{0,\infty,\Gamma_h^k} \lesssim \|A_h^k - P_h^k\|_{0,\infty,\Gamma_h^k} + h^{k+1}.$$

Therefore, it is sufficient to prove the postulated estimate for  $A_h^k$ . We use that from  $P_h^k \tilde{P}_h^k = P_h^k$  and  $P_h^k A_h^k = A_h^k$  it follows that:

$$A_h^k - P_h^k = P_h^k \left( A_h^k - I \right) = P_h^k \left( A_h^k - \tilde{P}_h^k \right).$$

To estimate  $A_h^k - \tilde{P}_h^k$ , Lemma 2.11 and  $(I - dH)^{-1} = I + \mathcal{O}(h^{k+1})$  are used and lead to:

$$\|A_h^k - \tilde{P}_h^k\|_{0,\infty,\Gamma_h^k} \lesssim h^{k+1}.$$

□

The following estimates can be obtained from Lemma 2.11 and 2.12 for functions  $\phi$  sufficiently smooth in  $G$  and all  $K^k \in \mathcal{T}_h^k$ :

$$\|\phi^E\|_{0,K^k} \approx \|\phi\|_{0,\mathbf{p}(K^k)}, \tag{2.19}$$

$$\|\nabla_{\Gamma_h^k} \phi^E\|_{0,K^k} \approx \|\nabla_{\Gamma} \phi\|_{0,\mathbf{p}(K^k)}. \tag{2.20}$$

## 2.5 Finite Element Spaces and Interpolation

To obtain finite element methods on the introduced discrete surfaces  $\Gamma_h^k$ , finite dimensional ansatz and test spaces on  $\Gamma_h^k$  have to be defined. Remember that,  $\widehat{K}$  is the reference element and  $G_K^k$  names the mapping from  $\widehat{K}$  to the higher order element  $K^k \in \mathcal{T}_h^k$ .  $\mathbb{P}_r(\widehat{K})$  names the space of polynomials degree  $r$  or less over  $\widehat{K}$ . Then, the continuous mapped Lagrange finite element space of order  $r$  is given by

$$X^r := \{v \in C^0(\Gamma_h^k) \mid v|_{K^k} = \widehat{v} \circ (G_K^k)^{-1} \text{ for a } \widehat{v} \in \mathbb{P}_r(\widehat{K}) \text{ for all } K^k \in \mathcal{T}_h^k\}.$$

The setting is called isoparametric if  $r = k$ , sub-parametric if  $k < r$  and super-parametric if  $k > r$ .

The inequalities given in Lemma 2.4 enable the standard estimations for integral transformations between the finite elements  $K^k$  and the reference element  $\widehat{K}$ . Thereby, some standard inequalities often used in the analysis of finite element methods can be transferred to surface finite elements:

### **Lemma 2.13 (Trace Inequality)**

Let  $v \in H^1(K^k)$ . Then it holds

$$\|v\|_{0,\partial K^k} \lesssim (h_K^{-1} \|v\|_{0,K^k}^2 + h_K |v|_{1,K^k}^2)^{1/2}.$$

### **Lemma 2.14 (Inverse Inequality)**

There exists a positive constant  $c_{inv}$  such that for all  $v_h \in X^r$  and  $K^k \in \mathcal{T}_h^k$  it holds

$$|v_h|_{1,K^k} \leq c_{inv} h_K^{-1} \|v_h\|_{0,K^k}.$$

In the later analysis an interpolation of continuous functions  $u^E : \Gamma_h^k \rightarrow \mathbb{R}$  into the finite element space  $X^r$  will be needed. An interpolator  $i^r : C^0(\Gamma_h^k) \rightarrow X^r$  is introduced following [22, Section 2.5] and [2, Section 5]. We denote by  $\widehat{i}^r$  the nodal Lagrange interpolator from  $C^1(\widehat{K})$  into the polynomial space  $\mathbb{P}^r(\widehat{K})$ . The interpolator on  $i^r : C^0(\Gamma_h^k) \rightarrow X^r$  can be defined from  $\widehat{i}^r$  element-wise by transformation back and forth:

$$i^r u^E|_{K^k} = \widehat{i}^r (u^E|_{K^k} \circ G_K^k) \circ (G_K^k)^{-1}.$$

On the smooth surface  $\Gamma$  an interpolator  $\widetilde{i}^r : C^0(\Gamma) \rightarrow \{v_h^L \mid v_h \in X^r\}$  for functions is given following the same approach

$$\widetilde{i}^r u|_{\widetilde{K}} = (i^r(u^E))^L.$$

The following interpolation estimate can be obtained for functions defined on the smooth surface:

**Lemma 2.15**

Let  $i^r : C^0(\Gamma_h^k) \rightarrow X^r$  be as defined above and  $u \in H^{m+1}(\Gamma)$ ,  $1 \leq m \leq r$ , then:

$$\|u^E - i^r(u^E)\|_{0,K^k} + h_K |u^E - i^r(u^E)|_{1,K^k} \lesssim h_K^{m+1} \|u\|_{m+1,\tilde{K}}. \quad (2.21)$$

**Proof.**

Using the definition of  $\tilde{i}^r$  presented above and the norm equivalences (2.19)–(2.20) it follows for  $l = 0, 1$ :

$$|u^E - i^r(u^E)|_{l,K^k} \lesssim \left| u - (i^r(u^E))^L \right|_{l,\tilde{K}} = \left| u - \tilde{i}^r u \right|_{l,\tilde{K}}.$$

The estimate

$$\left| u - \tilde{i}^r u \right|_{l,\tilde{K}} \lesssim h_K^{m+1-l} \|u\|_{m+1,\tilde{K}}$$

follows from interpolation estimations for  $\hat{i}^r$  and integral transformations and is given in [2].  $\square$

## Chapter 3

# Elliptic Equations on Surfaces

This section demonstrates the usage of surface finite elements for elliptic partial differential equations on a surface  $\Gamma$ . The following diffusion-convection-reaction equation on a closed surface  $\Gamma$  is considered as model problem:

$$-\varepsilon\Delta_{\Gamma}u + \nabla_{\Gamma} \cdot (\mathbf{w}u) + cu = f \quad \text{on } \Gamma. \quad (3.1)$$

The diffusion coefficient  $\varepsilon > 0$  is assumed to be constant and the given non-negative reaction coefficient  $c \in L^{\infty}(\Gamma)$ , the velocity field  $\mathbf{w} \in W^{1,\infty}(\Gamma)^{n+1}$ , and the right hand side  $f \in L^2(\Gamma)$ . Due to the steady state formulation of the problem, the surface  $\Gamma$  is fixed to its position and cannot move with the velocity field  $\mathbf{w}$ . Hence, the velocity field  $\mathbf{w}$  has to be tangential to the surface:

$$\mathbf{w} \cdot \mathbf{n} = 0 \quad \text{on } \Gamma.$$

Introducing  $\sigma := \nabla_{\Gamma} \cdot \mathbf{w} + c \in L^{\infty}(\Gamma)$ , the equation (3.1) can be reformulated in the following way:

$$-\varepsilon\Delta_{\Gamma}u + \mathbf{w} \cdot \nabla_{\Gamma}u + \sigma u = f \quad \text{on } \Gamma. \quad (3.2)$$

In this work two different settings are considered. Either the existence of a positive constant  $\sigma_0$ , such that:

$$\sigma - \frac{1}{2}\nabla_{\Gamma} \cdot \mathbf{w} \geq \sigma_0 > 0 \quad \text{on } \Gamma, \quad (3.3)$$

is supposed or the case of a missing  $L^2$ -control in equation (3.2) is studied:

$$\sigma - \frac{1}{2}\nabla_{\Gamma} \cdot \mathbf{w} = 0 \quad \text{on } \Gamma. \quad (3.4)$$

In Section 3.1 the diffusion-convection-reaction equation (3.2) under the condition (3.3) is studied. This assumption is common in the numerical analysis of diffusion-convection-reaction equations, compare [56]. A uniquely solvable weak

formulation is introduced and discretized using higher order surface approximations. An error analysis is carried out, where the orders of the surface and the function space approximation are handled independently. Thereby, special focus is taken on the convection-dominated case and all obtained estimations are semi-robust with respect to the diffusion coefficient.

Considering assumption (3.4), equation (3.2) is called diffusion-convection equation. This equation under the assumed condition is only solvable if  $\langle f, 1 \rangle_\Gamma = 0$  and the solution is only unique up to a constant. Therefore, an additional condition

$$\langle u, 1 \rangle_\Gamma = M \quad (3.5)$$

with a given value  $M$  is necessary to fix the solution.

Section 3.2 shows the differences of handling the diffusion-convection equation compared to the diffusion-convection-reaction equation. Following the outline of Section 3.1 the problem of missing  $L^2$ -control is handled. The chance of getting semi-robust estimates in this case is discussed and the obtained results are compared.

## 3.1 Diffusion Convection Reaction Equation

In this section a diffusion-convection-reaction equation on a closed surface  $\Gamma$

$$-\varepsilon \Delta_\Gamma u + \mathbf{w} \cdot \nabla_\Gamma u + \sigma u = f \quad \text{on } \Gamma \quad (3.6)$$

with the additional condition

$$\sigma - \frac{1}{2} \nabla_\Gamma \cdot \mathbf{w} \geq \sigma_0 > 0 \quad \text{on } \Gamma \quad (3.7)$$

for a constant  $\sigma_0$  is considered.

### 3.1.1 Weak Formulation

The surface finite element method is based on a weak formulation of the given equation (3.6). Therefore, the equation is multiplied by a test function  $v \in H^1(\Gamma)$  and integrated over the surface. The diffusion term is integrated by parts using formula (1.3). This yields:

#### **Problem 3.1 (*Weak Diffusion-Convection-Reaction Problem*)**

Find  $u \in V = H^1(\Gamma)$  such that for all  $v \in V$

$$a^{DCR}(u, v) = f^{DCR}(v)$$



with

$$\begin{aligned} a^{DCR}(u, v) &= \varepsilon \langle \nabla_{\Gamma} u, \nabla_{\Gamma} v \rangle_{\Gamma} + \langle \mathbf{w} \cdot \nabla_{\Gamma} u, v \rangle_{\Gamma} + \langle \sigma u, v \rangle_{\Gamma}, \\ f^{DCR}(v) &= \langle f, v \rangle_{\Gamma}. \end{aligned}$$

Corresponding to the bilinear form the triple norm:

$$\|v\|_{DCR} := (\varepsilon |v|_{1,\Gamma}^2 + \sigma_0 \|v\|_{0,\Gamma}^2)^{\frac{1}{2}}$$

is introduced. Actually, the triple norm is a norm on  $H^1(\Gamma)$ .

The unique solvability of Problem 3.1 shall be obtained by the Lax-Milgram theorem [51]. Therefore, the coercivity of the defined bilinear form  $a^{DCR}(\cdot, \cdot)$  is a main ingredient.

### Lemma 3.1

Under the assumption (3.7) the bilinear form  $a^{DCR}(\cdot, \cdot)$  is coercive in  $V$ :

$$a^{DCR}(v, v) \geq \|v\|_{DCR}^2 \quad \forall v \in V. \quad (3.8)$$

### Proof.

To prove the coercivity, the convection term in  $a^{DCR}(\cdot, \cdot)$  is partially integrated using formula (1.4):

$$\begin{aligned} \langle \mathbf{w} \cdot \nabla_{\Gamma} u, v \rangle_{\Gamma} &= -\langle \nabla_{\Gamma} \cdot (v \mathbf{w}), u \rangle_{\Gamma} + \langle u H \mathbf{n}, v \mathbf{w} \rangle_{\Gamma} \\ &= -\langle v \nabla_{\Gamma} \cdot \mathbf{w}, u \rangle_{\Gamma} - \langle \mathbf{w} \cdot \nabla_{\Gamma} v, u \rangle_{\Gamma}, \end{aligned}$$

where  $\mathbf{w} \cdot \mathbf{n} = 0$  on  $\Gamma$  is used.

The bilinear form  $a^{DCR}(v, v)$  can be reformulated and estimated using (3.7):

$$\begin{aligned} a^{DCR}(v, v) &= \varepsilon \langle \nabla_{\Gamma} v, \nabla_{\Gamma} v \rangle_{\Gamma} + \frac{1}{2} \langle v \mathbf{w}, \nabla_{\Gamma} v \rangle_{\Gamma} - \frac{1}{2} \langle v \mathbf{w}, \nabla_{\Gamma} v \rangle_{\Gamma} + \left\langle \sigma - \frac{1}{2} \nabla_{\Gamma} \cdot \mathbf{w} v, v \right\rangle_{\Gamma} \\ &\geq \varepsilon |v|_{1,\Gamma}^2 + \sigma_0 \|v\|_{0,\Gamma}^2 \end{aligned}$$

and (3.8) follows.  $\square$

Now, the unique solvability follows by the Lax-Milgram theorem. The required linearity of  $f^{DCR}(\cdot)$  and bilinearity of  $a^{DCR}(\cdot, \cdot)$  are obvious. The continuity of  $f^{DCR}(\cdot)$  and  $a^{DCR}(\cdot, \cdot)$  follows using the Cauchy-Schwarz inequality.

### Lemma 3.2

Problem 3.1 is uniquely solvable.

### 3.1.2 Discretized Formulation

To discretize the weak formulation, a triangulation of the given surface  $\Gamma$  and a finite element space have to be chosen. Higher order surface approximations  $\Gamma_h^k$ , as introduced in Section 2.2, are considered together with the mapped continuous Lagrange finite element spaces  $X^r$ , given in Section 2.5.

Making use of the introduced extension operator (2.4) the data given on  $\Gamma$  can be extended to the approximating surface  $\Gamma_h^k$ . The discrete formulation of Problem 3.1 reads:

#### **Problem 3.2** (*Discretized Diffusion-Convection-Reaction Problem*)

Find  $u_h \in X^r$  such that for all  $v_h \in X^r$

$$a_k^{DCR}(u_h, v_h) = f_h^{DCR}(v_h)$$

with

$$\begin{aligned} a_k^{DCR}(u_h, v_h) &= \varepsilon \left\langle \nabla_{\Gamma_h^k} u_h, \nabla_{\Gamma_h^k} v_h \right\rangle_{\Gamma_h^k} + \left\langle \mathbf{w}^E \cdot \nabla_{\Gamma_h^k} u_h, v_h \right\rangle_{\Gamma_h^k} + \left\langle \sigma^E u_h, v_h \right\rangle_{\Gamma_h^k}, \\ f_k^{DCR}(v_h) &= \left\langle f^E, v_h \right\rangle_{\Gamma_h^k}. \end{aligned}$$

Corresponding to this discretized formulation a mesh dependent norm on  $X^r$  is introduced via:

$$\| \| v_h \| \|_{DCR,k} := \left( \varepsilon |v_h|_{1,\Gamma_h^k}^2 + \sigma_0 \|v_h\|_{0,\Gamma_h^k}^2 \right)^{\frac{1}{2}}.$$

The unique solvability of Problem 3.2 is shown by proving the coercivity of  $a_h^{DCR}(\cdot, \cdot)$  in the discrete triple norm.

#### **Lemma 3.3**

If  $h$  is small enough (independent of  $\varepsilon$ ),  $a_k^{DCR}(\cdot, \cdot)$  is coercive in  $X^r$ :

$$a_k^{DCR}(v_h, v_h) \geq \frac{3}{4} \| \| v_h \| \|_{DCR,h}^2 \quad \forall v_h \in X^r$$

#### **Proof.**

The coercivity of  $a_k^{DCR}(\cdot, \cdot)$  follows as for  $a^{DCR}(\cdot, \cdot)$  in Lemma 3.1 by partial integra-

tion. Using  $\mathbf{n} \cdot \mathbf{w}^E = (\mathbf{n} \cdot \mathbf{w})^E = 0$ , hence  $P\mathbf{w}^E = \mathbf{w}^E$ , it follows:

$$\begin{aligned}
a_k^{DCR}(v_h, v_h) &= \varepsilon \left\langle \nabla_{\Gamma_h^k} v_h, \nabla_{\Gamma_h^k} v_h \right\rangle_{\Gamma_h^k} + \left\langle \mathbf{w}^E \cdot \nabla_{\Gamma_h^k} v_h, v_h \right\rangle_{\Gamma_h^k} + \left\langle \sigma^E v_h, v_h \right\rangle_{\Gamma_h^k} \\
&= \varepsilon \|\nabla_{\Gamma_h^k} v_h\|_{0, \Gamma_h^k}^2 + \frac{1}{2} \left\langle \mathbf{w}^E \cdot \nabla_{\Gamma_h^k} v_h, v_h \right\rangle_{\Gamma_h^k} - \frac{1}{2} \left\langle \mathbf{w}^E \cdot \nabla_{\Gamma_h^k} v_h, v_h \right\rangle_{\Gamma_h^k} \\
&\quad + \left\langle \left( \sigma^E - \frac{1}{2} \nabla_{\Gamma_h^k} \cdot \mathbf{w}^E \right) v_h, v_h \right\rangle_{\Gamma_h^k} + \frac{1}{2} \sum_{K \in \mathcal{T}_h^k} \int_{\partial K} \mathbf{w}^E \cdot \boldsymbol{\nu}_h^k v_h^2 d\mathbf{b}_h^k \\
&= \varepsilon \|\nabla_{\Gamma_h^k} v_h\|_{0, \Gamma_h^k}^2 \\
&\quad + \left\langle \left( \sigma^E - \frac{1}{2} (\nabla_{\Gamma} \cdot \mathbf{w})^E + \frac{1}{2} \left( (\nabla_{\Gamma} \cdot \mathbf{w})^E - \nabla_{\Gamma_h^k} \cdot \mathbf{w}^E \right) \right) v_h, v_h \right\rangle_{\Gamma_h^k} \\
&\quad + \frac{1}{2} \sum_{E \in \mathcal{E}_h^k} \int_E P\mathbf{w}^E \cdot (\boldsymbol{\nu}^+ + \boldsymbol{\nu}^-) v_h^2 d\mathbf{b}_h^k
\end{aligned}$$

The Lemmata 2.9 and 2.7 together with the trace inequality (Lemma 2.13) and the inverse inequality (Lemma 2.14) provides the existence of a positive constant  $C \in \mathbb{R}$ , such that:

$$a_k^{DCR}(v_h, v_h) \geq \varepsilon \|\nabla_{\Gamma_h^k} v_h\|_{0, \Gamma_h^k}^2 + \left( \sigma_0 - \frac{1}{2} C h^k (\|\nabla \mathbf{w}\|_{0, \infty, \Gamma} + \|\mathbf{w}\|_{0, \infty, \Gamma}) \right) \|v_h\|_{0, \Gamma_h^k}^2.$$

For  $h$  small enough, such that:

$$h^k \lesssim \frac{\sigma_0}{2C (\|\nabla \mathbf{w}\|_{0, \infty, \Gamma} + \|\mathbf{w}\|_{0, \infty, \Gamma})}, \quad (3.9)$$

the wanted result is obtained.  $\square$

Then, unique solvability is ensured by the Lax-Milgram theorem. The linearity of  $f_k^{DCR}(\cdot)$  and  $a_k^{DCR}(\cdot, \cdot)$  are obvious and continuity can be proven using  $\sigma \in L^\infty(\Gamma)$  and  $\mathbf{w} \in W^{1, \infty}(\Gamma)$ .

#### Lemma 3.4

*Problem 3.2 is uniquely solvable.*

### 3.1.3 Error Estimates

After introducing the weak and the discretized formulation of the diffusion-convection-reaction equation on a closed surface  $\Gamma$ , the errors occurring from solving the discretized problem instead of the continuous weak problem are topic of this section.

Thereby, the convection dominated case, i.e.  $\varepsilon \ll 1$ , is considered. Thus, the dependence of the error constants on  $\varepsilon$  are explicitly given.

Because the weak problem is given on the surface  $\Gamma$  and the discrete problem on the approximating surface  $\Gamma_h^k$ , their solutions are defined on different domains and cannot be compared directly. Hence, the extension operator is used to transfer the solution  $u$  of the weak problem onto  $\Gamma_h^k$ .

The error coming from the approximation of the infinite dimensional function space  $V$  by a finite dimensional space  $X^r$  is studied. An analysis of the geometric error introduced by the usage of an approximating surface  $\Gamma_h^k$  and the associated discrete surface operators follows. This is extended to a convergence result in the triple norm and convergence estimates in the  $L^2$ - and  $H^1$ -norm are concluded.

### Continuity Estimate

The error coming from approximating the infinite dimensional function space by a finite dimensional space  $X^r$  is considered. Therefore, the bilinear form  $a_h^{DCR}(\cdot, \cdot)$  is estimated for an ansatz function  $u^E - i^r(u^E)$  and a test function  $v_h$ . Thereby,  $i^r$  is the interpolator of order  $r$  introduced in Section 2.5.

#### Lemma 3.5

Let  $u \in H^{r+1}(\Gamma)$  and  $v_h \in X^r$ . Then, the following estimate holds

$$|a_k^{DCR}(u^E - i^r u^E, v_h)| \lesssim h^r \|u\|_{r+1, \Gamma} \|v_h\|_{DCR, k}.$$

#### Proof.

To shorten the following formulas  $\psi$  is set to  $\psi = u^E - i^r u^E$ . Then, it follows:

$$\begin{aligned} |a_k^{DCR}(\psi, v_h)| &\leq \left| \varepsilon \left\langle \nabla_{\Gamma_h^k} \psi, \nabla_{\Gamma_h^k} v_h \right\rangle_{\Gamma_h^k} \right| + \left| \left\langle \mathbf{w}^E \cdot \nabla_{\Gamma_h^k} \psi, v_h \right\rangle_{\Gamma_h^k} \right| + \left| \left\langle \sigma^E \psi, v_h \right\rangle_{\Gamma_h^k} \right| \\ &=: T_1 + T_2 + T_3. \end{aligned}$$

Now, the error is evaluated term by term. For the diffusion term  $T_1$  one gets:

$$T_1 = \left| \varepsilon \left\langle \nabla_{\Gamma_h^k} \psi, \nabla_{\Gamma_h^k} v_h \right\rangle_{\Gamma_h^k} \right| \leq \varepsilon |\psi|_{1, \Gamma_h^k} |v_h|_{1, \Gamma_h^k},$$

the convection term  $T_2$  leads to:

$$T_2 = \left| \left\langle \mathbf{w}^E \cdot \nabla_{\Gamma_h^k} \psi, v_h \right\rangle_{\Gamma_h^k} \right| \leq \|\mathbf{w}\|_{0, \infty, \Gamma} |\psi|_{1, \Gamma_h^k} \|v_h\|_{0, \Gamma_h^k},$$

and the reaction term  $T_3$  can be bounded by:

$$T_3 = \left| \left\langle \sigma^E \psi, v_h \right\rangle_{\Gamma_h^k} \right| \leq \|\sigma\|_{0, \infty, \Gamma} \|\psi\|_{0, \Gamma_h^k} \|v_h\|_{0, \Gamma_h^k}.$$

Adding everything together, using the interpolation property of  $i^r$  presented in (2.15)

and the definition of the triple norm yields:

$$\begin{aligned}
& |a_k^{DCR}(\psi, v_h)| \\
& \leq \left( \varepsilon^{1/2} |\psi|_{1, \Gamma_h^k} + \|\mathbf{w}\|_{0, \infty, \Gamma} \sigma_0^{-1/2} |\psi|_{1, \Gamma_h^k} + \|\sigma\|_{0, \infty, \Gamma} \sigma_0^{-1/2} \|\psi\|_{0, \Gamma_h^k} \right) \|v_h\|_{DCR, k} \\
& \lesssim h^r \|u\|_{r+1, \Gamma} \|v_h\|_{DCR, k}.
\end{aligned}$$

□

### Notice 3.1.1

By partial integration of the convection term the derivative can be moved from the ansatz to the test function in the proof of Lemma 3.5. This leads to a higher interpolation order for the ansatz function, but also to a  $H^1$ -semi norm of the test function. To bound the term against the triple norm of the test function the constant including the factor  $\varepsilon^{-1/2}$  is introduced and the estimation is no longer semi-robust. In brief, a semi-robust estimation of the interpolation error is obtained at the expense of one order for the continuity error of the convection term.

### Consistency Error

Due to the approximation of  $\Gamma$  by a non-smooth discrete surface  $\Gamma_h^k$  the integration domains and the surface operators differ in the continuous and the discrete setting. This introduces a geometric error, which is independent of the finite element space  $X^r$ . It only depends on the degree  $k$  of the Lagrange interpolation used to define  $\Gamma_h^k$ . Using the estimates obtained in Section 2.4 the following consistency result can be given for a solution  $u$  of the weak diffusion-convection-reaction problem 3.1:

### Lemma 3.6

For  $u \in V = H^1(\Gamma)$  being a solution of Problem 3.1, it holds for all  $v_h \in X^r$ :

$$|f_k^{DCR}(v_h) - a_k^{DCR}(u^E, v_h)| \lesssim (\|u\|_{1, \Gamma} + \|f\|_{0, \Gamma}) h^{k+1} \|v_h\|_{DCR, k}.$$

### Proof.

Assume an arbitrary  $v_h \in X^r$ . To estimate  $|f_k^{DCR}(v_h) - a_k^{DCR}(u^E, v_h)|$  the lifting operator defined in (2.5) is used. Because  $u$  is a solution of Problem 3.1 it follows  $a^{DCR}(u, v_h^L) - f^{DCR}(v_h^L) = 0$  and hence:

$$\begin{aligned}
& |f_k^{DCR}(v_h) - a_k^{DCR}(u^E, v_h)| \\
& = |f_k^{DCR}(v_h) - a_k^{DCR}(u^E, v_h) + (a^{DCR}(u, v_h^L) - f^{DCR}(v_h^L))| \\
& \leq |f_k^{DCR}(v_h) - f^{DCR}(v_h^L)| + |a_k^{DCR}(u^E, v_h) - a^{DCR}(u, v_h^L)|.
\end{aligned}$$

First, the terms coming from the bilinear form are estimated:

$$\begin{aligned}
|a_k^{DCR}(u^E, v_h) - a^{DCR}(u, v_h^L)| &\leq \varepsilon \left| \left\langle \nabla_{\Gamma_h^k} u^E, \nabla_{\Gamma_h^k} v_h \right\rangle_{\Gamma_h^k} - \left\langle \nabla_{\Gamma} u, \nabla_{\Gamma} v_h^L \right\rangle_{\Gamma} \right| \\
&\quad + \left| \left\langle \mathbf{w}^E \cdot \nabla_{\Gamma_h^k} u^E, v_h \right\rangle_{\Gamma_h^k} - \left\langle \mathbf{w} \cdot \nabla_{\Gamma} u, v_h^L \right\rangle_{\Gamma} \right| \\
&\quad + \left| \left\langle \sigma^E u^E, v_h \right\rangle_{\Gamma_h^k} - \left\langle \sigma u, v_h^L \right\rangle_{\Gamma} \right| \\
&=: T_1 + T_2 + T_3.
\end{aligned}$$

Using the integral transformation formula (2.17) and the Lemma 2.12 the term  $T_1$  is estimated by:

$$\begin{aligned}
T_1 &= \varepsilon \left| \left\langle \nabla_{\Gamma_h^k} u^E, \nabla_{\Gamma_h^k} v_h \right\rangle_{\Gamma_h^k} - \left\langle \nabla_{\Gamma} u, \nabla_{\Gamma} v_h^L \right\rangle_{\Gamma} \right| \\
&= \varepsilon \left| \left\langle \left( P_h^k - A_h^k \right) \nabla_{\Gamma_h^k} u^E, \nabla_{\Gamma_h^k} v_h \right\rangle_{\Gamma_h^k} \right| \\
&\leq \text{ess sup}_{\Gamma_h^k} \{ P_h^k - A_h^k \} \varepsilon \| \nabla_{\Gamma_h^k} u^E \|_{0, \Gamma_h^k} \| \nabla_{\Gamma_h^k} v_h \|_{0, \Gamma_h^k} \\
&\lesssim h^{k+1} \varepsilon |u^E|_{1, \Gamma_h^k} |v_h|_{1, \Gamma_h^k}.
\end{aligned}$$

The term  $T_2$  is evaluated using the transformation formula (2.18) and Lemma 2.12:

$$\begin{aligned}
T_2 &= \left| \left\langle \mathbf{w}^E \cdot \nabla_{\Gamma_h^k} u^E, v_h \right\rangle_{\Gamma_h^k} - \left\langle \mathbf{w} \cdot \nabla_{\Gamma} u, v_h^L \right\rangle_{\Gamma} \right| \\
&= \left| \left\langle \left( P_h^k - B_h^k \right) \mathbf{w}^E \cdot \nabla_{\Gamma_h^k} u^E, v_h \right\rangle_{\Gamma_h^k} \right| \\
&\leq \text{ess sup}_{\Gamma_h^k} \{ P_h^k - B_h^k \} \| \mathbf{w}^E \|_{0, \infty, \Gamma_h^k} \| v_h \|_{0, \Gamma_h^k} \| \nabla_{\Gamma_h^k} u^E \|_{0, \Gamma_h^k} \\
&\lesssim h^{k+1} \| \mathbf{w} \|_{0, \infty, \Gamma} |u^E|_{1, \Gamma_h^k} \| v_h \|_{0, \Gamma_h^k}.
\end{aligned}$$

The last term  $T_3$  is evaluated by using the transformation formula (2.15) and Lemma 2.11:

$$\begin{aligned}
T_3 &= \left| \left\langle \sigma^E u^E, v_h \right\rangle_{\Gamma_h^k} - \left\langle \sigma u, v_h^L \right\rangle_{\Gamma} \right| \\
&\leq \left| \left\langle \left( 1 - \mu_h^k \right) \sigma^E u^E, v_h \right\rangle_{\Gamma_h^k} \right| \\
&\leq \| 1 - \mu_h^k \|_{0, \infty, \Gamma_h^k} \| \sigma \|_{0, \infty, \Gamma} \| u^E \|_{0, \Gamma_h^k} \| v_h \|_{0, \Gamma_h^k} \\
&\lesssim h^{k+1} \| \sigma \|_{0, \infty, \Gamma_h^k} \| u^E \|_{0, \Gamma_h^k} \| v_h \|_{0, \Gamma_h^k}.
\end{aligned}$$

Summing up and using the norm equivalences (2.19)–(2.20) results in:

$$\begin{aligned}
|a_k^{DCR}(u^E, v_h) - a^{DCR}(u, v_h^L)| &\lesssim h^{k+1} \left( \varepsilon^{1/2} + \sigma_0^{-1/2} (\| \mathbf{w} \|_{0, \infty, \Gamma} + \| \sigma \|_{0, \infty, \Gamma}) \right) \| u \|_{1, \Gamma} \| v_h \|_{DCR, k} \\
&\lesssim h^{k+1} \| u \|_{1, \Gamma} \| v_h \|_{DCR, k}.
\end{aligned}$$

The error made by approximating the right hand side can be obtained by using the transformation formula (2.15) and Lemma 2.11 again:

$$\begin{aligned}
|f_k^{DCR}(v_h) - f^{DCR}(v_h^L)| &= \left| \langle f^E, v_h \rangle_{\Gamma_h^k} - \langle f, v_h^L \rangle_{\Gamma} \right| \\
&= \left| \left\langle \left(1 - \mu_h^k\right) f^E, v_h \right\rangle_{\Gamma_h^k} \right| \\
&\lesssim h^{k+1} \|f^E\|_{0, \Gamma_h^k} \|v_h\|_{0, \Gamma_h^k} \\
&\lesssim h^{k+1} \|f\|_{0, \Gamma} \|v_h\|_{DCR, k}.
\end{aligned}$$

Combining these results proves the lemma.  $\square$

### Convergence Error in $\|\cdot\|_{DCR, k}$

After the estimate of the continuity and the consistency error the total error is evaluated in the triple norm.

#### Theorem 3.7

Let  $u \in H^{r+1}(\Gamma)$  solve Problem 3.1 and  $u_h \in X^r$  solve Problem 3.2. Then, it can be concluded that:

$$\| \|u^E - u_h\| \|_{DCR, k} \lesssim h^r \|u\|_{r+1, \Gamma} + h^{k+1} \|u\|_{1, \Gamma} + h^{k+1} \|f\|_{0, \Gamma}.$$

#### Proof.

In a first step the error is split up using the interpolator  $i^r$  and a triangle inequality:

$$\| \|u^E - u_h\| \|_{DCR, k} \leq \| \|u^E - i^r(u^E)\| \|_{DCR, k} + \| \|i^r(u^E) - u_h\| \|_{DCR, k}.$$

The first summand is estimated using the interpolation properties of  $i^r$ , which are given in Lemma 2.15:

$$\begin{aligned}
\| \|u^E - i^r(u^E)\| \|_{DCR, k}^2 &= \varepsilon \|u^E - i^r(u^E)\|_{1, \Gamma_h^k}^2 + \sigma_0 \|u^E - i^r(u^E)\|_{0, \Gamma_h^k}^2 \\
&\lesssim (\varepsilon h^{2r} + \sigma_0 h^{2r+2}) \|u\|_{r+1, \Gamma}^2 \lesssim h^{2r} \|u\|_{r+1, \Gamma}^2.
\end{aligned}$$

For the second term  $\psi := i^r(u^E) - u_h$  is introduced. Obviously,  $\psi \in X^r$ . The coercivity of  $a_k^{DCR}(\cdot, \cdot)$  in  $X^r$ , compare Lemma 3.3, is used:

$$\begin{aligned}
\| \|i^r(u^E) - u_h\| \|_{DCR, k}^2 &\lesssim a_k^{DCR}(i^r(u^E) - u_h, \psi) \\
&= a_k^{DCR}(i^r(u^E) - u^E, \psi) + a_k^{DCR}(u^E - u_h, \psi).
\end{aligned}$$

The different terms of the sum can be bounded using Lemma 3.5 and Lemma 3.6:

$$|a_k^{DCR}(i^r(u^E) - u^E, \psi)| \lesssim h^r \|u\|_{r+1, \Gamma} \| \psi \|_{DCR, k}$$

and

$$\begin{aligned} |a_k^{DCR}(u^E - u_h, \psi)| &= |a_k^{DCR}(u^E, \psi) - f_k^{DCR}(\psi)| \\ &\lesssim h^{k+1} (\|u\|_{1,\Gamma} + \|f\|_{0,\Gamma}) \|\psi\|_{DCR,k}. \end{aligned}$$

Putting this together concludes the proof.  $\square$

The standard Galerkin surface finite method for diffusion-convection-reaction equations provides a semi-robust convergence of order  $k + 1$  with respect to the geometric approximation but only of order  $r$  with respect to the finite element approximation of the function space. Having a closer look on the estimate in Theorem 3.7, the optimality of the single estimation terms can be discussed. The geometric error is of overall order  $k + 1$  and therefore optimal. This is not the case for the finite element error. For the diffusion term the convergence of order  $r$  is optimal. The resulting error term is scaled with  $\varepsilon^{1/2}$  and thus vanishing in the convection dominated case. The reaction term also provides the expectable convergence of order  $r + 1$ . For the convection term a convergence of order  $r + 1$  would be expected, but one order is lost to obtain a semi-robust estimate, compare Notice 3.1.1. In Chapter 4 two different stabilization techniques, which shall overcome this drawback, are introduced.

### Convergence Error in the $L^2$ - and $H^1$ -norm

The estimate of  $u^E - u_h$  in the discrete triple norm enables also evaluations in the  $L^2$ - and the  $H^1$ -norm for diffusion-convection-reaction problems.

#### Corollar 3.8

Let  $u \in H^{r+1}(\Gamma)$  solve Problem 3.1 and  $u_h \in X^r$  solve Problem 3.2. It can be concluded that:

$$\|u - u_h^L\|_{0,\Gamma} \lesssim (h^r + h^{k+1}) \|u\|_{r+1,\Gamma} + h^{k+1} \|f\|_{0,\Gamma}$$

and

$$|u - u_h^L|_{1,\Gamma} \lesssim (h^r + h^{k+1}) \varepsilon^{-1/2} \|u\|_{r+1,\Gamma} + h^{k+1} \varepsilon^{-1/2} \|f\|_{0,\Gamma}.$$

#### Proof.

From the definition of the triple norm:

$$\|v_h\|_{DCR,k} = \left( \varepsilon |v_h|_{1,\Gamma_h^k}^2 + \sigma_0 \|v_h\|_{0,\Gamma_h^k}^2 \right)^{1/2}$$

it can be obtained that:

$$\|v_h\|_{0,\Gamma_h^k} \leq \sigma_0^{-1/2} \|v_h\|_{DCR,k} \quad \text{and} \quad |v_h|_{1,\Gamma_h^k} \leq \varepsilon^{-1/2} \|v_h\|_{DCR,k}.$$



Together with Theorem 3.7 and the norm equivalences (2.19)–(2.20) the postulated result can be concluded.  $\square$

**Notice 3.1.2**

*It is known for bulk equations that an improved error estimate in the  $L^2$ -norm can be expected for regular solution functions. A technique well known as Aubin-Nitsche duality method can be used to prove this higher order convergence. The same arguments can be transferred to surface equations as well.*

## 3.2 Diffusion Convection Equation

In this section the diffusion-convection equation is studied. Hence, the equation

$$-\varepsilon\Delta_\Gamma u + \mathbf{w} \cdot \nabla_\Gamma u + \sigma u = f \quad \text{on } \Gamma \quad (3.10)$$

on a closed surface  $\Gamma$  under the assumption

$$\sigma - \frac{1}{2}\nabla_\Gamma \cdot \mathbf{w} = 0 \quad \text{on } \Gamma \quad (3.11)$$

is considered.

Due to  $c$  being assumed to be non-negative and  $\sigma = \nabla_\Gamma \cdot \mathbf{w} + c$ , from assumption (3.11) it follows  $\nabla_\Gamma \cdot \mathbf{w} \leq 0$ . Integrating  $\nabla_\Gamma \cdot \mathbf{w}$  over  $\Gamma$  and using the formula (1.4) for partial integration lead to:

$$\int_\Gamma \nabla_\Gamma \cdot \mathbf{w} ds = - \int_\Gamma \mathbf{w} \cdot \nabla_\Gamma 1 ds + \int_\Gamma \mathbf{w} \cdot \mathbf{n} \mathcal{H} ds = 0.$$

Thereby, the condition  $\mathbf{w} \cdot \mathbf{n} = 0$  was used. Hence, assumption (3.11) and  $\mathbf{w} \cdot \mathbf{n} = 0$  result in:

$$\nabla_\Gamma \cdot \mathbf{w} = 0 \quad \text{on } \Gamma \quad (3.12)$$

and thus  $\sigma = 0$ . The diffusion-convection problem can be rewritten as:

$$-\varepsilon\Delta_\Gamma u + \mathbf{w} \cdot \nabla_\Gamma u = f \quad \text{on } \Gamma. \quad (3.13)$$

This equation under condition (3.12) does not provide a unique solution. If  $u$  is a solution of equation (3.13), then also  $u + \tilde{u}$  for every constant  $\tilde{u} \in \mathbb{R}$  is a solution. An additional condition is needed to fix one solution. Here, we use:

$$\langle u, 1 \rangle_\Gamma = M \quad \text{for a given } M \in \mathbb{R}. \quad (3.14)$$

Further, a solvability condition on the right hand side of (3.13) arises. Taking the integral of  $f$  over  $\Gamma$ , replacing  $f$  by the left hand side of the equation and partial integration using formulas (1.3) and (1.4) provide:

$$\begin{aligned} \int_{\Gamma} f ds &= \int_{\Gamma} -\varepsilon \Delta_{\Gamma} u ds + \int_{\Gamma} \mathbf{w} \cdot \nabla_{\Gamma} u ds \\ &= \int_{\Gamma} \varepsilon \nabla_{\Gamma} u \cdot \nabla_{\Gamma} 1 ds - \int_{\Gamma} u \nabla_{\Gamma} \cdot \mathbf{w} ds + \int_{\Gamma} u \mathbf{w} \cdot \mathbf{n} \mathcal{H} ds = 0. \end{aligned}$$

In the following the solvability condition  $\langle f, 1 \rangle_{\Gamma} = 0$  is assumed to be fulfilled. The derivation of the weak and the discretized problem basically follow the same ideas as in the previous section. The same holds true for big parts of the error analysis. These techniques are only referred to and not presented again. The main issue is the missing  $L^2$ -control and the changes required to overcome this drawback in the numerical analysis.

### 3.2.1 Problem Formulation

The weak formulation is obtained following the same steps as in Section 3.1. Only the additional condition (3.14) has to be incorporated into the ansatz and the test space:

**Problem 3.3 (*Weak Diffusion-Convection Problem*)**

Find  $u \in V = H^1(\Gamma)$  with  $\langle u, 1 \rangle_{\Gamma} = M$  such that for all  $v \in V_0 = \{v \in H^1(\Gamma) \mid \langle v, 1 \rangle_{\Gamma} = 0\}$

$$a^{DC}(u, v) = f^{DC}(v)$$

with

$$\begin{aligned} a^{DC}(u, v) &= \varepsilon \langle \nabla_{\Gamma} u, \nabla_{\Gamma} v \rangle_{\Gamma} + \langle \mathbf{w} \cdot \nabla_{\Gamma} u, v \rangle_{\Gamma}, \\ f^{DC}(v) &= \langle f, v \rangle_{\Gamma}. \end{aligned}$$

According to the bilinear form  $a^{DC}(\cdot, \cdot)$  the triple norm for diffusion-convection equations is set to:

$$\| \| v \| \|_{DC} := \varepsilon^{1/2} | \cdot |_{1, \Gamma}.$$

The missing reaction term in the problem formulation leads to the missing  $L^2$ -control in the corresponding triple norm.  $\| \cdot \|_{DC}$  is only a semi-norm in  $H^1(\Gamma)$  but due to the Poincare inequality (Theorem 1.3) it is a norm in  $V_0$ .

To show unique solvability of Problem 3.3 the coercivity of  $a^{DC}(\cdot, \cdot)$  in  $V_0$  is proven:

**Lemma 3.9**

The bilinear form  $a^{DC}(\cdot, \cdot)$  is coercive in  $V_0$ :

$$a^{DC}(v, v) = \|v\|_{DC}^2 \quad \forall v \in V_0. \quad (3.15)$$

**Proof.**

Following the ideas used in the proof of Theorem 3.1 the bilinear form can be directly estimated by:

$$a^{DC}(v, v) = \varepsilon |v|_{1,\Gamma}^2 = \|v\|_{DC}^2.$$

□

The proof of unique solvability of Problem 3.3 is done in two steps. At first, solvability is proven and afterwards the uniqueness of the solution is shown. To conclude solvability we recognize that :

$$\{u \in H^1(\Gamma) \mid \langle u, 1 \rangle_\Gamma = M\} \neq \emptyset$$

because the constant  $\tilde{u} = \frac{1}{|\Gamma|}M$  is element of this set. Using that  $a^{DC}(\tilde{u}, v) = 0$  for all  $v \in V_0$ , Problem 3.3 can be reformulated in the equivalent problem:

**Problem 3.4**

Find  $u - \tilde{u} = u_0 \in V_0$  such that for all  $v \in V_0$

$$a^{DC}(u_0, v) = f^{DC}(v).$$

Because  $a^{DC}(\cdot, \cdot)$  is bilinear, continuous and coercive in  $V_0$ , and  $f^{DC}(\cdot)$  is linear and continuous,  $u_0$  is uniquely defined due to the Lax-Milgram theorem. Hence,  $u = u_0 + \tilde{u}$  is a solution of Problem 3.3.

Uniqueness can be seen by taking two solutions  $u_1$  and  $u_2$  of Problem 3.3. Then,  $u_1 - u_2 \in V_0$  and solves Problem 3.4 with a homogeneous right hand side. Because Problem 3.4 is uniquely solvable and  $u_0 = 0$  is a valid solution, it follows  $u_1 = u_2$ .

**Lemma 3.10**

Problem 3.3 is uniquely solvable.

**3.2.2 Discretized Formulation**

To define a discrete formulation of Problem 3.3, the same setting as in Section 3.1 is used. That means a surface approximation  $\Gamma_h^k$  of order  $k$  and an approximation of the solution space by  $X^r$  of order  $r$  are considered.

To prove unique solvability for the discretized diffusion-convection-reaction problem partial integration of the convection term is used, compare Theorem 3.3. This introduces integrals over the element edges. To obtain coercivity of the problem

a condition on the element size is required. Because of the missing  $L^2$ -control this condition would not be independent of  $\varepsilon$  in case of diffusion-convection equations. More precisely, a condition of kind  $h \lesssim \varepsilon$  occurs, which is impractical.

To overcome this problem, the following equality in the continuous setting is utilized, compare (1.4):

$$\langle \mathbf{w} \cdot \nabla_{\Gamma} u, v \rangle_{\Gamma} = - \langle \mathbf{w} \cdot \nabla_{\Gamma} v, u \rangle_{\Gamma} - \langle \nabla_{\Gamma} \cdot \mathbf{w}, uv \rangle_{\Gamma} + \langle u \mathcal{H} v \mathbf{w} \cdot \mathbf{n} \rangle_{\Gamma}.$$

Making use of the assumptions  $\mathbf{w} \cdot \mathbf{n} = 0$  and  $\nabla_{\Gamma} \cdot \mathbf{w} = 0$  on  $\Gamma$  the convection term can be rewritten as follows:

$$\langle \mathbf{w} \cdot \nabla_{\Gamma} u, v \rangle_{\Gamma} = \frac{1}{2} (\langle \mathbf{w} \cdot \nabla_{\Gamma} u, v \rangle_{\Gamma} - \langle \mathbf{w} \cdot \nabla_{\Gamma} v, u \rangle_{\Gamma}). \quad (3.16)$$

The discretized problem is then obtained using this skew-symmetric formulation of the convection term.

**Problem 3.5 (*Discretized Diffusion-Convection Problem*)**

Find  $u_h \in X^r$  with  $\langle u_h, 1 \rangle_{\Gamma_h^k} = M$  such that  
for all  $v_h \in X_0^r = \{v_h \in X^r \mid \langle v_h, 1 \rangle_{\Gamma_h^k} = 0\}$

$$a_k^{DC}(u_h, v_h) = f_k^{DC}(v_h)$$

with

$$\begin{aligned} a_k^{DC}(u_h, v_h) &= \varepsilon \left\langle \nabla_{\Gamma_h^k} u_h, \nabla_{\Gamma_h^k} v_h \right\rangle_{\Gamma_h^k} + \frac{1}{2} \left\langle \mathbf{w}^E \cdot \nabla_{\Gamma_h^k} u_h, v_h \right\rangle_{\Gamma_h^k} \\ &\quad - \frac{1}{2} \left\langle \mathbf{w}^E \cdot \nabla_{\Gamma_h^k} v_h, u_h \right\rangle_{\Gamma_h^k}, \\ f_k^{DC}(v_h) &= \langle f^E, v_h \rangle_{\Gamma_h^k}. \end{aligned}$$

According to the bilinear form  $a_k^{DC}(\cdot)$  the following mesh dependent norm:

$$\| \| v_h \| \|_{DC,h} = \varepsilon^{1/2} |v_h|_{1,\Gamma_h^k}$$

is introduced. As  $\| \cdot \|_{DC}$  in the continuous case,  $\| \cdot \|_{DC,k}$  is only a semi-norm on  $X^r$  but a norm on  $X_0^r$ . Hence, coercivity in  $X_0^r$  and unique solvability of the Problem 3.5 can be concluded following the ideas from the last section.

**Lemma 3.11**

The bilinear form  $a_k^{DC}(\cdot, \cdot)$  is coercive in  $X_0^r$ :

$$a_k^{DC}(v_h, v_h) = \| \| v_h \| \|_{DC,k}^2 \quad \forall v_h \in X_0^r.$$

**Proof.**

The estimation of the bilinear form follows directly by inserting  $v_h$  as ansatz and test function:

$$\begin{aligned} a_h(v_h, v_h) &= \varepsilon \left\langle \nabla_{\Gamma_h^k} v_h, \nabla_{\Gamma_h^k} v_h \right\rangle_{\Gamma_h^k} + \frac{1}{2} \left( \left\langle \mathbf{w}^E \cdot \nabla_{\Gamma_h^k} v_h, v_h \right\rangle_{\Gamma_h^k} - \left\langle \mathbf{w}^E \cdot \nabla_{\Gamma_h^k} v_h, v_h \right\rangle_{\Gamma_h^k} \right) \\ &= \varepsilon |v_h|_{1, \Gamma_h^k} = \|v_h\|_{DC, k}^2. \end{aligned}$$

Thereby, the Poincare type inequality from Theorem 1.3, which is valid for all  $v_h \in X_0^r$ , is used. This provides the coercivity of  $a_k^{DC}(\cdot, \cdot)$  in  $X_0^r$ .  $\square$

To prove uniqueness and existence of the solution of Problem 3.5, the same ansatz as in the continuous case is utilized. First, it is shown that:

$$\{v_h \in X^r \mid \langle v_h, 1 \rangle_{\Gamma_h^k} = M\} \neq \emptyset$$

by stating the element  $\tilde{u}_h = \frac{1}{|\Gamma_h^k|} M$ . Then, an equivalent formulation of Problem 3.5 is given by:

**Problem 3.6**

Find  $u_h - \tilde{u}_h = u_{h,0} \in X_0^r$  such that for all  $v_h \in X_0^r$

$$a_k^{DC}(u_{h,0}, v_h) = f_k^{DC}(v_h) - a_k^{DC}(\tilde{u}_h, v_h).$$

The unique solvability of this problem is concluded from the coercivity of  $a_k^{DC}(\cdot, \cdot)$  and the Lax-Milgram theorem. Hereby, linearity of the right hand side and bilinearity  $a_k^{DC}(\cdot, \cdot)$  are obvious. Continuity is given due to  $\mathbf{w} \in W^{1,\infty}(\Gamma)$ . Hence,  $u_h = u_{h,0} + \tilde{u}_h$  is a solution of Problem 3.5.

The uniqueness of the solution can be seen by assuming the existence of two solutions  $u_{h,1}$  and  $u_{h,2}$ . Their difference  $u_{h,1} - u_{h,2}$  is a solution of Problem 3.6 with a homogeneous right hand side. Due to  $u_{h,1} - u_{h,2} = 0$  is the unique solution,  $u_{h,1} = u_{h,2}$  can be concluded. This shows:

**Lemma 3.12**

Problem 3.5 is uniquely solvable.

**3.2.3 Error Estimates**

Whereas in the analysis of the diffusion-convection-reaction problem a semi-robust error estimate can be obtained, the missing  $L^2$ -control inhibits this for the diffusion-convection problem. Therefore, estimates with an optimal order of convergence are presented but they still depend on the diffusion parameter  $\varepsilon$  in an inconvenient manner. Unfortunately, this drawback is natural for diffusion-convection equations and no semi-robust estimates can be obtained at all.

The analysis is presented following the same schedule as in Section 3.1.3 to achieve a better comparability. After studying the error coming from the approximation of the function space and the one occurring due to geometric approximations separately, the main result of this section is an estimate of the convergence error in the mesh dependent triple norm.

The triple norm of the diffusion-convection problem provides no  $L^2$ -control and as a result

$$\| \| \| u^E - u_h \| \|_{DC,k} = \| \| \| (u_0 + \tilde{u})^E - (u_{h,0} - \tilde{u}_h) \| \|_{DC,k} = \| \| \| u_0^E - u_{h,0} \| \|_{DC,k}.$$

Thereby, the notations introduced in Sections 3.2.1 and 3.2.2 are used. In particular,  $\tilde{u}$  and  $\tilde{u}_h$  are constants and  $u_0$  and  $u_{h,0}$  solve the adapted Problems 3.4 and 3.6, respectively. This together with the obtained coercivity in  $V_0$  and  $X_0^r$  motivates to study Problems 3.4 and 3.6 instead of Problems 3.3 and 3.5.

### Continuity Estimate

In the case of diffusion-convection-reaction equations it has already been stated that by partial integration of the convection term a higher order can be obtained, compare Notice 3.1.1. This was renounced to get semi robust estimations. For diffusion-convection equations semi-robust estimations cannot be achieved and thus partial integration of the convection term is used.

#### Lemma 3.13

For  $u \in H^{r+1}(\Gamma)$  and  $v_h \in X_0^r$ , it can be shown that

$$|a_k^{DC}(u^E - i^r u^E, v_h)| \lesssim h^r (\varepsilon^{1/2} + h\varepsilon^{-1/2}) \|u\|_{r+1,\Gamma} \|v_h\|_{DC,k}.$$

#### Proof.

As in the proof of Theorem 3.5,  $\psi$  is defined as  $\psi := u^E - i^r u^E$ . Inserting this leads to:

$$\begin{aligned} |a_k^{DC}(\psi, v_h)| &\leq \left| \varepsilon \left\langle \nabla_{\Gamma_h^k} \psi, \nabla_{\Gamma_h^k} v_h \right\rangle_{\Gamma_h^k} \right| + \frac{1}{2} \left| \left\langle \mathbf{w}^E \cdot \nabla_{\Gamma_h^k} \psi, v_h \right\rangle_{\Gamma_h^k} \right| \\ &\quad + \frac{1}{2} \left| \left\langle \mathbf{w}^E \cdot \nabla_{\Gamma_h^k} v_h, \psi \right\rangle_{\Gamma_h^k} \right| \\ &\lesssim h^r \varepsilon^{1/2} \|u\|_{r+1,\Gamma} \|v_h\|_{DC,k} + T_2 + T_3, \end{aligned}$$

where the diffusion term is estimated as in Lemma 3.5.

$T_3$  can be directly evaluated and together with the interpolation properties of  $i^r$  provides an order of  $h^{r+1}$ :

$$\begin{aligned} T_3 &= \left| \left\langle \mathbf{w}^E \cdot \nabla_{\Gamma_h^k} v_h, \psi \right\rangle_{\Gamma_h^k} \right| \leq \|\mathbf{w}\|_{0,\infty,\Gamma} \|\psi\|_{0,\Gamma_h^k} |v_h|_{1,\Gamma_h^k} \\ &\lesssim \varepsilon^{-1/2} h^{r+1} \|u\|_{r+1,\Gamma} \|v_h\|_{DC,k}. \end{aligned}$$

To obtain an error of the same order for  $T_2$ , the gradient has to be moved from  $\psi$  to  $v_h$  by partial integration. This introduces boundary terms over the element edges:

$$\begin{aligned} T_2 &= \left| \left\langle \mathbf{w}^E \cdot \nabla_{\Gamma_h^k} \psi, v_h \right\rangle_{\Gamma_h^k} \right| \\ &\leq \left| \left\langle \mathbf{w}^E \cdot \nabla_{\Gamma_h^k} v_h, \psi \right\rangle_{\Gamma_h^k} \right| + \left| \sum_{K \in \mathcal{T}_h^k} \int_{\partial K} \mathbf{w}^E \cdot \boldsymbol{\nu}_h^k \psi v_h d\mathbf{b}_h^k \right| \\ &= T_3 + \sum_{E \in \mathcal{E}_h^k} \left| \int_E P\mathbf{w}^E \cdot (\boldsymbol{\nu}^+ - \boldsymbol{\nu}^-) \psi v_h d\mathbf{b}_h^k \right|, \end{aligned}$$

where it was used that  $P\mathbf{w}^E = \mathbf{w}^E$  and  $\boldsymbol{\nu}^+$  and  $\boldsymbol{\nu}^-$  name the co-normals belonging to the two elements connected to the edge  $E$ . Lemmas 2.9 and 2.6 together with the trace inequality (Lemma 2.13) lead to:

$$\begin{aligned} T_2 &\lesssim T_3 + \sum_{E \in \mathcal{E}_h^k} h^{2k} \|\mathbf{w}\|_{0,\infty,\Gamma} \|\psi\|_{0,E} \|v_h\|_{0,E} \\ &\lesssim T_3 + h^{2k} \sum_{K \in \mathcal{T}_h^k} (h_K^{-1} \|\psi\|_{0,K}^2 + h_K |\psi|_{1,K}^2)^{1/2} (h_K^{-1} \|v_h\|_{0,K}^2 + h_K |v_h|_{1,K}^2)^{1/2}. \end{aligned}$$

Using the Poincare inequality (Lemma 1.3) and  $k \geq 1$  yields:

$$\begin{aligned} T_2 &\lesssim T_3 + h^{2k} \sum_{K \in \mathcal{T}_h^k} h_K^{r+1/2} \|u\|_{r+1,K} (h_K^{-1} \|v_h\|_{0,K}^2 + h_K |v_h|_{1,K}^2)^{1/2} \\ &\lesssim T_3 + h^{2k+r} \|u\|_{r+1,\Gamma} (\|v_h\|_{0,\Gamma} + h |v_h|_{1,\Gamma}) \\ &\lesssim \varepsilon^{-1/2} h^{r+1} \|u\|_{r+1,\Gamma} \|v_h\|_{DC,k}. \end{aligned}$$

Adding up the gained estimates yields the postulated result.  $\square$

### Consistency Error

The proof of the geometric error follows the ideas of the proof of Theorem 3.6. Only the formulation of the convection term differs from the one referred to in Theorem 3.6. The convection term of the weak formulation is handled by partial integration to mimic the skew-symmetry of the discretized formulation, see equation (3.16). The same consistency order as for the diffusion-convection-reaction problem is obtained. That is expected, because this error reflects the geometric approximations and the same discrete surface  $\Gamma_h^k$  is used in both cases.

**Lemma 3.14**

For  $u_0 \in V_0$  being a solution of Problem 3.4 and  $v_h \in X_0^r$ , it holds:

$$|f_k^{DC}(v_h) - a_k^{DC}(u_0^E, v_h)| \lesssim h^{k+1} \varepsilon^{-1/2} (\|u\|_{1,\Gamma} + \|f\|_{0,\Gamma}) \|v_h\|_{DC,k}.$$

**Proof.**

Following the proof of Theorem 3.6 only  $\left| \langle \mathbf{w}^E \cdot \nabla_{\Gamma_h^k} v_h, u^E \rangle_{\Gamma_h^k} - \langle \mathbf{w} \cdot \nabla_{\Gamma} v_h^L, u \rangle_{\Gamma} \right|$  has to be evaluated. The estimates of all other terms can be taken directly from Theorem 3.6. This term is handled using (2.18), Lemma 2.12 and the norm equivalences (2.19)–(2.20):

$$\begin{aligned} & \left| \langle \mathbf{w}^E \cdot \nabla_{\Gamma_h^k} v_h, u^E \rangle_{\Gamma_h^k} - \langle \mathbf{w} \cdot \nabla_{\Gamma} v_h^L, u \rangle_{\Gamma} \right| \\ &= \left| \langle (P_h^k - B_h^k) (\mathbf{w}^E \cdot \nabla_{\Gamma_h^k} v_h, u^E) \rangle_{\Gamma_h^k} \right| \\ &\leq \text{ess sup}_{\Gamma_h^k} \{P_h^k - B_h^k\} \|\mathbf{w}^E\|_{0,\infty,\Gamma_h^k} \|u^E\|_{0,\Gamma_h^k} \|\nabla_{\Gamma_h^k} v_h\|_{0,\Gamma_h^k} \\ &\lesssim h^{k+1} \varepsilon^{-1/2} \|u\|_{0,\Gamma} \|v_h\|_{DC,k}. \end{aligned}$$

Combining this with the known estimates and utilizing the Poincare inequality (Theorem 1.3) proves the lemma.  $\square$

**Convergence Error in  $\|\cdot\|_{DC,k}$** 

As in the case of diffusion-convection-reaction equations from the continuity and the consistency error estimates the convergence error can be bounded. Thereby, a special treatment of the term  $i^r(u_0^E) - u_{h,0}$  is necessary. In the case of diffusion-convection-reaction equations the coercivity holds true in  $X^r$  and by definition  $i^r(u_0^E) - u_{h,0} \in X^r$ . However, for diffusion-convection equations coercivity can only be obtained in  $X_0^r$  and in general  $i^r(u_0^E) - u_{h,0} \notin X_0^r$ . A workaround is presented in the proof of the next theorem.

**Theorem 3.15**

If  $u_0 \in V_0$  solves Problem (3.4),  $u_{h,0} \in X_0^r$  solves Problem (3.6) and it is assumed that  $u_0 \in H^{r+1}(\Gamma)$ , the following holds

$$\|u_0^E - u_{h,0}\|_{DC,k} \lesssim [h^r (\varepsilon^{1/2} + h\varepsilon^{-1/2}) + h^{k+1} \varepsilon^{-1/2}] \|u_0\|_{r+1,\Gamma} + h^{k+1} \varepsilon^{-1/2} \|f\|_{0,\Gamma}.$$

**Proof.**

This proof is following the ideas presented in the proof of Theorem 3.7. Therefore,  $\chi$  is set to  $\chi := i^r(u_0^E) - u_{h,0} \in X^r$ . Unfortunately, in general  $\langle \chi, 1 \rangle_{\Gamma_h^k} \neq 0$  and hence  $\chi \notin X_0^r$ . A constant  $C \in \mathbb{R}$  is introduced such that:

$$\langle \chi + C, 1 \rangle_{\Gamma_h^k} = \langle i^r(u_0^E) + C, 1 \rangle_{\Gamma_h^k} = 0.$$



Then,  $\chi + C \in X_0^r$  and the coercivity can be utilized.

The following terms have to be estimated:

- (1)  $\| \|u_0^E - i^r(u_0^E) - C\| \|_{DC,k}$
- (2)  $a_k^{DC}(i^r(u_0^E) - u_0^E, \chi + C)$
- (3)  $a_k^{DC}(u_0^E - u_{h,0}, \chi + C) = a_k^{DC}(u_0^E, \chi + C) - f_k^{DC}(\chi + C)$
- (4)  $a_k^{DC}(C, \chi + C)$ .

Term (1) can be estimated by the interpolation properties of  $i^r$  given in Lemma 2.15:

$$\| \|u_0^E - i^r(u_0^E) - C\| \|_{DC,k}^2 = \varepsilon |u_0^E - i^r(u_0^E)|_{1,\Gamma_h^k}^2 \lesssim \varepsilon h^{2r} \|u_0\|_{r+1,\Gamma}^2.$$

The terms (2) and (3) are bounded by Lemma 3.13 and Lemma 3.14.

The last term is evaluated using  $C \in \mathbb{R}$ :

$$\begin{aligned} a_k^{DC}(C, \chi + C) &= \frac{1}{2} \left| \left\langle \mathbf{w}^E \cdot \nabla_{\Gamma_h^k}(\chi + C), C \right\rangle_{\Gamma_h^k} \right| \\ &\leq |C| \left| \left\langle \mathbf{w}^E \cdot \nabla_{\Gamma_h^k} \chi, 1 \right\rangle_{\Gamma_h^k} \right| \\ &\leq |C| \| \mathbf{w}^E \|_{0,\infty,\Gamma} |\Gamma_h^k| |\chi|_{1,\Gamma_h^k}. \end{aligned}$$

$|\Gamma_h^k|$  can be bounded by interpolation formula (2.15) and Lemma 2.12:

$$\begin{aligned} \|\Gamma\| - |\Gamma_h^k| &= |\langle 1, 1 \rangle_{\Gamma} - \langle 1, 1 \rangle_{\Gamma_h^k}| = \left| \left\langle 1, \mu_h^k - 1 \right\rangle_{\Gamma_h^k} \right| \lesssim h^{k+1} |\Gamma_h^k| \\ \Rightarrow |\Gamma_h^k| &\lesssim (1 + h^{k+1}) |\Gamma|. \end{aligned} \tag{3.17}$$

The value of  $C$  has to be estimated next. Therefore, the definition of  $C$  is recalled:

$$\langle \chi + C, 1 \rangle_{\Gamma_h^k} = 0 \Rightarrow C = \frac{\langle \chi, 1 \rangle_{\Gamma_h^k}}{|\Gamma_h^k|}.$$

To evaluate  $|\langle \chi, 1 \rangle_{\Gamma_h^k}|$  it is used that  $u_{h,0} \in X_0^r$  and  $u_0 \in V_0$ . Hence,  $\langle u_{h,0}, 1 \rangle_{\Gamma_h^k} = 0$  and  $\langle u_0, 1 \rangle_{\Gamma} = 0$ . It holds:

$$\begin{aligned} \left| \langle \chi, 1 \rangle_{\Gamma_h^k} \right| &= \left| \langle i^r(u_0^E) - u_{h,0}, 1 \rangle_{\Gamma_h^k} \right| \\ &= \left| \langle i^r(u_0^E), 1 \rangle_{\Gamma_h^k} - \langle u_0, 1 \rangle_{\Gamma} \right| \\ &\leq \left| \langle i^r(u_0^E) - u_0^E, 1 \rangle_{\Gamma_h^k} \right| + \left| \langle u_0^E, 1 - \mu_h^k \rangle_{\Gamma_h^k} \right|. \end{aligned}$$

Now, the interpolation properties of  $i^r$ , see Lemma 2.15, and Lemma 2.11 lead to:

$$\begin{aligned} |\langle \chi, 1 \rangle_{\Gamma_h^k}| &\lesssim h^{r+1} \|u_0\|_{r+1, \Gamma} \left| \Gamma_h^k \right|^{1/2} + h^{k+1} \|u_0\|_{0, \Gamma} \left| \Gamma_h^k \right|^{1/2} \\ &\lesssim \left( h^{r+1} + h^{k+1} \right) \|u_0\|_{r+1, \Gamma} \left| \Gamma_h^k \right|^{1/2} \end{aligned}$$

and it follows that:

$$|C| \lesssim \left( h^{r+1} + h^{k+1} \right) \|u_0\|_{r+1, \Gamma} \left| \Gamma_h^k \right|^{-1/2}. \quad (3.18)$$

Inserting this and the estimate of  $|\Gamma_h^k|$  into the estimation of  $|a_k^{DC}(C, \chi + C)|$  gives:

$$\begin{aligned} |a_k^{DC}(C, \chi + C)| &\lesssim \left( h^{r+1} + h^{k+1} \right) \|u_0\|_{r+1, \Gamma} \left( \left( 1 + h^{k+1} \right) |\Gamma| \right)^{1/2} |\psi|_{1, \Gamma_h^k} \\ &\lesssim \left( h^{r+1} + h^{k+1} \right) \varepsilon^{-1/2} \|u_0\|_{r+1, \Gamma} \|\psi\|_{DC, k}. \end{aligned}$$

Summing up and using  $\|\chi + C\|_{DC, k} = \|\chi\|_{DC, k}$  lead to:

$$\begin{aligned} \|u_0^E - u_{h,0}\|_{DC, k} &\lesssim h^r \varepsilon^{1/2} \|u_0\|_{r+1, \Gamma} \\ &\quad + h^r \left( \varepsilon^{1/2} + h \varepsilon^{-1/2} \right) \|u_0\|_{r+1, \Gamma} \\ &\quad + h^{k+1} \varepsilon^{-1/2} \left( \|u^E\|_{1, \Gamma} + \|f\|_{0, \Gamma} \right) \\ &\quad + \left( h^{r+1} + h^{k+1} \right) \varepsilon^{-1/2} \|u_0\|_{r+1, \Gamma}. \end{aligned}$$

Condensing these terms gives the estimate of Theorem 3.15.  $\square$

The convergence error obviously reproduces the peculiarities discussed for the interpolation error. A higher convergence error in the convection term is achieved but no semi-robustness can be expected. The lower order convergence term, coming from the diffusion term, vanishes if  $\varepsilon \rightarrow 0$  and a convergence of order  $h^{r+1} + h^{k+1}$  can be expected. But the constant of the error estimation becomes arbitrarily bad for small diffusion parameters.

### Convergence Error in the $L^2$ - and $H^1$ - norm

It has to be remembered that until now, only the error  $u_0^E - u_{h,0}$  has been studied. To get estimates for  $u^E - u_h$  it is used that  $u = u_0 + \tilde{u}$  and  $u_h = u_{h,0} + \tilde{u}_h$  with the constants  $\tilde{u}, \tilde{u}_h \in \mathbb{R}$  given in sections 3.2.1 and 3.2.2. It follows:

#### Lemma 3.16

Let  $\tilde{u} \in \mathbb{R}$  and  $\tilde{u}_h \in \mathbb{R}$  be given by  $\tilde{u} = M/|\Gamma|$  and  $\tilde{u}_h = M/|\Gamma_h^k|$ , then it holds:

$$\|\tilde{u}^E - \tilde{u}_h\|_{0, \Gamma_h^k} \lesssim h^{k+1} M.$$

**Proof.**

The result is obtained by expressing  $\tilde{u}_h$  in terms of  $\tilde{u}$  utilizing Lemma 2.11:

$$\tilde{u}_h = \frac{M |\Gamma|}{M |\Gamma_h^k|} \tilde{u} = \left( \frac{|\Gamma| - |\Gamma_h^k|}{|\Gamma_h^k|} + 1 \right) \tilde{u} \lesssim \left( \frac{h^{k+1} |\Gamma_h^k|}{|\Gamma_h^k|} + 1 \right) \tilde{u}.$$

Notice that  $\tilde{u}$  and  $\tilde{u}_h$  are constants. Hence, the extension  $\tilde{u}^E$  of  $\tilde{u}$  is the constant itself. This yields:

$$\begin{aligned} \|\tilde{u}^E - \tilde{u}_h\|_{0, \Gamma_h^k} &\lesssim \|\tilde{u}^E - (1 + h^{k+1}) \tilde{u}^E\|_{0, \Gamma_h^k} \\ &= h^{k+1} \|\tilde{u}^E\|_{0, \Gamma_h^k} \\ &= h^{k+1} \frac{M}{|\Gamma|} |\Gamma_h^k|^{1/2} \lesssim h^{k+1} M. \end{aligned}$$

Thereby, equation (3.17) is used, compare the proof of Theorem 3.15.  $\square$

Now, everything is provided to give a convergence error estimate in the  $L^2$ - and the  $H^1$ -norm.

**Corollar 3.17**

Let  $u \in H^{r+1}(\Gamma)$  solve Problem 3.3 and  $u_h \in X$  solve Problem 3.5. Then, it can be concluded that:

$$\begin{aligned} \|u^E - u_h\|_{1, \Gamma_h^k} &\lesssim [h^r + (h^{r+1} + h^{k+1}) \varepsilon^{-1}] (\|u\|_{r+1, \Gamma} + M) \\ &\quad + h^{k+1} \varepsilon^{-1} \|f\|_{0, \Gamma}. \end{aligned}$$

**Proof.**

The estimation of  $u^E - u_h$  in the  $H^1$ -semi-norm is directly obtained from the definition of the triple norm  $\|\cdot\|_{DC,k}$  and Lemma 3.15:

$$\begin{aligned} \|u^E - u_h\|_{1, \Gamma_h^k} &= \varepsilon^{-1/2} \|u^E - u_h\|_{DC,k} \\ &= \varepsilon^{-1/2} \|u_0^E - u_{h,0}\|_{DC,k} \\ &\lesssim [h^r + (h^{r+1} + h^{k+1}) \varepsilon^{-1}] \|u_0\|_{r+1, \Gamma} \\ &\quad + h^{k+1} \varepsilon^{-1} \|f\|_{0, \Gamma}. \end{aligned}$$

To get an error bound in the  $L^2$ -norm the Poincare inequality and Lemma 3.16 are used. Unfortunately, the same problem as in Theorem 3.15 occurs. For  $\psi := u_0^E - u_{h,0}$  we get  $\psi \in X^r$  but  $\psi \notin X_0^r$  and the Poincare inequality cannot be applied to  $\psi$  directly. Again, a constant  $C \in \mathbb{R}$  is introduced such that  $\langle \psi + C \rangle_{\Gamma_h^k} = 0$  and  $\psi + C \in X_0^r$ . From

equations (3.17) and (3.18) obtained in the proof of Theorem 3.15 it follows that:

$$\begin{aligned} \|C\|_{0,\Gamma_h^k} &= |C| |\Gamma_h^k|^{1/2} \lesssim (h^{r+1} + h^{k+1}) \left( (1 + h^{k+1}) |\Gamma| \right)^{1/2} \|u_0\|_{0,\Gamma} \\ &\lesssim (h^{r+1} + h^{k+1}) \|u_0\|_{0,\Gamma}. \end{aligned}$$

Using Lemma 3.16 and the Poincare inequality it can be concluded that:

$$\begin{aligned} \|u^E - u_h\|_{0,\Gamma_h^k} &\leq \|\psi + C\|_{0,\Gamma_h^k} + \|C\|_{0,\Gamma_h^k} + \|\tilde{u}^E - \tilde{u}_h\|_{0,\Gamma_h^k} \\ &\lesssim |\psi|_{1,\Gamma_h^k} + (h^{r+1} + h^{k+1}) \|u_0\|_{0,\Gamma} + h^{k+1} M \\ &\lesssim \varepsilon^{-1/2} \|u_0^E - u_{h,0}\|_{DC,h} + (h^{r+1} + h^{k+1}) \|u_0\|_{0,\Gamma} + h^{k+1} M \\ &\lesssim \left[ h^r + (h^{r+1} + h^{k+1}) \varepsilon^{-1} \right] \|u_0\|_{r+1,\Gamma} \\ &\quad + h^{k+1} \varepsilon^{-1} \|f\|_{0,\Gamma} + h^{k+1} M. \end{aligned}$$

As a last step to conclude the proof, the norms of the unknown  $u_0^E$  shall be expressed in terms of the  $u$  and  $M$ :

$$\|u_0\|_{k+1,\Gamma} = \|u - \tilde{u}\|_{k+1,\Gamma_h^k} \lesssim \|u\|_{k+1,\Gamma} + \|\tilde{u}\|_{0,\Gamma} \lesssim \|u\|_{k+1,\Gamma_h^k} + M.$$

□

## Chapter 4

# Stabilization Techniques on Surfaces

In the previous chapter an error analysis for the diffusion-convection-reaction and the diffusion-convection equation on surfaces has been presented. In the case of diffusion-convection-reaction equations even semi-robust estimates have been achieved. Nevertheless, the discussed method of standard Galerkin surface finite elements for transport equations succumbs a problem well known for bulk equations. In the convection-dominated case, non-physical oscillations can occur if the triangulation is not fine enough. The same behaviour can be observed for surface equations, compare [61] and Section 6.3.

As already presented in Section 1.1, many different stabilization techniques have been developed and studied for transport equations in the bulk. The only reference found in the literature on the stabilization of convection-dominated surface transport equations is a publication by Olshanskii, Reusken and Xu in 2014 [61]. They have studied the Streamline-Upwind-Petrov-Galerkin (SUPG) stabilization method for a first order trace finite element method. A shared error analysis for the diffusion-convection-reaction and the diffusion-convection equation is given. The constant  $C$  in the presented error estimate depend only mildly on the diffusion parameter  $\varepsilon$ . More precisely, the constant of the convergence estimate, obtained in the mesh depending energy norm corresponding to the SUPG-stabilized formulation, depends on  $\varepsilon^{-1/2}$ .

In this work, stabilization techniques for higher order fitted surface finite elements are given. The Local Projection Stabilization (LPS) for transport equations on surfaces is studied. Semi-robust error estimates for convection-dominated diffusion-convection-reaction equations on closed surfaces are presented. Additionally, the surface variant of the SUPG method introduced in [61] is transferred to fitted finite elements of higher order. The applicability of these techniques to diffusion-convection equations is discussed.

## 4.1 Local Projection Stabilization

The Local Projection Stabilization is a projection based stabilization technique, which is defined element-wise. It is aimed to keep control over the gradient of the ansatz function in the case of a vanishing diffusion parameter. For unstabilized elliptic equations the  $H^1$ -control depends strongly on  $\varepsilon$ . For a decreasing diffusion parameter the bound of the  $H^1$ -semi norm becomes weaker. This loss of control over the derivatives leads to the appearance of oscillations in convection dominated cases, compare Section 6.3. In the LPS method, control over the higher order modes of the gradient is added and thus oscillations are damped. In the following, the LPS on surfaces is introduced. Thereby, the diffusion-convection-reaction problem on a closed surface, as studied in Section 3.1, is considered as an example problem.

We introduce a projection space  $D^r$ , which is normally a lower order discontinuous finite element space on the same surface approximation as the ansatz space  $X^r$ . A projection  $\pi_K : L^2(K) \rightarrow D^r(K)$  is defined element-wise for all  $K \in \mathcal{T}_h^k$  and the difference between a function and its projection is named fluctuation  $\kappa_K = id - \pi_K$ .

Now, the stabilization term used in LPS is given by:

$$S_k^{LPS}(u_h, v_h) = \sum_{K \in \mathcal{T}_h^k} \alpha_K \left\langle \kappa_K \left( \nabla_{\Gamma_h^k} u_h \right), \kappa_K \left( \nabla_{\Gamma_h^k} v_h \right) \right\rangle_K \quad (4.1)$$

with  $\alpha_K$  being an element-wise constant stabilization parameter. Throughout the following convergence analysis it will turn out that  $\alpha_K = \alpha^2 h_K$  with a fixed  $\alpha \in \mathbb{R}$  leads to optimal error estimates.

### 4.1.1 Stabilized Formulation

Using the stabilization term (4.1) the LPS stabilized formulation of the diffusion-convection-reaction problem on a closed surface reads:

**Problem 4.1 (*LPS Stabilized Problem*)**

Find  $u_h \in X^r$  such that for all  $v_h \in X^r$

$$a_k^{LPS}(u_h, v_h) = f_k^{LPS}(v_h)$$

with

$$\begin{aligned} a_k^{LPS}(u_h, v_h) &= a_k^{DCR}(u_h, v_h) + S_k^{LPS}(u_h, v_h), \\ f_k^{LPS}(v_h) &= f_k^{DCR}(v_h). \end{aligned}$$

The associated mesh-dependent triple norm is given by:

$$\| \| v_h \| \|_{LPS,k} := \left( \varepsilon |v_h|_{1,\Gamma_h^k}^2 + \sigma_0 \|u\|_{0,\Gamma_h^k}^2 + \sum_{K \in \mathcal{T}_h^k} \alpha_K \|\kappa_K \nabla_{\Gamma_h^k} v_h\|_{0,K}^2 \right)^{\frac{1}{2}}.$$

and is actually a norm on  $X^r$ .

According to this norm, coercivity of  $a_k^{LPS}(\cdot, \cdot)$  for small  $h$  can be proven using the results of Lemma 3.3 and unique solvability on fine meshes follows:

**Lemma 4.1**

For  $v_h \in X^r$  and  $h$  small enough, such that (3.9) holds,  $a_k^{LPS}(\cdot, \cdot)$  is coercive in  $X^r$ :

$$a_k^{LPS}(v_h, v_h) \geq \frac{3}{4} \| \| v_h \| \|_{LPS,k}^2 \quad \forall v_h \in X^r$$

and Problem 4.1 is uniquely solvable.

**Proof.**

Coercivity for  $a_k^{LPS}(\cdot, \cdot)$  is shown by using the estimate obtained in Lemma 3.3:

$$\begin{aligned} a_k^{LPS}(v_h, v_h) &= a_k^{DCR}(v_h, v_h) + S_k^{LPS}(v_h, v_h) \\ &\geq \frac{3}{4} \| \| v_h \| \|_{DCR,k}^2 + \sum_{K \in \mathcal{T}_h^k} \alpha_K \|\kappa_K \nabla_{\Gamma_h^k} v_h\|_{0,K}^2 \\ &\geq \frac{3}{4} \| \| v_h \| \|_{LPS,k}^2. \end{aligned}$$

Linearity and continuity of  $a_k^{LPS}(\cdot, \cdot)$  and  $f_k^{LPS}(\cdot)$  are obtained straight forward. Hence, Problem 4.1 is uniquely solvable for small  $h$  due to the Lax-Milgram theorem.  $\square$

## 4.1.2 Error Estimates

In this section, an error estimate is taken out for Problem 4.1. This problem differs from the standard Galerkin diffusion-convection-reaction problem only in the additional stabilization term. Thus, it would be sufficient to obtain the necessary evaluations for the stabilization term to conclude an error estimate of the whole problem. Nevertheless, from LPS methods for bulk equations it is known that the bounds for the convection term, as achieved in Section 3.1.3, can be improved using the stronger triple norm together with a special interpolant.

At first the existence of such an interpolator under the given assumptions is shown. Then, this result is used to obtain an improved convergence error estimate for the stabilized diffusion-convection-reaction equation.

### Orthogonal Interpolation

As known from the LPS for bulk equation [55], the finite element space  $X^r$  and  $D^r$  are assumed to fulfil three assumptions. For surface equations the difference between the smooth and the discrete surface has to be taken into account. Error estimates shall depend on the integrals of the given data and the exact solution over  $\Gamma$  instead of integrals over  $\Gamma_h^k$ . Therefore, in the assumed inequalities, given below, the right hand sides are formulated depending on integrals over  $\Gamma$  instead of  $\Gamma_h^k$ :

(A1) For the fluctuation operator  $\kappa_K$  it holds:

$$\|\kappa_K \phi\|_{0,K} \lesssim h_K^l |\phi^L|_{l,\mathbf{p}(K)} \quad \forall \phi \in H^l(K), \forall K \in \mathcal{T}_h^k, 0 \leq l \leq r.$$

(A2) It exists an interpolator  $i^r : H^2(\Gamma_h^k) \rightarrow X^r$  of order  $r + 1$ :

$$\|\phi - i^r \phi\|_{0,K} + h_K |\phi - i^r \phi|_{1,K} \lesssim h_K^l \|\phi^L\|_{l,\mathbf{p}(K)} \quad \forall \phi \in H^l(K), \\ \forall K \in \mathcal{T}_h^k, 2 \leq l \leq r + 1.$$

(A3) A local inf-sup condition is fulfilled by  $X^r$  and  $D^r$ :

$$\inf_{q_h \in D^r(K)} \sup_{v_h \in X^r(K)} \frac{\langle v_h, q_h \rangle_K}{\|v_h\|_{0,K} \|q_h\|_{0,K}} \geq \beta \quad \forall K \in \mathcal{T}_h^k$$

with  $\beta > 0$  being a constant independent of  $h$  and

$$D^r(K) := \{q_h|_K \mid q_h \in D^r\}, \quad X^r(K) := \{v_h|_K \mid v_h \in X^r, v_h|_{\partial K} = 0\}.$$

Recognize that these assumptions are defined in an element-wise manner. In the case of a linear surface approximation the elements  $K$  are flat and the  $n$ -dimensional surface elements can be considered as  $(n - 1)$ -dimensional bulk elements. Hence, the results obtained for LPS in [55] and [56] can directly be used in this case. In these papers, it is shown that the assumptions (A2) and (A3) entail the existence of a special interpolation operator  $j^r$ , which is orthogonal to  $D^r$ . This result can be directly transferred to the case of higher order surface approximations:

#### Lemma 4.2

If the assumptions (A2) and (A3) are met by the spaces  $X^r$  and  $D^r$ , an interpolator  $j^r : H^2(\Gamma_h^k) \rightarrow X^r$  fulfilling the orthogonality condition:

$$\langle \phi - j^r \phi, q_h \rangle_{\Gamma_h^k} = 0 \quad \forall q_h \in D^r, \forall \phi \in H^1(\Gamma_h^k)$$



and the interpolation property for  $2 \leq l \leq r + 1$ :

$$\|\phi - j^r \phi\|_{0,K} + h_K |\phi - j^r \phi|_{1,K} \lesssim h_K^l \|\phi^L\|_{l,\mathbf{P}(K)} \quad \forall \phi \in H^l(K), \forall K \in \mathcal{T}_h^k,$$

exists.

**Proof.**

Due to the element-wise definition of the assumptions, the proof can be taken from [55, Theorem 2.2]. The main ingredient is the equivalence of the inf-sup-condition and the property:

The operator  $B : X(K) \rightarrow D(K)'$  given by  $\langle Bv_h, q_h \rangle_{D(K)} := \langle v_h, q_h \rangle_M$  for all  $v_h \in X(K)$  and  $q_h \in D(K)$  is an isomorphism from  $W^\perp$  onto the dual space of  $D(K)$  with  $W := \{v_h \in X(K) \mid \langle v_h, q_h \rangle_K = 0 \forall q_h \in D(K)\}$ .

shown in [39, Lemma I.4.1].  $\square$

### Consistency Estimate

Aside from the geometric error coming from the surface approximation the added stabilization term leads to an inconsistent problem formulation even for exactly approximated surfaces, e.g. polyhedral surfaces. The additional consistency error is evaluated in the next lemma.

**Lemma 4.3**

For  $u \in H^{r+1}(\Gamma)$ ,  $\alpha_K = \alpha^2 h_K$  and (A1) be fulfilled, one gets for all  $v_h \in X^r$ :

$$\begin{aligned} & \left| (f_k^{DCR}(v_h) - f_k^{LPS}(v_h)) - (a_k^{DCR}(u^E, v_h) - a_k^{LPS}(u^E, v_h)) \right| \\ & \lesssim h^{r+1/2} \|u\|_{r+1,\Gamma} \|v_h\|_{LPS,k}. \end{aligned}$$

**Proof.**

Using the definitions of the right hand form  $f_k^{LPS}(v_h) = f_k^{DCR}(v_h)$  and the bilinear form  $a_k^{LPS}(u^E, v_h) = a_k^{DCR}(u^E, v_h) + S_k^{LPS}(u^E, v_h)$ , and assumption (A1) it follows that:

$$\begin{aligned} & \left| (f_k^{DCR}(v_h) - f_k^{LPS}(v_h)) - (a_k^{DCR}(u^E, v_h) - a_k^{LPS}(u^E, v_h)) \right| \\ & = |S_k^{LPS}(u^E, v_h)| \\ & = \left| \sum_{K \in \mathcal{T}_h^k} \alpha_K \left\langle \kappa_K \nabla_{\Gamma_h^k} u^E, \kappa_K \nabla_{\Gamma_h^k} v_h \right\rangle_K \right| \\ & \lesssim \sum_{K \in \mathcal{T}_h^k} \alpha_K h_K^r |\nabla_{\Gamma_h^k} u^E|_{r,K} \|\kappa_K \nabla_{\Gamma_h^k} v_h\|_{0,K} \\ & \lesssim h^{r+1/2} \|u\|_{r+1,\Gamma} \|v_h\|_{LPS,k}. \end{aligned}$$

$\square$

### Continuity Estimate

Next, a continuity estimate for the LPS stabilized formulation is proven. Recognize that the orthogonal interpolator  $j^r$  provides the same interpolation properties as the standard Lagrange interpolator  $i^r$ . Consequently, the result of Theorem 3.5 is also valid if  $i^r$  is replaced by  $j^r$ . Nevertheless, the additional stabilization term has to be studied and the orthogonality condition fulfilled by the newly introduced interpolator can be used to improve the estimation of the convection term.

#### Lemma 4.4

Let  $u \in H^{r+1}(\Gamma)$ ,  $v_h \in X^r$ , (A1)–(A3) be fulfilled and  $j^r$  be the interpolator given by Theorem 4.2. Then, for  $\alpha_K = \alpha^2 h_K$  the following holds:

$$|a_k^{LPS}(u^E - j^r u^E, v_h)| \lesssim h^r (\varepsilon^{1/2} + h^{1/2}) \|u\|_{r+1, \Gamma} \|v_h\|_{LPS, h}.$$

#### Proof.

Writing shortly  $\psi := u^E - j^r u^E$  it follows:

$$\begin{aligned} |a_k^{LPS}(\psi, v_h)| &\leq \left| \varepsilon \left\langle \nabla_{\Gamma_h^k} \psi, \nabla_{\Gamma_h^k} v_h \right\rangle_{\Gamma_h^k} \right| + \left| \left\langle \mathbf{w}^E \cdot \nabla_{\Gamma_h^k} \psi, v_h \right\rangle_{\Gamma_h^k} \right| + \left| \left\langle \sigma^E \psi, v_h \right\rangle_{\Gamma_h^k} \right| \\ &\quad + \left| \sum_{K \in \mathcal{T}_h^k} \left\langle \alpha_K \kappa_K \left( \nabla_{\Gamma_h^k} \psi \right), \kappa_K \left( \nabla_{\Gamma_h^k} v_h \right) \right\rangle_K \right| \\ &=: T_1 + T_2 + T_3 + T_4. \end{aligned}$$

The terms  $T_1$  and  $T_3$  are evaluated as in Theorem 3.5 using the interpolation properties of  $j^r$ :

$$\begin{aligned} T_1 &\lesssim \varepsilon^{1/2} h^r \|u\|_{r+1, \Gamma} \|v_h\|_{LPS, h} \\ T_3 &\lesssim h^{r+1} \|u\|_{r+1, \Gamma} \|v_h\|_{LPS, h}. \end{aligned}$$

The convection term  $T_2$  is partially integrated to gain a higher interpolation order from the  $L^2$ - norm of  $\psi$  instead of the  $H^1$ -semi-norm:

$$\begin{aligned} T_2 &\leq \left| \left\langle \mathbf{w}^E \cdot \nabla_{\Gamma_h^k} v_h, \psi \right\rangle_{\Gamma_h^k} \right| + \left| \left\langle \nabla_{\Gamma_h^k} \cdot \mathbf{w}^E v_h, \psi \right\rangle_{\Gamma_h^k} \right| + \left| \sum_{K \in \mathcal{T}_h^k} \int_{\partial K} v_h \psi \mathbf{w}^E \cdot \boldsymbol{\nu}_h^k d\mathbf{b}_h^k \right| \\ &=: T_2^1 + T_2^2 + T_2^3. \end{aligned}$$

If the term  $T_2^1$  is evaluated directly one gets:

$$T_2^1 \lesssim \varepsilon^{-1/2} h^{r+1} \|u\|_{r+1, \Gamma} \|v_h\|_{LPS, k}$$

and a negative power of  $\varepsilon$  is introduced, which has to be avoided to obtain semi-robust estimates. Thus, we make use of the stronger LPS triple norm  $\|\cdot\|_{LPS, k}$  compared to the standard Galerkin triple norm  $\|\cdot\|_{DCR, k}$  and the orthogonality property of  $j^r$ . A

constant  $\tilde{\mathbf{w}}_K^E \in \mathbb{P}_0(K)$  is introduced as the integral mean value of  $\mathbf{w}^E$  over  $K$ . Then  $T_2^1$  can be rewritten:

$$\begin{aligned} T_2^1 &= \left| \left\langle \mathbf{w}^E \cdot \nabla_{\Gamma_h^k} v_h, \psi \right\rangle_{\Gamma_h^k} \right| \\ &= \left| \sum_{K \in \mathcal{T}_h^k} \left\langle (\mathbf{w}^E - \tilde{\mathbf{w}}_K^E) \cdot \nabla_{\Gamma_h^k} v_h, \psi \right\rangle_K + \left\langle \tilde{\mathbf{w}}_K^E \cdot \nabla_{\Gamma_h^k} v_h, \psi \right\rangle_K \right| \\ &\lesssim \sum_{K \in \mathcal{T}_h^k} \|\mathbf{w}^E - \tilde{\mathbf{w}}_K^E\|_{0,\infty,K} |v_h|_{1,K} \|\psi\|_{0,K} + \sum_{K \in \mathcal{T}_h^k} \left| \left\langle \tilde{\mathbf{w}}_K^E \cdot \nabla_{\Gamma_h^k} v_h, \psi \right\rangle_K \right|. \end{aligned}$$

An interpolation result and the inverse inequality (Lemma 2.14) are used to estimate the first summand. The second one is handled by using the orthogonality property of the interpolator  $j^r$  and subtracting the term  $\left\langle \tilde{\mathbf{w}}_K^E \cdot \pi_K \left( \nabla_{\Gamma_h^k} v_h \right), \psi \right\rangle_K$  for every element. This term equals zero because  $\pi_K(\nabla_{\Gamma_h^k} v_h) \in D^r$ .

$$\begin{aligned} T_2^1 &\lesssim \sum_{K \in \mathcal{T}_h^k} h_K \|\nabla_{\Gamma_h^k} \mathbf{w}^E\|_{0,\infty,K} |v_h|_{1,K} \|\psi\|_{0,K} \\ &\quad + \left| \sum_{K \in \mathcal{T}_h^k} \left\langle \tilde{\mathbf{w}}_K^E \cdot \left( \nabla_{\Gamma_h^k} v_h - \pi_K \left( \nabla_{\Gamma_h^k} v_h \right) \right), \psi \right\rangle_K \right| \\ &\lesssim \sum_{K \in \mathcal{T}_h^k} \left( \|\nabla_{\Gamma} \mathbf{w}\|_{0,\infty,\Gamma} \|v_h\|_{0,K} \|\psi\|_{0,K} + \|\mathbf{w}\|_{0,\infty,\Gamma} \|\kappa_K \left( \nabla_{\Gamma_h^k} v_h \right)\|_{0,K} \|\psi\|_{0,K} \right) \\ &\lesssim \|v_h\|_{0,\Gamma_h^k} \|\psi\|_{0,\Gamma_h^k} + \sum_{K \in \mathcal{T}_h^k} \left\| \kappa_K \left( \nabla_{\Gamma_h^k} v_h \right) \right\|_{0,K} \|\psi\|_{0,K} \\ &\lesssim h^{r+1} \|u\|_{r+1,\Gamma} \|v_h\|_{LPS,k} + \sum_{K \in \mathcal{T}_h^k} h_K^{r+1} \alpha_K^{-1/2} \|u\|_{r+1,\mathbf{P}(K)} \alpha_K^{1/2} \left\| \kappa_K \left( \nabla_{\Gamma_h^k} v_h \right) \right\|_{0,K} \\ &\lesssim h^{r+1/2} \|u\|_{r+1,\Gamma} \|v_h\|_{LPS,k}. \end{aligned}$$

The term  $T_2^2$  can be estimated using Lemma 2.7 and the fact, that the given velocity field  $\mathbf{w}$  is divergence free on  $\Gamma$ :

$$\begin{aligned} T_2^2 &= \left| \left\langle \nabla_{\Gamma_h^k} \cdot \mathbf{w}^E v_h, \psi \right\rangle_{\Gamma_h^k} \right| \\ &= \left| \left\langle \left( \nabla_{\Gamma_h^k} \cdot \mathbf{w}^E - (\nabla_{\Gamma} \cdot \mathbf{w})^E \right) v_h, \psi \right\rangle_{\Gamma_h^k} \right| \\ &\lesssim h^k |\mathbf{w}|_{1,\infty,\Gamma} \|v_h\|_{0,\Gamma_h^k} \|\psi\|_{0,\Gamma_h^k} \\ &\lesssim h^{k+r+1} \|u\|_{r+1,\Gamma} \|v_h\|_{LPS,k} \end{aligned}$$

To evaluate the term  $T_2^3$  we use the assumption  $\mathbf{w} \cdot \mathbf{n} = 0$  on  $\Gamma$ . It follows that  $\mathbf{w}^E \cdot \mathbf{n} = (\mathbf{w} \cdot \mathbf{n})^E = 0$  on  $\Gamma_h^k$  and hence  $P\mathbf{w}^E(\mathbf{x}) = \mathbf{w}^E(\mathbf{x})$  for  $\mathbf{x} \in \Gamma_h^k$ . Using

Lemma 2.9 yields:

$$\begin{aligned}
T_2^3 &= \left| \sum_{K \in \mathcal{T}_h^k} \int_{\partial K} \mathbf{w}^E \cdot \boldsymbol{\nu}_h^k v_h \psi d\mathbf{b}_h^k \right| \\
&= \left| \sum_{E \in \mathcal{E}_h^k} \int_E P \mathbf{w}^E \cdot (\boldsymbol{\nu}^+ + \boldsymbol{\nu}^-) v_h \psi d\mathbf{b}_h^k \right| \\
&\lesssim \sum_{E \in \mathcal{E}_h^k} \|\mathbf{w}^E\|_{0,\infty,E} |P(\boldsymbol{\nu}^+ + \boldsymbol{\nu}^-)| \|v_h\|_{0,E} \|\psi\|_{0,E} \\
&\lesssim \sum_{E \in \mathcal{E}_h^k} h_K^{2k} \|v_h\|_{0,E} \|\psi\|_{0,E}.
\end{aligned}$$

Utilizing the trace theorem (Lemma 2.13) and the inverse inequality (Lemma 2.14) provides:

$$\begin{aligned}
T_2^3 &\lesssim h^{2k-1} \|v_h\|_{0,\Gamma_h^k} \left( \|\psi\|_{0,\Gamma_h^k} + h |\psi|_{1,\Gamma_h^k} \right) \\
&\lesssim h^{2k+r} \|u\|_{r+1,\Gamma} \|v_h\|_{LPS,k}.
\end{aligned}$$

The last summand  $T_4$  can be bounded using the assumption (A1):

$$\begin{aligned}
T_4 &\leq \sum_{K \in \mathcal{T}_h^k} \left| \alpha_K \left\langle \kappa_K \left( \nabla_{\Gamma_h^k} \psi \right), \kappa_K \left( \nabla_{\Gamma_h^k} v_h \right) \right\rangle_K \right| \\
&\leq \sum_{K \in \mathcal{T}_h^k} \alpha_K \left\| \kappa_K \left( \nabla_{\Gamma_h^k} \psi \right) \right\|_{0,K} \left\| \kappa_K \left( \nabla_{\Gamma_h^k} v_h \right) \right\|_{0,K} \\
&\lesssim \sum_{K \in \mathcal{T}_h^k} \alpha_K \|\nabla_{\Gamma_h^k} \psi\|_{0,K} \|\kappa_K \nabla_{\Gamma_h^k} v_h\|_{0,K} \\
&\lesssim \alpha h^{1/2} |\psi|_{1,\Gamma_h^k} \|v_h\|_{LPS,k} \\
&\lesssim h^{r+1/2} \|u\|_{r+1,\Gamma} \|v_h\|_{LPS,k}.
\end{aligned}$$

Taking the sum over all, the postulated inequality follows.  $\square$

This result is compared to Lemma 3.5. For the diffusion and the reaction term the same order is obtained in both Lemmas. For the estimation of the convection term the order is increased by  $h^{1/2}$  compared to the standard Galerkin approach.

#### Notice 4.1.1

Having a closer look on the proofs of the Theorems 4.3 and 4.4 the optimal asymptotic choice of  $\alpha_K$  can be concluded. For a small diffusion parameter  $\varepsilon$  the continuity estimate is dominated by the error obtained for the convection term. This is of order  $h_K^{r+1} \alpha_K^{-1/2}$  on each element  $K$ . On the other hand the consistency

error coming from the additional stabilization term is bounded with an order of  $h_K^r \alpha_K^{1/2}$ . Hence, the optimal asymptotic choice of  $\alpha_K$  is  $\alpha_K \sim h_K$ , as already assumed above.

### Convergence Estimate in $\|\cdot\|_{LPS,k}$

To give an overall convergence result for Problem 4.1 the above error estimates are used. Hence, the improvement obtained for the continuity error of the convection term is transferred to the convergence estimate.

#### Theorem 4.5

Let  $u_h \in X^r$  be the discrete solution of the Problem 4.1,  $u \in H^{r+1}(\Gamma)$  the solution of the Problem 3.1,  $\alpha_K = \alpha^2 h_K$ , and assumptions (A1)–(A3) be fulfilled. Assuming that  $h$  is small enough to fulfil (3.9) it holds:

$$\|u^E - u_h\|_{LPS,k} \lesssim h^{k+1} (\|u\|_{1,\Gamma} + \|f\|_{0,\Gamma}) + h^r (\varepsilon^{1/2} + h^{1/2}) \|u\|_{r+1,\Gamma}.$$

#### Proof.

Let  $j^r : H^2(\Gamma_h^k) \rightarrow X^r$  be the orthogonal interpolation operator given in Lemma 4.2. Then, using the triangle inequality yields:

$$\|u^E - u_h\|_{LPS,k} \leq \|u^E - j^r u^E\|_{LPS,k} + \|j^r u^E - u_h\|_{LPS,k}. \quad (4.2)$$

The first term of (4.2) can be estimated using assumption (A1) and the interpolation properties of  $j^r$ :

$$\begin{aligned} & \|u^E - j^r u^E\|_{LPS,k}^2 \\ &= \varepsilon \left\| \nabla_{\Gamma_h^k} (u^E - j^r u^E) \right\|_{0,\Gamma_h^k}^2 + \sigma_0 \|u^E - j^r u^E\|_{0,\Gamma_h^k}^2 \\ &+ \sum_{K \in \mathcal{T}_h^k} \alpha_K \left\| \kappa_K \nabla_{\Gamma_h^k} (u^E - j^r u^E) \right\|_{0,K}^2 \\ &\lesssim (\varepsilon h^{2r} + h^{2r+2}) \|u\|_{r+1,\Gamma}^2 + \sum_{K \in \mathcal{T}_h^k} \alpha_K \left\| \nabla_{\Gamma_h^k} (u^E - j^r u^E) \right\|_{0,K}^2 \\ &\lesssim h^{2r} (\varepsilon + h) \|u\|_{r+1,\Gamma}^2. \end{aligned}$$

The second term of (4.2) is handled by making use of the coercivity proven in Lemma 4.1. Setting  $\psi := u_h - j^r u^E$  one gets:

$$\begin{aligned} \|j^r u^E - u_h\|_{LPS,k}^2 &\lesssim a_k^{LPS}(u_h - j^r u^E, \psi) \\ &= a_k^{LPS}(u_h - u^E, \psi) + a_k^{LPS}(u^E - j^r u^E, \psi) \\ &= f_k^{LPS}(u_h, \psi) - a_k^{LPS}(u^E, \psi) + a_k^{LPS}(u^E - j^r u^E, \psi). \end{aligned}$$

Making use of Lemma 3.6, Lemma 4.3 and Lemma 4.4 it follows that:

$$\begin{aligned} \|\psi\|_{LPS,k} &\lesssim h^{k+1} (\|u\|_{1,\Gamma} + \|f\|_{0,\Gamma}) \\ &\quad + h^{r+1} \|u\|_{r+1,\Gamma} \\ &\quad + h^r \left( \varepsilon^{1/2} + h^{-1/2} \right) \|u\|_{r+1,\Gamma}. \end{aligned}$$

By adding up all the equations, the expected result is gained.  $\square$

Comparing this convergence result with the convergence result obtained in Theorem 3.7, an improvement for the error coming from the discretization of  $H^1(\Gamma_h^k)$  by the finite element space  $X^r$  can be seen. For  $\varepsilon \rightarrow 0$  an asymptotic behaviour like  $h^{r+1/2}$  instead of  $h^r$  is achieved in the triple norm. Naturally, no difference appears in the errors coming from the surface approximation.

### Convergence Estimates in the $L^2$ - and $H^1$ -norm

Because the LPS triple norm provides direct control over the  $L^2$ - and the  $H^1$ -norm, estimations in these norms can be obtained directly from Theorem 4.5. Therefore, the definition of  $\|\cdot\|_{LPS,k}$  is recalled and using the norm equivalences (2.19)–(2.20) it follows:

$$\begin{aligned} \|u - u_h^L\|_{0,\Gamma} &\leq \|u^E - u_h\|_{0,\Gamma_h^k} \lesssim \|u^E - u_h\|_{LPS,k} \\ |u - u_h^L|_{1,\Gamma} &\leq |u^E - u_h|_{1,\Gamma_h^k} \lesssim \varepsilon^{-1/2} \|u^E - u_h\|_{LPS,k}. \end{aligned}$$

This leads to the following error estimates:

#### Corollar 4.6

*Under the same conditions as in Theorem 4.5 it follows:*

$$\|u - u_h^L\|_{0,\Gamma} \lesssim h^{k+1} (\|u\|_{1,\Gamma} + \|f\|_{0,\Gamma}) + h^r (\varepsilon^{1/2} + h^{1/2}) \|u\|_{r+1,\Gamma}$$

and

$$|u - u_h^L|_{1,\Gamma} \lesssim h^{k+1} \varepsilon^{-1/2} (\|u\|_{1,\Gamma} + \|f\|_{0,\Gamma}) + h^r (1 + \varepsilon^{-1/2} h^{1/2}) \|u\|_{r+1,\Gamma}.$$

### 4.1.3 LPS for Diffusion-Convection Equations

The improvement in the continuity error for the convection term provided by the LPS stabilization is based on two main points:

- the  $L^2$ -control provided by the triple norm  $\|\cdot\|_{LPS,k}$  coming from the  $L^2$ -control of the  $\|\cdot\|_{DCR,k}$  norm and

- the reduced interpolation order obtained in the standard Galerkin finite element method due to the need of a semi-robust estimate.

In the case of diffusion-convection equations the interpolation error of the convection term is already bounded by  $h^{r+1}$ , see the proof of Lemma 3.13. Further, no  $L^2$ -control can be obtained. Hence, LPS stabilization does not lead to improved interpolation estimates for diffusion-convection equations.

Nevertheless, a LPS stabilized problem and the corresponding stronger triple norm can be defined similarly to Section 4.1.1. Coercivity in that stronger norm can be proven for diffusion-convection equations, too. Thus, LPS still increases the stability for diffusion-convection equations but does not yield an improved convergence order.

#### 4.1.4 Choices for $X^r$ and $D^r$

The error analysis above is based on three assumptions for the finite element space  $X^r$ , the projection space  $D^r$  and an element-wise projection operator  $\pi_K : L^2(K) \rightarrow D^r(K)$ . In this section, possible choices fulfilling these assumptions are presented. Thereby, two conflicting requirements have to be taken into account. On the one hand,  $D^r$  has to be big enough to guarantee the assumption (A1). On the other hand, the projection space has to be small enough compared with  $X^r$  to meet the inf-sup-condition (A3).

Let  $G_K^k : \widehat{K} \rightarrow K$  be the mapping from the reference element to the higher order element  $K \in \mathcal{T}_h^k$ , as given in Section 2.2, and  $\mathbb{P}_r(K)$  the space of polynomials of degree  $r$  or less over  $K$ . The mapped finite element spaces are given by the ansatz  $\widehat{X}^r$  and the projection space  $\widehat{D}^r$  on the reference element  $\widehat{K}$ :

$$\begin{aligned} X^r &= \{v \in C^0(\Gamma_h^k) \mid v|_{K^k} \circ G_K^k \in \widehat{X}^r\}, \\ D^r &= \{q \in L^2(\Gamma_h^k) \mid q|_{K^k} \circ G_K^k \in \widehat{D}^r\}. \end{aligned}$$

In the following, it is discussed how to choose the spaces  $\widehat{X}^r$  and  $\widehat{D}^r$ .

The existence of an interpolator of order  $r+1$ , as postulated in assumption (A2), is obvious for spaces  $\widehat{X}^r$  containing the polynomials of order  $r$ . The standard Lagrange interpolation into the space already provides the necessary estimations, see Lemma 2.15.

Assumption (A1) is met by taking  $\pi_K : L^2(K) \rightarrow D^r$  as an element-wise  $L^2$ -interpolator via

$$\langle \phi^L, q_h^L \rangle_{\mathbf{p}(K)} = \langle (\pi_K \phi)^L, q_h^L \rangle_{\mathbf{p}(K)} \quad \forall q_h \in D^r(K)$$

and  $\widehat{D}^r \supset \mathbb{P}_{r-1}(\widehat{K})$ . It can be concluded that  $\pi_K$  is the identity on  $D^r(K)$ . The Bramble-Hilbert lemma, compare [19, Theorem 4.1.3], provides then the approximation properties stated in assumption (A1).

The choice  $\widehat{X}^r = \mathbb{P}_r(\widehat{K})$  and  $\widehat{D}^r = \mathbb{P}_{r-1}(\widehat{K})$  fulfils the assumptions (A1) and (A2) but fails for assumption (A3).  $\widehat{X}^r$  can be enriched such that the inf-sup-condition holds. This problem is studied for bulk equations in [55]. There, it is used that an inf-sup-condition proven on the reference element  $\widehat{K}$  can be directly transferred to affine finite elements. A similar result is obtained for the isoparametric surface elements used here:

**Theorem 4.7**

Let  $\widehat{K}$  be the reference element of the mapped surface finite element space  $X^r$  and the mapping  $G_K^k : \widehat{K} \rightarrow K$  as given in Section 2.2. Providing an inf-sup-condition on  $\widehat{K}$ :

$$\inf_{\widehat{q} \in \widehat{D}^r} \sup_{\widehat{v} \in \widehat{X}_0^r} \frac{(\widehat{v}, \widehat{q})_{\widehat{K}}}{\|\widehat{v}\|_{0, \widehat{K}} \|\widehat{q}\|_{0, \widehat{K}}} \geq \widehat{\beta} > 0$$

with  $\widehat{X}_0^r := \{\widehat{v} \in \widehat{X}^r \mid \widehat{v}|_{\partial \widehat{K}} = 0\}$  it follows an inf-sup-condition on all elements  $K$ :

$$\inf_{q_h \in D^r(K)} \sup_{v_h \in X^r(K)} \frac{(v_h, q_h)_K}{\|v_h\|_{0, K} \|q_h\|_{0, K}} \geq \beta_K > 0$$

with  $D^r(K) := \{q_h|_K \mid q_h \in D^r\}$  and  $X^r(K) := \{v_h|_K \mid v_h \in X^r, v_h|_{\partial K} = 0\}$ . All  $\beta_K$  are bounded uniquely from below by a constant  $\beta > 0$ .

**Proof.**

In Theorem 2.2 it is given that:

$$\left| F_K(\widehat{K}) \right| n! (1 - c_K)^n \leq \left| \sqrt{\det \left( (DG_K^k)^T DG_K^k \right)} \right| \leq \left| F_K(\widehat{K}) \right| n! (1 + c_K)^n$$

for all mappings  $G_K^k : \widehat{K} \rightarrow K$ . Setting  $v_h \circ G_K^k = \widehat{v} \in \widehat{X}_0^r$  for an arbitrary  $v_h \in X^r(K)$  and  $q_h \circ G_K^k = \widehat{q} \in \widehat{D}^r$  for an arbitrary  $q_h \in D^r(K)$  it follows:

$$\begin{aligned} \frac{(v_h, q_h)_K}{\|v_h\|_{0, K} \|q_h\|_{0, K}} &\geq \frac{(\widehat{v}, \widehat{q})}{\|\widehat{v}\|_{0, \widehat{K}} \|\widehat{q}\|_{0, \widehat{K}}} \cdot \frac{|F_K(\widehat{K})| n! (1 + c_K)^n}{|F_K(\widehat{K})| n! (1 - c_K)^n} \\ &\geq \widetilde{\beta} \left( \frac{1 + c_K}{1 - c_K} \right)^n = \widetilde{\beta} \left( 1 + \frac{2c_K}{1 - c_K} \right)^n \geq \widehat{\beta}. \end{aligned}$$

□

Using this result, assumption (A3) can be obtained directly from an inf-sup condition on the reference element. This inf-sup condition is proven amongst others for the choice  $\widehat{X}^r = \mathbb{P}_r^{\text{bubble}}$  and  $\widehat{D}^r = \mathbb{P}_{r-1}^{\text{disc}}$  [55]. There, the finite element space of continuous element-wise functions of order  $r$  or less is enriched by bubble functions on each element. These bubble functions have only support on the inner



of every element. This prevents a high coupling. More precisely, a function  $\widehat{b}$  is given as:

$$\widehat{b} := (n+1)^{n+1} \prod_{i=1}^{n+1} \lambda_i.$$

Thereby,  $\lambda_i$ ,  $i = 1, \dots, n+1$ , are the barycentric coordinates in the reference element  $\widehat{K}$ . Then  $\mathbb{P}_r^{\text{bubble}}(\widehat{K})$  is set to  $\mathbb{P}_r^{\text{bubble}}(\widehat{K}) = \mathbb{P}_r(\widehat{K}) + \widehat{b}\mathbb{P}_{r-1}(\widehat{K})$  and the finite element and the projection space are given by

$$\widehat{X}^r = \mathbb{P}_r^{\text{bubble}} \quad \text{and} \quad \widehat{D}^r = \mathbb{P}_{r-1}.$$

A comparison of the dimensions of  $\widehat{X}_0^r(\widehat{K})$  and  $\widehat{D}^r(\widehat{K})$  proves the minimality of the enrichment, see [55].

## 4.2 Streamline-Upwind-Petrov-Galerkin Stabilization

Another common stabilization technique for transport equations is the Streamline-Upwind-Petrov-Galerkin (SUPG) stabilization. The stabilization term for the SUPG stabilization is obtained by adding the partial differential equation to the continuous weak formulation of the problem. If  $u \in H^2(\Gamma)$  solves Problem 3.6, it follows that for all  $v \in H^1(\Gamma)$

$$(-\varepsilon \Delta_{\Gamma} u + \mathbf{w} \cdot \nabla_{\Gamma} u + \sigma u) \mathbf{w} \cdot \nabla_{\Gamma} v = f \mathbf{w} \cdot \nabla_{\Gamma} v \quad \text{on } \Gamma.$$

Discretizing this term in the same way as described in Section 3.1.2 and scaling the result with a stabilization parameter  $\alpha_K$  on each element  $K \in \mathcal{T}_h^k$  yields:

$$\begin{aligned} \sum_{K \in \mathcal{T}_h^k} \alpha_K \langle -\varepsilon \Delta_{\Gamma_h^k} u_h + \mathbf{w}^E \cdot \nabla_{\Gamma_h^k} u_h + \sigma^E u_h, \mathbf{w}^E \cdot \nabla_{\Gamma_h^k} v_h \rangle_K \\ = \sum_{K \in \mathcal{T}_h^k} \langle f^E, \mathbf{w}^E \cdot \nabla_{\Gamma_h^k} v_h \rangle_K. \end{aligned} \quad (4.3)$$

Having a closer look at the error analysis taken out later, it is highly motivated to choose

$$0 < \alpha_K \leq \frac{1}{2} \min \left\{ \frac{h_K^2}{\varepsilon c_{inv}^2}, \frac{\sigma_0 h_K}{\|\sigma\|_{0,\infty,K}} \right\}. \quad (4.4)$$

Thereby,  $c_{inv}$  is the constant from the inverse inequality, compare Theorem 2.14.

### 4.2.1 Stabilized Formulation

The SUPG stabilized formulation of Problem 3.1 is obtained by adding (4.3) to the standard discretized formulation, see Problem 3.2. It reads:

#### Problem 4.2 (*SUPG Stabilized Problem*)

Find  $u_h \in X^r$ , such that for all  $v_h \in X^r$

$$a_k^{SUPG}(u_h, v_h) = f_k^{SUPG}(v_h)$$

with

$$\begin{aligned} a_k^{SUPG}(u_h, v_h) &= a_k^{DCR}(u_h, v_h) + S_k^{SUPG}(u_h, v_h), \\ S_k^{SUPG}(u_h, v_h) &= \sum_{K \in \mathcal{T}_h^k} \alpha_K \left\langle -\varepsilon \Delta_{\Gamma_h^k} u_h + \mathbf{w}^E \cdot \nabla_{\Gamma_h^k} u_h + \sigma^E u_h, \mathbf{w}^E \cdot \nabla_{\Gamma_h^k} v_h \right\rangle_K, \\ f_k^{SUPG}(v_h) &= f_h^{DCR}(v_h) + \sum_{K \in \mathcal{T}_h^k} \left\langle f^E, \mathbf{w}^E \cdot \nabla_{\Gamma_h^k} v_h \right\rangle_K. \end{aligned}$$

As in the case of LPS a stronger mesh dependent norm compared to the unstabilized surface finite element method is introduced:

$$\| \| v_h \| \|_{SUPG,k} := \left( \varepsilon |v_h|_{1,\Gamma_h^k}^2 + \sigma_0 \|v_h\|_{0,\Gamma_h^k}^2 + \sum_{K \in \mathcal{T}_h^k} \alpha_K \| \mathbf{w}^E \cdot \nabla_{\Gamma_h^k} v_h \|_{0,K}^2 \right)^{1/2},$$

and coercivity of the stabilized bilinear form  $a_k^{SUPG}(\cdot, \cdot)$  in  $X^r$  can be proven. This provides unique solvability of Problem 4.2:

#### Theorem 4.8

If  $h$  is small enough to fulfil (3.9), the bilinear form  $a_k^{SUPG}(\cdot, \cdot)$  is coercive in  $X^r$ :

$$a_k^{SUPG}(v_h, v_h) \geq \frac{1}{4} \| \| v_h \| \|_{SUPG,k}^2 \quad \text{for all } v_h \in X^r$$

and Problem 4.2 is uniquely solvable.

#### Proof.

At first the result of Lemma 3.3 and the definition of  $\| \| \cdot \| \|_{SUPG,k}$  are used. It follows that:

$$\begin{aligned}
a_k^{SUPG}(v_h, v_h) &= a_k^{DCR}(v_h, v_h) \\
&\quad + \sum_{K \in \mathcal{T}_h^k} \alpha_K \left\langle -\varepsilon \Delta_{\Gamma_h^k} v_h + \mathbf{w}^E \cdot \nabla_{\Gamma_h^k} v_h + \sigma^E v_h, \mathbf{w}^E \cdot \nabla_{\Gamma_h^k} v_h \right\rangle_K \\
&\geq \frac{3}{4} \|v_h\|_{DCR,k}^2 - \sum_{K \in \mathcal{T}_h^k} \alpha_K \left\langle \varepsilon \Delta_{\Gamma_h^k} v_h, \mathbf{w}^E \cdot \nabla_{\Gamma_h^k} v_h \right\rangle_K \\
&\quad + \sum_{K \in \mathcal{T}_h^k} \alpha_K \left\langle \mathbf{w}^E \cdot \nabla_{\Gamma_h^k} v_h, \mathbf{w}^E \cdot \nabla_{\Gamma_h^k} v_h \right\rangle_K \\
&\quad + \sum_{K \in \mathcal{T}_h^k} \alpha_K \left\langle \sigma^E v_h, \mathbf{w}^E \cdot \nabla_{\Gamma_h^k} v_h \right\rangle_K \\
&\geq \frac{3}{4} \|v_h\|_{SUPG,k}^2 - \sum_{K \in \mathcal{T}_h^k} \alpha_K \left\langle \varepsilon \Delta_{\Gamma_h^k} v_h, \mathbf{w}^E \cdot \nabla_{\Gamma_h^k} v_h \right\rangle_K \\
&\quad + \sum_{K \in \mathcal{T}_h^k} \alpha_K \left\langle \sigma^E v_h, \mathbf{w}^E \cdot \nabla_{\Gamma_h^k} v_h \right\rangle_K.
\end{aligned}$$

The occurring additional terms are bounded using the Cauchy-Schwarz inequality, Young's inequality, the inverse inequality (Lemma 2.14), and (4.4):

$$\begin{aligned}
\left| \alpha_K \left\langle \varepsilon \Delta_{\Gamma_h^k} v_h, \mathbf{w}^E \cdot \nabla_{\Gamma_h^k} v_h \right\rangle_K \right| &\leq \varepsilon \alpha_K \|\Delta_{\Gamma_h^k} v_h\|_{0,K} \|\mathbf{w}^E \cdot \nabla_{\Gamma_h^k} v_h\|_{0,K} \\
&\leq \varepsilon \alpha_K h_K^{-1} c_{inv} \|\nabla_{\Gamma_h^k} v_h\|_{0,K} \|\mathbf{w}^E \cdot \nabla_{\Gamma_h^k} v_h\|_{0,K} \\
&\leq \frac{1}{\sqrt{2}} \varepsilon^{1/2} \|\nabla_{\Gamma_h^k} v_h\|_{0,K} \alpha_K^{1/2} \|\mathbf{w}^E \cdot \nabla_{\Gamma_h^k} v_h\|_{0,K} \\
&\leq \frac{1}{2} \left( \varepsilon \|\nabla_{\Gamma_h^k} v_h\|_{0,K}^2 + \frac{1}{2} \alpha_K \|\mathbf{w}^E \cdot \nabla_{\Gamma_h^k} v_h\|_{0,K}^2 \right), \\
\left| \alpha_K \left\langle \sigma^E v_h, \mathbf{w}^E \cdot \nabla_{\Gamma_h^k} v_h \right\rangle_K \right| &\leq \sigma_{0,\infty,K} \alpha_K \|v_h\|_{0,K} \|\mathbf{w}^E \cdot \nabla_{\Gamma_h^k} v_h\|_{0,K} \\
&\leq \frac{1}{\sqrt{2}} \sigma_0^{1/2} \|v_h\|_{0,K} \alpha_K^{1/2} \|\mathbf{w}^E \cdot \nabla_{\Gamma_h^k} v_h\|_{0,K} \\
&\leq \frac{1}{2} \left( \sigma_0 \|v_h\|_{0,K}^2 + \frac{1}{2} \alpha_K \|\mathbf{w}^E \cdot \nabla_{\Gamma_h^k} v_h\|_{0,K}^2 \right).
\end{aligned}$$

It follows:

$$a_h^{SUPG}(v_h, v_h) \geq \frac{3}{4} \|v_h\|_{SUPG,k}^2 - \frac{1}{2} \|v_h\|_{SUPG,k}^2 = \frac{1}{4} \|v_h\|_{SUPG,k}^2.$$

□

## 4.2.2 Error Estimates

The semi-robust estimate obtained for the standard Galerkin surface finite element method for diffusion-convection-reaction equations does not provide an optimal interpolation error for the convection term. The stabilization with SUPG enables coercivity in a stronger norm. This is used to get a higher order continuity error for the convection term and hence for the convergence estimate. This technique together with the estimate of the additional terms coming from the stabilization are topic of this section.

### Continuity Estimate

The additional term of the  $\|\cdot\|_{SUPG,k}$  compared to the  $\|\cdot\|_{DCR,k}$  enables a semi-robust estimation of  $\langle \mathbf{w}^E \cdot \nabla_{\Gamma_h^k} v_h, u^E - i^r u^E \rangle_{\Gamma_h^k}$ . Partial integration is used to shift the gradient in the convection term from the ansatz function to the test function. A higher order estimate can be obtained for the convection term.

#### Lemma 4.9

Let  $u \in H^{r+1}$  and  $v_h \in X^r$ . Then, it holds:

$$|a_k^{SUPG}(u^E - i^r u^E, v_h)| \lesssim h^r (\varepsilon^{1/2} + h^{1/2}) \|u\|_{r+1,\Gamma} \|v_h\|_{SUPG,k}.$$

#### Proof.

Setting  $\phi := u^E - i^r u^E$  and using partial integration for the convection term, it follows using a triangle inequality:

$$\begin{aligned} |a_h^{SUPG}(\phi, v_h)| &\leq \left| \varepsilon \langle \nabla_{\Gamma_h^k} \phi, \nabla_{\Gamma_h^k} v_h \rangle_{\Gamma_h^k} \right| + \left| \langle \mathbf{w}^E \cdot \nabla_{\Gamma_h^k} v_h, \phi \rangle_{\Gamma_h^k} \right| \\ &\quad + \left| \langle (\sigma^E - \nabla_{\Gamma_h^k} \cdot \mathbf{w}^E) \phi, v_h \rangle_{\Gamma_h^k} \right| + \left| \sum_{K \in \mathcal{T}_h^k} \int_{\partial K} \mathbf{w}^E \cdot \boldsymbol{\nu}_h^k \phi v_h d\mathbf{b}_h^k \right| \\ &\quad + |S_{SUPG}(\phi, v_h)| \\ &:= T_1 + T_2 + T_3 + T_4 + T_5. \end{aligned}$$

These terms are evaluated one by one.  $T_1$  is handled as in the unstabilized case by direct estimation using the Cauchy-Schwarz inequality and the interpolation properties of  $i^r$ :

$$T_1 \leq \varepsilon |\phi|_{1,\Gamma_h^k} |v_h|_{1,\Gamma_h^k} \leq \varepsilon^{1/2} h^r \|u\|_{r+1,\Gamma} \|v_h\|_{SUPG,k}.$$

The convection term is bounded making use of the stronger SUPG-triple norm and equation (4.4):

$$\begin{aligned} T_2 &= \sum_{K \in \mathcal{T}_h^k} \left\langle \mathbf{w}^E \cdot \nabla_{\Gamma_h^k} v_h, \phi \right\rangle_K \leq \sum_{K \in \mathcal{T}_h^k} \alpha_K^{-1/2} \|\phi\|_{0,K} \alpha_K^{1/2} \|\mathbf{w}^E \cdot \nabla_{\Gamma_h^k} v_h\|_{0,K^k} \\ &\lesssim h^{r+1/2} \|u\|_{r+1,\Gamma} \|v_h\|_{SUPG,k}. \end{aligned}$$

To estimate term  $T_3$ , Lemma 2.7 is utilized:

$$\begin{aligned} T_3 &\leq \|\sigma^E - \nabla_{\Gamma_h^k} \cdot \mathbf{w}^E\|_{0,\infty,\Gamma_h^k} \|\phi\|_{0,\Gamma_h^k} \|v_h\|_{0,\Gamma_h^k} \\ &\leq \left( \|\sigma - \nabla_{\Gamma} \cdot \mathbf{w}\|_{0,\infty,\Gamma} + \|(\nabla_{\Gamma} \cdot \mathbf{w})^E - \nabla_{\Gamma_h^k} \cdot \mathbf{w}^E\|_{0,\infty,\Gamma_h^k} \right) h^{r+1} \|u\|_{r+1,\Gamma} \|v_h\|_{SUPG,k} \\ &\leq \left( \|\sigma\|_{0,\infty,\Gamma} + |\mathbf{w}|_{1,\infty,\Gamma} + h^k |\mathbf{w}|_{1,\infty,\Gamma} \right) h^{r+1} \|u\|_{r+1,\Gamma} \|v_h\|_{SUPG,k} \\ &\lesssim h^{r+1} \|u\|_{r+1,\Gamma} \|v_h\|_{SUPG,k}. \end{aligned}$$

The partial integration on the non-smooth surface introduces the integrals over the element edges given in  $T_4$ . This term is estimated in the same way as term  $T_2^3$  in the proof of Lemma 4.4:

$$T_4 \leq h^{2k+r} \|u\|_{r+1,\Gamma} \|v_h\|_{SUPG,k}.$$

From (4.4) a bound for  $T_5$  is obtained:

$$\begin{aligned} T_5 &\leq \left( \sum_{K \in \mathcal{T}_h^k} \alpha_K \left( \varepsilon^2 \|\Delta_{\Gamma_h^k} \phi\|_{0,K}^2 + \|\mathbf{w}^E \cdot \nabla_{\Gamma_h^k} \phi\|_{0,K}^2 + \|\sigma \phi\|_{0,K}^2 \right) \right)^{1/2} \|v_h\|_{SUPG,k} \\ &\lesssim \left( \sum_{K \in \mathcal{T}_h^k} \alpha_K^{1/2} \left( \varepsilon^2 h^{2r-2} + \|\mathbf{w}\|_{0,\infty,\Gamma}^2 h^{2r} + \|\sigma\|_{0,\infty,\Gamma}^2 h^{2r+2} \right) \right)^{1/2} \|u\|_{r+1,\Gamma} \|v_h\|_{SUPG,k} \\ &\lesssim \left( \sum_{K \in \mathcal{T}_h^k} \left( \frac{1}{c_{inv}^2} \varepsilon h_K^{2r} + \sigma_0 \|\sigma\|_{0,\infty,\Gamma}^{-2} \|\mathbf{w}\|_{0,\infty,\Gamma}^2 h_K^{2r+1} + \sigma_0 h_K^{2r+3} \right) \right)^{1/2} \\ &\quad \times \|u\|_{r+1,\Gamma} \|v_h\|_{SUPG,h} \\ &\lesssim \left( \varepsilon^{1/2} + h^{1/2} \right) h^r \|u\|_{r+1,\Gamma} \|v_h\|_{SUPG,k}. \end{aligned}$$

Adding up everything results in the postulated estimate.  $\square$

### Consistency Error

The SUPG method is known as a consistent stabilization technique for bulk equations. The stabilization term contains the continuous formulation of the problem and thus using the exact solution as ansatz function leads to a vanishing

stabilization term. No consistency error occurs. Unfortunately, this is no longer true for surface equations. The surface operators on the given surface  $\Gamma$  are different from the ones on the discrete surface  $\Gamma_h^k$ . Therefore, geometric errors are introduced for the SUPG stabilization terms in the bilinear form and the right hand side:

**Lemma 4.10**

Let  $u \in H^2(\Gamma)$  be a solution of Problem 3.1,  $v_h \in X^r$ , and  $\alpha_K$  fulfil (4.4), then it holds:

$$\begin{aligned} & |(f_k^{SUPG}(v_h) - f_k^{DCR}(v_h)) - (a_k^{SUPG}(u^E, v_h) - a_k^{DCR}(u^E, v_h))| \\ & \lesssim h^{k+1} (\varepsilon^{1/2} + h^{1/2}) \|u\|_{1,\Gamma} \|v_h\|_{SUPG,k}. \end{aligned}$$

**Proof.**

A reordering of the terms provides:

$$\begin{aligned} & |(f_k^{SUPG}(v_h) - f_k^{DCR}(v_h)) - (a_k^{SUPG}(u^E, v_h) - a_k^{DCR}(u^E, v_h)_{DCR})| \\ & = \left| \sum_{K \in \mathcal{T}_h^k} \alpha_K \left\langle f^E, \mathbf{w}^E \cdot \nabla_{\Gamma_h^k} v_h \right\rangle_K \right. \\ & \quad \left. + \sum_{K \in \mathcal{T}_h^k} \alpha_K \left\langle -\varepsilon \Delta_{\Gamma_h^k} u^E + \mathbf{w}^E \cdot \nabla_{\Gamma_h^k} u^E + \sigma u^E, \mathbf{w}^E \cdot \nabla_{\Gamma_h^k} v_h \right\rangle_K \right| \\ & \leq \left| \sum_{K \in \mathcal{T}_h^k} \alpha_K \left\langle -\varepsilon \Delta_{\Gamma_h^k} u^E + \mathbf{w}^E \cdot \nabla_{\Gamma_h^k} u^E + \sigma u^E - f^E, \mathbf{w}^E \cdot \nabla_{\Gamma_h^k} v_h \right\rangle_K \right|. \end{aligned}$$

Due to  $u$  being a solution of the continuous diffusion-convection-reaction problem, it holds:

$$-\varepsilon \Delta_{\Gamma} u + \mathbf{w} \cdot \nabla_{\Gamma} u + \sigma u = f \quad \text{on } \Gamma.$$

This can be used to add a valid zero to the above estimate:

$$\begin{aligned} & |(f_k^{SUPG}(v_h) - f_k^{DCR}(v_h)) - (a_k^{SUPG}(u^E, v_h) - a_k^{DCR}(u^E, v_h)_{DCR})| \\ & \leq \left| \sum_{K \in \mathcal{T}_h^r} \alpha_K \left\langle -\varepsilon \Delta_{\Gamma_h^k} u^E + \mathbf{w}^E \cdot \nabla_{\Gamma_h^k} u^E + \sigma u^E - f^E, \mathbf{w}^E \cdot \nabla_{\Gamma_h^k} v_h \right\rangle_K \right. \\ & \quad \left. - \sum_{K \in \mathcal{T}_h^r} \alpha_K \left\langle (-\varepsilon \Delta_{\Gamma} u + \mathbf{w} \cdot \nabla_{\Gamma} u + \sigma u - f)^E, \mathbf{w}^E \cdot \nabla_{\Gamma_h^k} v_h \right\rangle_K \right| \end{aligned}$$

$$\begin{aligned}
&\leq \left| \sum_{K \in \mathcal{T}_h^r} \alpha_K \varepsilon \left\langle \Delta_{\Gamma_h^k} u^E - (\Delta_{\Gamma} u)^E, \mathbf{w}^E \cdot \nabla_{\Gamma_h^k} v_h \right\rangle_K \right| \\
&+ \left| \sum_{K \in \mathcal{T}_h^r} \alpha_K \left\langle \mathbf{w}^E \cdot \nabla_{\Gamma_h^k} u^E - (\mathbf{w} \cdot \nabla_{\Gamma} u)^E, \mathbf{w}^E \cdot \nabla_{\Gamma_h^k} v_h \right\rangle_K \right| \\
&+ \left| \sum_{K \in \mathcal{T}_h^r} \alpha_K \left\langle \sigma^E u^E - (\sigma u)^E, \mathbf{w}^E \cdot \nabla_{\Gamma_h^k} v_h \right\rangle_K \right| \\
&+ \left| \sum_{K \in \mathcal{T}_h^r} \alpha_K \left\langle f^E - f^E, \mathbf{w}^E \cdot \nabla_{\Gamma_h^k} v_h \right\rangle_K \right|.
\end{aligned}$$

The last two terms vanish due to  $(\sigma u)^E = \sigma^E u^E$ .

To estimate the first two summands, the results from Section 2.3 are used. The first term can be bounded with the estimate of Lemma 2.8 and formula (4.4):

$$\begin{aligned}
&\left| \sum_{K \in \mathcal{T}_h^k} \alpha_K \varepsilon \left\langle \Delta_{\Gamma_h^k} u^E - (\Delta_{\Gamma} u)^E, \mathbf{w}^E \cdot \nabla_{\Gamma_h^k} v_h \right\rangle_K \right| \\
&\lesssim \frac{h}{c_{inv}} \varepsilon^{1/2} \left( \sum_{K \in \mathcal{T}_h^k} \|\Delta_{\Gamma_h^k} u^E - (\Delta_{\Gamma} u)^E\|_{0,K}^2 \right)^{1/2} \|v_h\|_{SUPG,k} \\
&\leq h^{k+1} \varepsilon^{1/2} \frac{1}{c_{inv}} \|u\|_{2,\Gamma} \|v_h\|_{SUPG,k}.
\end{aligned}$$

The term coming from the convection part is handled by applying formula (2.12) and  $\mathbf{w}^E \cdot \mathbf{n}^E = (\mathbf{w} \cdot \mathbf{n})^E = 0$ . It follows  $\mathbf{w}^E \tilde{P}_h^r = \mathbf{w}^E$  and hence:

$$\begin{aligned}
\mathbf{w}^E \cdot \nabla_{\Gamma_h^k} u^E - (\mathbf{w} \cdot \nabla_{\Gamma} u)^E &= \mathbf{w}^E \cdot \left( \nabla_{\Gamma_h^k} u^E - (\nabla_{\Gamma} u)^E \right) \\
&= \mathbf{w}^E \tilde{P}_h^r \left( I - (I - dH)^{-1} \tilde{P}_h^r \right) \nabla_{\Gamma_h^k} u^E \\
&= \mathbf{w}^E \left( \tilde{P}_h^r - (\mu_h^r)^{-1} B_h \right) \nabla_{\Gamma_h^k} u^E.
\end{aligned}$$

It can be easily seen that Lemmas 2.11 and 2.12 provide:

$$\| \tilde{P}_h^k - (\mu_h^r)^{-1} B_h^k \|_{0,\infty,\Gamma_h^k} \leq \| \tilde{P}_h^k - B_h^k \|_{0,\infty,\Gamma_h^k} + \left\| \frac{\mu_h^k - 1}{\mu_h^k} \right\|_{0,\infty,\Gamma_h^k} \| B_h^k \|_{0,\infty,\Gamma_h^k} \lesssim h^{k+1}.$$

Employing this, the second term yields:

$$\begin{aligned}
& \left| \sum_{K \in \mathcal{T}_h^k} \alpha_K \left\langle \mathbf{w}^E \cdot \nabla_{\Gamma_h^k} u^E - (\mathbf{w} \cdot \nabla_{\Gamma} u)^E, \mathbf{w}^E \cdot \nabla_{\Gamma_h^k} v_h \right\rangle_K \right| \\
& \lesssim \|\tilde{F}_h^k - (\mu_h^k)^{-1} B_h\|_{0,\infty,\Gamma_h^k} \left( \sum_{K \in \mathcal{T}_h^k} \alpha_K \|\mathbf{w}\|_{0,\infty,\Gamma}^2 |u^E|_{1,K}^2 \right)^{1/2} \|v_h\|_{SUPG,k} \\
& \lesssim h^{k+3/2} \sigma_0^{-1/2} \|\sigma\|_{0,\infty,\Gamma}^{-1} \|\mathbf{w}\|_{0,\infty,\Gamma} \|u\|_{1,\Gamma} \|v_h\|_{SUPG,k} \\
& \lesssim h^{k+3/2} \|u\|_{1,\Gamma} \|v_h\|_{SUPG,k}.
\end{aligned}$$

Thereby, the norm equivalence (2.20) was used. Combining this with the results above proves the lemma.  $\square$

### Convergence Errors in $\|\cdot\|_{SUPG,k}$

The improved estimate of the interpolation error also leads to an improved estimate of the convergence in the corresponding triple norm. The proof is following the scheme used for the LPS, compare Theorem 4.5.

#### Theorem 4.11

Let  $u_h \in X^r$  be the solution of Problem 4.2,  $u \in H^{r+1}(\Gamma)$  the solution of Problem 3.1 and  $\alpha_K$  as given in (4.4). Assuming that  $h$  small enough to fulfil (3.9), it holds:

$$\| \|u^E - u_h\| \|_{SUPG,k} \lesssim h^{k+1} (\|u\|_{1,\Gamma} + \|f\|_{0,\Gamma}) + h^r (\varepsilon^{1/2} + h^{1/2}) \|u\|_{r+1,\Gamma}.$$

#### Proof.

Setting  $\psi = i^r(u^E) - u_h \in X^r$  and using a triangle inequality, it follows:

$$\| \|u^E - u_h\| \|_{SUPG,k} \leq \| \|u^E - i^r u^E\| \|_{SUPG,k} + \| \psi \|_{SUPG,k}.$$

The first term is bounded using the interpolation properties of  $i^r$ , see Theorem 2.15, and the bounds for  $\alpha_K$  given in (4.4):

$$\begin{aligned}
\| \|u^E - i^r u^E\| \|_{SUPG,k}^2 &= \varepsilon |u^E - i^r u^E|_{1,\Gamma_h^k}^2 + \sigma_0 \|u^E - i^r u^E\|_{0,\Gamma_h^k}^2 \\
&+ \sum_{K \in \mathcal{T}_h^k} \alpha_K \|\mathbf{w}^E \cdot \nabla_{\Gamma_h^k} (u^E - i^r u^E)\|_{0,K}^2 \\
&\lesssim \left( \varepsilon h^{2r} + \sigma_0 h^{2r+2} + h \sigma_0 \|\sigma\|_{0,\infty,\Gamma}^{-2} \|\mathbf{w}\|_{0,\infty,\Gamma}^2 h^{2r} \right) \|u\|_{r+1,\Gamma}^2 \\
&\lesssim h^{2r} (\varepsilon + h) \|u\|_{r+1,\Gamma}^2.
\end{aligned}$$

The second term is evaluated following the standard scheme, compare Theorem 3.7 or



Theorem 4.5. Using the coercivity given in Theorem 4.8, Lemma 3.6, Lemma 4.9, and Lemma 4.10 one gets:

$$\begin{aligned}
\|\psi\|_{SUPG,k}^2 &\lesssim |a_k^{SUPG}(i^r u^E - u^E, \psi)| + |a_k^{SUPG}(u^E - u_h, \psi)| \\
&\lesssim |a_k^{SUPG}(i^r u^E - u^E, \psi)| + |a_k^{SUPG}(u^E, \psi) - f_k^{SUPG}(\psi)| \\
&\lesssim h^{k+1} (\|u\|_{r+1,\Gamma} + \|f\|_{0,\Gamma}) \|\psi\|_{SUPG,k} + h^r (\varepsilon^{1/2} + h^{1/2}) \\
&\quad \times \|u\|_{r+1,\Gamma} \|\psi\|_{SUPG,k} \\
\Rightarrow \|\psi\|_{SUPG,k} &\lesssim h^{k+1} (\|u\|_{r+1,\Gamma} + \|f\|_{0,\Gamma}) + h^r (\varepsilon^{1/2} + h^{1/2}) \|u\|_{r+1,\Gamma}.
\end{aligned}$$

□

It can be seen that the SUPG stabilized finite element method for diffusion-convection-reaction equations provides the same order of convergence as the LPS stabilized method. But it requires the evaluation of the Laplace-Beltrami operator for the mapped finite element space. This is quite complex to implement, see formula (2.13). Additionally, the Laplace-Beltrami operator has to be evaluated for every integration point used in numerical integration. This leads to increasing assembling costs. Otherwise, the LPS is based on the fluctuations of ansatz and test functions, which also have to be calculated. But this can be reduced to the assembling of a matrix of size  $\dim(\widehat{D}^r) \times \dim(\widehat{D}^r)$  and the calculation of the fluctuations of the reference basis functions. Therefore, the LPS stabilization technique is favoured here.

### Convergence Error in $L^2$ - and $H^1$ -norm

Due to the definition of the triple norm  $\|\cdot\|_{SUPG,k}$ , estimates in the  $H^1$ - and  $L^2$ -norm can directly be obtained from the estimate presented in Theorem 4.11.

#### Corollar 4.12

Let  $u_h \in X^r$  be the discrete solution of the Problem 4.2,  $u \in H^{r+1}(\Gamma)$  the solution of the Problem 3.1 and  $\alpha_K$  as given in (4.4). Assuming that  $h$  is small enough to fulfil (3.9), it holds:

$$\|u - u_h^L\|_{0,\Gamma} \lesssim h^{k+1} (\|u\|_{1,\Gamma} + \|f\|_{0,\Gamma}) + h^r (\varepsilon^{1/2} + h^{1/2}) \|u\|_{r+1,\Gamma}.$$

and

$$|u - u_h^L|_{1,\Gamma} \lesssim h^{k+1} \varepsilon^{-1/2} (\|u\|_{1,\Gamma} + \|f\|_{0,\Gamma}) + h^r (1 + \varepsilon^{-1/2} h^{1/2}) \|u\|_{r+1,\Gamma}.$$

### 4.2.3 SUPG for Diffusion-Convection Equations

Using the SUPG approach for diffusion-convection equations, coercivity in the corresponding stronger norm can be proven in the same way as for diffusion-convection-reaction equations. This provides a higher stability of the discrete solution than for the standard Galerkin approach. Nevertheless, recalling that the continuity error for the convection term is already of order  $r + 1$ , an improvement of the interpolation and hence the convergence error is not possible. Further, the SUPG stabilization does not allow the improvement towards a semi-robust estimate, because no  $L^2$ -control is provided by the stabilization term.

## Chapter 5

# Mixed Boundary Conditions

After studying diffusion-convection-reactions and diffusion-convection equations on closed surfaces and their stabilizations, open surfaces  $\Gamma$  with a  $C^{r+1}$  boundary  $\partial\Gamma$  are considered.

The boundary is assumed to consist of a relatively open Neumann boundary part  $(\partial\Gamma)_N$  and a Dirichlet boundary part  $(\partial\Gamma)_D = \Gamma \setminus (\partial\Gamma)_N$ . The boundary conditions are given by:

$$u = 0 \quad \text{on } (\partial\Gamma)_D, \quad (5.1)$$

$$\varepsilon \nabla_\Gamma u \cdot \boldsymbol{\nu} = u_N \quad \text{on } (\partial\Gamma)_N \quad (5.2)$$

for a given function  $u_N \in H^{-1/2}((\partial\Gamma)_N)$ .

### Notice 5.0.1

*The restriction to homogeneous Dirichlet boundary conditions is owed to readability. Inhomogeneous Dirichlet boundary conditions can be handled following the same steps as used to incorporate the additional condition into the diffusion-convection problem, compare Section 3.2. First, a function  $\tilde{u} \in H^2(\Gamma)$ , which fulfils the inhomogeneous Dirichlet boundary conditions, is required. Then, the problem is rewritten into an equivalent formulation to get  $u - \tilde{u}$ . This formulation provides homogeneous Dirichlet boundary conditions.*

Further, an inflow boundary  $(\partial\Gamma)^-$  and an outflow boundary  $(\partial\Gamma)^+$  are defined via:

$$(\partial\Gamma)^- = \{\mathbf{x} \in \partial\Gamma \mid \mathbf{w} \cdot \boldsymbol{\nu} < 0\},$$

$$(\partial\Gamma)^+ = \{\mathbf{x} \in \partial\Gamma \mid \mathbf{w} \cdot \boldsymbol{\nu} > 0\} \quad \text{and}$$

$$(\partial\Gamma)^0 = \partial\Gamma \setminus ((\partial\Gamma)^- \cup (\partial\Gamma)^+) = \{\mathbf{x} \in \partial\Gamma \mid \mathbf{w} \cdot \boldsymbol{\nu} = 0\},$$

where  $\boldsymbol{\nu}$  is the co-normal to the boundary  $\partial\Gamma$  as introduced in Section 1.2. As it is common for equations with mixed boundary conditions in the bulk, see e.g. [56], it is assumed that the inflow boundary is contained in the Dirichlet boundary

part:

$$(\partial\Gamma)^- \subset (\partial\Gamma)_D.$$

In the following, the incorporation of the two different boundary conditions is shown for the case of the diffusion-convection-reaction equation in Section 5.1. Unique solvability of the upcoming weak and discretized formulations is proven and the additional terms occurring in the error estimates are evaluated. The main work flow can be taken over for diffusion-convection equations. The situations, where a special treatment is needed, will be pointed out in Section 5.2.

## 5.1 Boundary Conditions for the Diffusion-Convection-Reaction Equation

To demonstrate the handling of open surfaces and the corresponding boundary conditions the LPS stabilized diffusion-convection-reaction problem is considered throughout this section. The presented results transfer to the unstabilized problem by setting the stabilization parameter  $\alpha$  to zero. To handle SUPG stabilized equations the same scheme can be used based on the analysis from Section 4.2. The main issues occurring with open surfaces  $\Gamma$  are the evaluation of integrals over the boundary and the incorporation of the given boundary conditions. The homogeneous Dirichlet boundary conditions are introduced strongly by restriction of the ansatz and the test space to  $V_D$ :

$$V_D = \{u \in H^1(\Gamma) \mid u = 0 \text{ on } (\partial\Gamma)_D\}.$$

In contrast to Dirichlet boundary conditions, Neumann boundary conditions are introduced weakly. Remember, that the diffusion part of the continuous equation, after multiplying with a test function and integration over  $\Gamma$ , has been partially integrated. For a closed surface no boundary integrals occur. But for surfaces with a boundary:

$$-\varepsilon \langle \Delta_\Gamma u, v \rangle_\Gamma = \varepsilon \langle \nabla_\Gamma u, \nabla_\Gamma v \rangle_\Gamma - \varepsilon \int_{\partial\Gamma} \nabla_\Gamma u \cdot \boldsymbol{\nu} v \, d\mathbf{b}$$

is obtained. On the boundary part, where Dirichlet boundary conditions are given, the test functions  $v$  are set to zero. The boundary integrals reduce to an integral over  $(\partial\Gamma)_N$  and  $\varepsilon \nabla_\Gamma u \cdot \boldsymbol{\nu} = u_N$  can be plugged in:

### **Problem 5.1 (Weak Problem with Boundary Conditions)**

Find  $u \in V_D$  such that for all  $v \in V_D$

$$a^{DCR}(u, v) = f^{DCR}(v) + \int_{(\partial\Gamma)_N} u_N v \, d\mathbf{b}.$$

Coercivity of the bilinear form  $a^{DCR}$  is already proven in Lemma 3.1. The unique solvability of Problem 5.1 is given by the next Lemma:

**Lemma 5.1**

*Problem 5.1 is uniquely solvable.*

**Proof.**

From the proof of Lemma 3.1 it is already known that  $a^{DCR}$  is bilinear and continuous. Additional, the bilinear form is coercive in  $V = H^1(\Gamma)$  and thus in  $V_D$ . The right hand side  $f^{DCR}(v) + \int_{(\partial\Gamma)_N} u_N v d\mathbf{b}$  is linear in  $v$  and continuous for every fixed  $u_N$ . Therefore, unique solvability of Problem 5.1 follows from the Lax-Milgram Theorem.  $\square$

### 5.1.1 Discretized Formulation

To discretize the problem a discretization of the Dirichlet boundary  $(\partial\Gamma_h^k)_D$  and the Neumann boundary  $(\partial\Gamma_h^k)_N$  are needed, such that  $(\partial\Gamma_h^k)_D \cup (\partial\Gamma_h^k)_N = \partial\Gamma_h^k$ . Therefore, it is assumed that the boundary conditions are defined element-wise. Then, there exist boundary edges  $E_i \in \mathcal{E}_{h,B}^k$  such that  $\mathbf{p}(\bigcup E_i) = (\partial\Gamma)_D$ , where  $\mathbf{p}$  is the closest point projection from the discrete surface  $\Gamma_h^k$  to the smooth surface  $\Gamma$  introduced in Section 2.1. The union of these edges is set as the discretized Dirichlet boundary  $\bigcup E_i = (\partial\Gamma_h^k)_D$ .

The discrete Neumann boundary is given as  $(\partial\Gamma_h^k)_N = \partial\Gamma_h^k \setminus (\partial\Gamma_h^k)_D$ . By construction it follows that:

$$\mathbf{p}((\partial\Gamma_h^k)_N) = \mathbf{p}(\partial\Gamma_h^k \setminus (\partial\Gamma_h^k)_D) = \partial\Gamma \setminus (\partial\Gamma)_D = (\partial\Gamma)_N.$$

Thus, the function  $u_N$  can simply be extended to the discrete surface via:

$$u_{N,h} = u_N^E.$$

In the same way as it was done for the smooth setting, the discrete in- and outflow boundaries are set to:

$$\begin{aligned} (\partial\Gamma_h^k)^- &= \{\mathbf{x} \in \partial\Gamma_h^k \mid \mathbf{w}^E \cdot \boldsymbol{\nu}_h^k < 0\}, \\ (\partial\Gamma_h^k)^+ &= \{\mathbf{x} \in \partial\Gamma_h^k \mid \mathbf{w}^E \cdot \boldsymbol{\nu}_h^k > 0\} \quad \text{and} \\ (\partial\Gamma_h^k)^0 &= \partial\Gamma_h^k \setminus \left( (\partial\Gamma_h^k)^- \cup (\partial\Gamma_h^k)^+ \right) = \{\mathbf{x} \in \partial\Gamma_h^k \mid \mathbf{w}^E \cdot \boldsymbol{\nu}_h^k = 0\}, \end{aligned}$$

where  $\boldsymbol{\nu}_h^k$  is the discrete co-normal to the boundary  $\partial\Gamma_h^k$ . As for the boundary parts on  $\Gamma$  it is assumed that the discrete inflow boundary is contained in the discretized Dirichlet boundary part:

$$(\partial\Gamma_h^k)^- \subset (\partial\Gamma_h^k)_D.$$

Recalling the LPS stabilized diffusion-convection-reaction problem 4.1, the problem formulation on an open surface reads:

**Problem 5.2 (Stabilized Problem with Boundary Conditions)**

Find  $u_h \in X_D^r = \{u_h \in X^r \mid u_h = 0 \text{ on } (\partial\Gamma_h^k)_D\}$  such that for all  $v_h \in X_D^r$

$$a_k^{LPS}(u_h, v_h) = f_k^{LPS}(v_h) + \int_{(\partial\Gamma_h^k)_N} u_N^E v d\mathbf{b}_h^k.$$

Coercivity of the bilinear form  $a_h^{LPS}$  in  $X^r$  has already been proven in the  $\|\cdot\|_{LPS,k}$ -norm in Lemma 4.1, but is shown here for a stronger triple norm including boundary integrals:

$$\|v_h\|_{BC,k} = \left( \|v_h\|_{LPS,h}^2 + \frac{1}{2} \|\mathbf{w}^E \cdot \boldsymbol{\nu}_h^k\|_{0,(\partial\Gamma_h^k)_N}^2 \right)^{1/2}.$$

**Lemma 5.2**

For  $h$  small enough the bilinear form  $a_k^{LPS}$  is coercive in  $X_D^r$ :

$$a_k^{LPS}(v_h, v_h) \geq \frac{3}{4} \|v_h\|_{BC,k}^2 \quad \forall v_h \in X_D^r$$

and Problem 5.2 is uniquely solvable.

**Proof.**

First, the coercivity of the bilinear form is proven. As in the proof of Lemma 3.1 the convection term is partially integrated. For an open surface not only integrals over inner edges but additional integrals over the boundary edges occur:

$$\begin{aligned} a_k^{LPS}(v_h, v_h) &= \varepsilon \left\langle \nabla_{\Gamma_h^k} v_h, \nabla_{\Gamma_h^k} v_h \right\rangle_{\Gamma_h^k} + \left\langle \mathbf{w}^E \cdot \nabla_{\Gamma_h^k} v_h, v_h \right\rangle_{\Gamma_h^k} + \langle \sigma^E v_h, v_h \rangle_{\Gamma_h^k} + S_k^{LPS}(v_h, v_h) \\ &\geq \varepsilon \|\nabla_{\Gamma_h^k} v_h\|_{0,\Gamma_h^k}^2 + \frac{1}{2} \left\langle \mathbf{w}^E \cdot \nabla_{\Gamma_h^k} v_h, v_h \right\rangle_{\Gamma_h^k} - \frac{1}{2} \left\langle \mathbf{w}^E \cdot \nabla_{\Gamma_h^k} v_h, v_h \right\rangle_{\Gamma_h^k} \\ &\quad + \left\langle \left( \sigma^E - \frac{1}{2} \nabla_{\Gamma_h^k} \cdot \mathbf{w}^E \right) v_h, v_h \right\rangle_{\Gamma_h^k} + \frac{1}{2} \sum_{E \in \mathcal{E}_{h,I}^k} \int_E P \mathbf{w}^E \cdot (\boldsymbol{\nu}^+ + \boldsymbol{\nu}^-) v_h^2 d\mathbf{b}_h^k \\ &\quad + \frac{1}{2} \sum_{E \in \mathcal{E}_{h,B}^k} \int_E \mathbf{w}^E \cdot \boldsymbol{\nu}_h^k v_h^2 d\mathbf{b}_h^k + S_k^{LPS}(v_h, v_h). \end{aligned}$$

In the proofs of Lemma 3.3 and Lemma 4.1 nearly all of the summands have already been estimated. Using these estimates leads to:

$$a_k^{LPS}(v_h, v_h) \geq \frac{3}{4} \|v_h\|_{LPS,k}^2 + \frac{1}{2} \sum_{E \in \mathcal{E}_{h,B}^k} \int_E \mathbf{w}^E \cdot \boldsymbol{\nu}_h^k v_h^2 d\mathbf{b}_h^k.$$

Recalling that the boundary conditions are given element-wise and  $v_h = 0$  on the

Dirichlet boundary yields:

$$\sum_{E \in \mathcal{E}_{h,B}^k} \int_E \mathbf{w}^E \cdot \boldsymbol{\nu}_h^k v_h^2 d\mathbf{b}_h^k = \sum_{E \in (\partial\Gamma_h^k)_N} \int_E \mathbf{w}^E \cdot \boldsymbol{\nu}_h^k v_h^2 d\mathbf{b}_h^k.$$

Since the discrete inflow boundary is assumed to be contained in the discretized Dirichlet boundary  $(\partial\Gamma_h^k)_D$ , it holds  $\mathbf{w}^E \cdot \boldsymbol{\nu}_h^k \geq 0$  on the discretized Neumann boundary  $(\partial\Gamma_h^k)_N$ . Thus, it can be concluded:

$$\sum_{E \in \mathcal{E}_{h,B}^k} \int_E \mathbf{w}^E \cdot \boldsymbol{\nu}_h^k v_h^2 d\mathbf{b}_h^k = \| |\mathbf{w}^E \cdot \boldsymbol{\nu}_h^k|^{1/2} v_h \|_{0,(\partial\Gamma_h^k)_N}^2$$

and hence

$$a_k^{LPS}(v_h, v_h) \geq \frac{3}{4} \| \|v_h\| \|_{LPS,k}^2 + \frac{1}{2} \| |\mathbf{w}^E \cdot \boldsymbol{\nu}_h^k|^{1/2} v_h \|_{0,(\partial\Gamma_h^k)_N}^2 \geq \frac{3}{4} \| \|v_h\| \|_{BC,k}^2.$$

The unique solvability follows directly using the Lax-Milgram Theorem. □

## 5.1.2 Error Estimates

The error between the solution  $u$  of the weak problem 5.1 and the solution  $u_h$  of the stabilized problem 5.2 on surfaces with boundary is studied in this section. Thereby, several intermediate results can be taken from the analysis of LPS stabilized problems on closed surfaces. Here, only the estimates of the newly introduced terms is discussed. For already presented estimates only a reference is provided.

### Continuity Error

At first we take a look on the continuity error. The continuity error only depends on the bilinear form  $a_k^{LPS}$  and is not influenced by the right hand side of the problem formulation. But partial integration was used in the proof of Theorem 4.4. From this, integrals over element edges have to be evaluated. For open surfaces, integrals over boundary edges occur and have to be bounded. This can be handled using the additional term of the  $\| \cdot \|_{BC,k}$ -norm.

#### Lemma 5.3

Let  $u \in H^{r+1}(\Gamma)$ ,  $v_h \in X_D^r$ , (A1)–(A3) be fulfilled and  $j^r$  be the interpolator given in Lemma 4.2. Then, for  $\alpha_K = \alpha^2 h_K$  the following holds:

$$|a_k^{LPS}(u^E - j^r u^E, v_h)| \lesssim h^r (\varepsilon^{1/2} + h^{1/2}) \|u\|_{r+1,\Gamma} \|v_h\|_{BC,k}.$$

**Proof.**

The proof can mainly be taken from Lemma 4.4. Having a look at the proof of that lemma, most of the terms are evaluated without using that  $\Gamma$  is a closed surface and can be taken over without further changes. Only the evaluation of the integrals over element edges coming from partial integration has to be considered separately. Let again  $\psi := u^E - j^r u^E$ , then referring to the numbering introduced in the proof of Lemma 4.4:

$$\begin{aligned} T_2^3 &= \left| \sum_{K \in \mathcal{T}_h^k} \int_{\partial K} v_h \psi \mathbf{w}^E \cdot \boldsymbol{\nu}_h^k d\mathbf{b}_h^k \right| \\ &\leq \left| \sum_{E \in \mathcal{E}_{h,I}^k} \int_E v_h \psi \mathbf{w}^E \cdot (\boldsymbol{\nu}^+ - \boldsymbol{\nu}^-) d\mathbf{b}_h^k \right| + \left| \sum_{E \in \mathcal{E}_{h,B}^k} \int_E v_h \psi \mathbf{w}^E \cdot \boldsymbol{\nu}_h^k d\mathbf{b}_h^k \right|. \end{aligned}$$

The first integral over the inner edges can be bounded as in the proof of Lemma 4.4 by:

$$\left| \sum_{E \in \mathcal{E}_{h,I}^k} \int_E v_h \psi \mathbf{w}^E \cdot (\boldsymbol{\nu}^+ + \boldsymbol{\nu}^-) d\mathbf{b}_h^k \right| \lesssim h^{r+2k} \|u\|_{r+1,\Gamma} \|v_h\|_{LPS,k}.$$

To evaluate the integral over the boundary edges, it is used, that  $v_h = 0$  on  $(\partial\Gamma_h^k)_D$  and that the discrete inflow boundary  $(\partial\Gamma_h^k)^-$  is assumed to be part of the discrete Dirichlet boundary. Therefore,  $\mathbf{w}^E \cdot \boldsymbol{\nu}_h^k \geq 0$  on  $(\partial\Gamma_h^k)_N$  and it follows:

$$\begin{aligned} \left| \sum_{E \in \mathcal{E}_{h,B}^k} \int_E v_h \psi \mathbf{w}^E \cdot \boldsymbol{\nu}_h^k d\mathbf{b}_h^k \right| &= \left| \sum_{E \in (\partial\Gamma_h^k)_N} \int_E v_h \psi \mathbf{w}^E \cdot \boldsymbol{\nu}_h^k d\mathbf{b}_h^k \right| \\ &\lesssim \left| \sum_{E \in (\partial\Gamma_h^k)_N} \int_E v_h \psi |\mathbf{w}^E \cdot \boldsymbol{\nu}_h^k| d\mathbf{b}_h^k \right| \\ &\lesssim \|\mathbf{w}\|_{0,\infty,\Gamma}^{1/2} \left| \sum_{E \in (\partial\Gamma_h^k)_N} \int_E v_h \psi |\mathbf{w}^E \cdot \boldsymbol{\nu}_h^k|^{1/2} d\mathbf{b}_h^k \right| \\ &\lesssim \|\psi\|_{0,(\partial\Gamma_h^k)_N} \|v_h\|_{BC,k}. \end{aligned}$$

Using the trace inequality for  $\psi$  provides:

$$\left| \sum_{E \in \mathcal{E}_{h,B}^k} \int_E v_h \psi \mathbf{w}^E \cdot \boldsymbol{\nu}_h^k d\mathbf{b}_h^k \right| \lesssim h^{r+1/2} \|u\|_{r+1,\Gamma} \|v_h\|_{BC,k}.$$

Together with the results from Lemma 4.4 the lemma can be concluded.  $\square$



### Consistency Estimate

In the estimate of the consistency error, the additional term on the right hand side of the problem formulation has to be bounded. But no partial integration was used to prove the consistency estimate of the LPS stabilized problem, compare Lemma 4.3.

#### Lemma 5.4

Let  $u \in V_D \cap H^{r+1}$  be the solution of Problem 5.1,  $\alpha_K = \alpha^2 h_K$  and (A1) be fulfilled, then it holds for all  $v_h \in X_D^r$ :

$$\begin{aligned} \left| f_k^{LPS}(v_h) + \int_{(\partial\Gamma_h^k)_N} u_N^E v \, d\mathbf{b}_h^k - a_k^{LPS}(u^E, v_h) \right| \\ \lesssim h^r (\varepsilon^{1/2} + h^{1/2}) \|u\|_{r+1,\Gamma} \|v_h\|_{BC,k} \\ + h^{k+1} (\|u\|_{1,\Gamma} + \|f\|_{0,\Gamma} + \|u_N\|_{0,(\partial\Gamma)_N}) \|v_h\|_{BC,k}. \end{aligned}$$

#### Proof.

At first it is used that  $u$  is a solution of Problem 5.1. This yields:

$$\begin{aligned} \left| f_k^{LPS}(v_h) + \int_{(\partial\Gamma_h^k)_N} u_N^E v \, d\mathbf{b}_h^k - a_k^{LPS}(u^E, v_h) \right| \\ = \left| f_k^{LPS}(v_h) + \int_{(\partial\Gamma_h^k)_N} u_N^E v_h \, d\mathbf{b}_h^k - a_k^{LPS}(u^E, v_h) \right. \\ \left. - f^{DCR}(v_h^L) - \int_{(\partial\Gamma)_N} u_N v_h^L \, d\mathbf{b} + a^{DCR}(u, v_h^L) \right| \\ \leq \left| (f_k^{LPS}(v_h) - f^{DCR}(v_h^L)) - (a_k^{LPS}(u^E, v_h) - a^{DCR}(u, v_h^L)) \right| \\ + \left| \int_{(\partial\Gamma_h^k)_N} u_N^E v_h \, d\mathbf{b}_h^k - \int_{(\partial\Gamma)_N} u_N v_h^L \, d\mathbf{b} \right|. \end{aligned}$$

The first term is evaluated combining Lemma 3.6 and Lemma 4.3:

$$\begin{aligned} \left| (f_k^{LPS}(v_h) - f^{DCR}(v_h^L)) - (a_k^{LPS}(u^E, v_h) - a^{DCR}(u, v_h^L)) \right| \\ \lesssim h^{r+1/2} \|u\|_{r+1,\Gamma} \|v_h\|_{LPS,k} + h^{k+1} (\|u\|_{1,\Gamma} + \|f\|_{0,\Gamma}) \|v_h\|_{DCR,k} \\ \lesssim h^{r+1/2} \|u\|_{r+1,\Gamma} \|v_h\|_{BC,k} + h^{k+1} (\|u\|_{1,\Gamma} + \|f\|_{0,\Gamma}) \|v_h\|_{BC,k}. \end{aligned}$$

The last term to estimate is the boundary term, where Lemma 2.11, the trace inequality

(Lemma 2.13), and the inverse inequality (Lemma 2.14) are used:

$$\begin{aligned} \left| \int_{(\partial\Gamma_h^k)_N} u_N^E v_h d\mathbf{b}_h^k - \int_{(\partial\Gamma)_N} u_N v_h^L d\mathbf{b} \right| &= \left| \int_{(\partial\Gamma_h^k)_N} u_N^E v_h (1 - \theta_h^k) d\mathbf{b}_h^k \right| \\ &\lesssim h^{k+1} \|u_N^E\|_{0,(\partial\Gamma_h^k)_N} \|v_h\|_{0,(\partial\Gamma_h^k)_N} \\ &\lesssim h^{k+1/2} \|u_N\|_{0,(\partial\Gamma)_N} \|v_h\|_{0,\Gamma_h^k} \\ &\lesssim h^{k+1/2} \|u_N\|_{0,(\partial\Gamma)_N} \|v_h\|_{BC,k}. \end{aligned}$$

□

### Convergence Error in $\|\cdot\|_{BC,k}$

After the estimate of the continuity and the consistency errors, the convergence error for the difference of  $u$  and  $u_h$  can be evaluated in the  $\|\cdot\|_{BC,k}$ -norm.

#### Theorem 5.5

Let  $u \in V_D \cap H^{r+1}(\Gamma)$  be a solution of Problem (5.1) and  $u_h \in X_D^r$  a solution of Problem (5.2). Further let  $h$  be small enough to fulfil (3.9),  $\alpha_K = \alpha^2 h_K$ , and assumptions (A1)-(A3) be fulfilled. Then, it can be concluded that:

$$\| \|u_0^E - u_{h,0}\| \|_{BC,k} \lesssim h^r (\varepsilon^{1/2} + h^{1/2}) \|u\|_{r+1,\Gamma} + h^{k+1} (\|u\|_{1,\Gamma} + \|f\|_{0,\Gamma} + \|u_N\|_{0,(\partial\Gamma)_N}).$$

#### Proof.

In a first step the error is split up using a triangle inequality:

$$\| \|u^E - u_h\| \|_{BC,k} \leq \| \|u^E - j^r(u^E)\| \|_{BC,k} + \| \|j^r(u^E) - u_h\| \|_{BC,k}.$$

The first summand is estimated using the interpolation properties of  $j^r$  given in Lemma 4.2 and the trace inequality (Lemma 2.13):

$$\begin{aligned} \| \|u^E - j^r(u^E)\| \|_{BC,k}^2 &= \| \|u^E - j^r(u^E)\| \|_{LPS,k}^2 + \| |\mathbf{w}^E \cdot \boldsymbol{\nu}_h^k|^{1/2} (u^E - j^r(u^E)) \|_{(0,\partial\Gamma_h^k)_N}^2 \\ &\lesssim h^{2r} (\varepsilon + h) \|u\|_{r+1,\Gamma}^2 + h^{2r+1} \|u\|_{r+1,\Gamma}^2, \end{aligned}$$

where the estimate of the first term is taken from the proof of Lemma 4.5.

For the second term  $\psi := j^r(u^E) - u_h$  is introduced. Obviously,  $\psi \in X_D^r$ . The coercivity of  $a_k^{LPS}(\cdot, \cdot)$  in  $X_D^r$ , compare Lemma 5.1, is used:

$$\begin{aligned} \| \|j^r(u^E) - u_h\| \|_h^2 &\lesssim a_h(j^r(u^E) - u_h, \psi) \\ &= a_h(j^r(u^E) - u^E, \psi) + a_h(u^E - u_h, \psi) \end{aligned}$$

The different terms of the sum can be bounded using Lemma 5.3 and Lemma 5.4. Adding everything up proves the theorem. □

It can be seen that the same convergence order can be obtained for diffusion-convection-reaction equations on closed and open surfaces. Furthermore, one can observe that Neumann boundary conditions influence the error in the same way as the right hand side due to the weak incorporation of the Neumann boundary conditions.

### Convergence Error in $L^2$ and $H^1$

The estimation of  $u^E - u_h$  in the problem dependent discrete triple norm also enables evaluations in the  $L^2$ - and the  $H^1$ -norm for diffusion-convection-reaction problems.

#### Corollar 5.6

Let  $u \in V_D \cap H^{r+1}(\Gamma)$  solve Problem 5.1 and  $u_h \in X_D^r$  solve Problem 5.2. Further let  $h$  be small enough to fulfil (3.9),  $\alpha_K = \alpha^2 h_K$ , and assumptions (A1)-(A3) be fulfilled. Then, it can be concluded that:

$$\|u - u_h^L\|_{0,\Gamma} \lesssim h^r (\varepsilon^{1/2} + h^{1/2}) \|u\|_{r+1,\Gamma} + h^{k+1} (\|u\|_{r+1,\Gamma} + \|f\|_{0,\Gamma} + \|u_N\|_{0,\Gamma})$$

and

$$|u - u_h^L|_{1,\Gamma} \lesssim h^r (1 + \varepsilon^{-1/2} h^{1/2}) \|u\|_{r+1,\Gamma} + h^{k+1} \varepsilon^{-1/2} (\|u\|_{r+1,\Gamma} + \|f\|_{0,\Gamma} + \|u_N\|_{0,\Gamma}).$$

#### Proof.

From the norm equivalences and the definition of the triple norm  $\|\cdot\|_{BC,k}$  it follows:

$$\|u - u_h^L\|_{0,\Gamma} \lesssim \|u^E - u_h\|_{0,\Gamma_h^k} \leq \|u_0^E - u_{h,0}\|_{BC,k}$$

and

$$|u - u_h|_{1,\Gamma} \lesssim |u^E - u_h|_{1,\Gamma_h^k} \leq \varepsilon^{-1/2} \|u_0^E - u_{h,0}\|_{BC,k}.$$

Together with Theorem 5.5 the postulated result can be concluded.  $\square$

## 5.2 Boundary Conditions for the Diffusion-Convection Equation

Now, the diffusion-convection equation on surfaces with boundary is considered:

$$\begin{aligned} -\varepsilon \Delta_\Gamma u + \mathbf{w} \cdot \nabla_\Gamma u &= f \quad \text{on } \Gamma, \\ u &= 0 \quad \text{on } (\partial\Gamma)_D, \\ \varepsilon \nabla_\Gamma u \cdot \boldsymbol{\nu} &= u_N \quad \text{on } (\partial\Gamma)_N. \end{aligned}$$

In this case, the existence or nonexistence of Dirichlet boundary conditions, e.g. the measure of  $(\partial\Gamma)_D$ , plays an important role for the error analysis.

First, the case of only Neumann boundary conditions ( $|\partial\Gamma)_D| = 0$ ) is considered. As in the case of diffusion-convection equations on closed surfaces, an additional condition is needed to provide coercivity and get uniqueness of the solution. Thereby, the triple norm is not enriched as it is done for diffusion-convection-reaction equations on open surfaces. Therefore, the error analysis follows the techniques presented in Section 3.2.3. The additional integrals over the boundary edges in the different estimates can be evaluated as follows :

- Interpolation error:

$$\begin{aligned} \int_{(\partial\Gamma_h^k)_N} \mathbf{w}^E \cdot \boldsymbol{\nu}_h^k \psi v_h d\mathbf{b}_h^k &\lesssim \|\mathbf{w}\|_{0,\infty,\Gamma} \|\psi\|_{0,(\partial\Gamma_h^k)_N} \|v_h\|_{0,(\partial\Gamma_h^k)_N} \\ &\lesssim h^r \|u\|_{r+1,\Gamma} |v_h|_{1,\Gamma_h^k} \\ &\lesssim h^r \varepsilon^{-1/2} \|u\|_{r+1,\Gamma} \|v_h\|_{DC,k}. \end{aligned}$$

- Consistency error:

$$\begin{aligned} \left| \int_{(\partial\Gamma_h^k)_N} u_{N,h} v_h d\mathbf{b}_h^k - \int_{(\partial\Gamma)_N} u_N v_h^L d\mathbf{b} \right| &\lesssim \left| \int_{(\partial\Gamma_h^k)_N} u_N^E v_h - u_N^E v_h \theta_h^k d\mathbf{b}_h^k \right| \\ &\lesssim h^{k+1/2} \|u_N\|_{0,(\partial\Gamma)_N} |v_h|_{1,\Gamma_h^k} \\ &\lesssim h^{k+1/2} \varepsilon^{-1/2} \|u_N\|_{0,\partial\Gamma} \|v_h\|_{DC,k}. \end{aligned}$$

Here, the norm equivalences (2.19)–(2.20), the trace inequality (Lemma 2.13) and the inverse inequality (Lemma 2.14) are used. Convergence results follow in the same way as in Theorem 3.15 and Corollar 3.17.

If Dirichlet boundary conditions are defined on a Dirichlet boundary part  $(\partial\Gamma)_D$  of positive measure, the Poincare inequality holds in  $V_D$  and  $X_D^r$ . Then, the triple norms  $\|\cdot\|_{DC}$  and  $\|\cdot\|_{DC,k}$  are norms in  $V_D$  and  $X_D^r$ , respectively. Unique solvability is obtained and no additional condition is needed. The error analysis now follows the scheme given in Section 5.1. Only three small adjustments have to be considered:

- The discrete triple norm is not enriched by the additional boundary term  $\|\mathbf{w}^E \cdot \boldsymbol{\nu}_h^k\|_{0,(\partial\Gamma_h^k)_N}^{1/2} v_h$ . Instead the boundary integrals are estimated as shown above.
- The inequality  $\|\cdot\|_{0,\Gamma_h^k} \lesssim \sigma_0^{-1/2} \|\cdot\|_{LPS,BC}$  used in the analysis of the diffusion-convection-reaction problem has to be replaced by

$$\|\cdot\|_{0,\Gamma_h^k} \lesssim |\cdot|_{1,\Gamma_h^k} \lesssim \varepsilon^{-1/2} \|\cdot\|_{DC,h}.$$

The obtained estimates are no longer semi-robust.

- No reaction and stabilization terms have to be considered.

# Chapter 6

## Numerical Results

A code, written in the Julia programming language, for surface finite elements has been developed by the author. It is able to handle 2- and 3-dimensional problems and includes Local Projection Stabilization techniques. The first section of this chapter provides a rough overview of the implementation techniques provided by Julia and used in the finite element code. Further the actual implemented setting is described and possible enhancements are pointed out.

The following sections are dedicated to different numerical examples. At first a diffusion-reaction equation with a known exact solution and continuous right hand side is considered. The numerically obtained convergence orders of by the LPS stabilized and unstabilized finite element method are compared to the theoretical results. The impact of surface and solution space approximation is discussed. In Section 6.3 a diffusion-reaction equation with a discontinuous right hand side on an closed 1D surface in  $\mathbb{R}^2$  is studied. The discontinuity leads to a layer in the solution for small diffusion parameters. A diffusion-convection equation on a bounded 2D surface in  $\mathbb{R}^3$  is studied in Section 6.4. There, a discontinuous Dirichlet boundary condition at the inflow boundary provides an internal layer along the corresponding streamlines. In the example shown in the last section a boundary layer develops due to non fitting Dirichlet boundary conditions at the outflow boundary. Around all of the described layers oscillations occur for finite element methods if the mesh is not fine enough. The power of the introduced LPS method to suppress and localize these oscillations is shown.

### 6.1 Implementation

In connection with the presented numerical analysis, a code for Local Projection Stabilization for surface finite elements has been developed. A couple of different objectives have been taken into account: the code should be fast, flexible, maintainable, and enhanceable but still compact and easy to implement. An attempt to meet all of these claims was carried out by choosing the programming language

Julia [7], which is still under development. Julia calls itself a

high-level, high-performance dynamic programming language for technical computing, with syntax that is familiar to users of other technical computing environments <sup>1</sup>

and is a relatively young open source language licensed under the MIT license. Most of the syntax is very close to the Matlab syntax and therefore easy to read and write for those already familiar with Matlab or Octave.

Julia provides several further advantages and possibilities, which have widely been used in the concept of the code:

- LLVM-based just-in-time compiler

Julia is an interpreted programming language with a just-in-time compiler. The code is compiled on-the-fly and executed without the need to create an executable file inbetween. This enables a performance comparable to high-level programming languages as C or Fortran.

- Function Overloading

Julia enables function overloading. Functions are not only given by their name but by their name and set of parameters. One function with the same name can be implemented for different parameter sets in a different ways without a tremendous usage of if-else constructions.

This is used for example to provide a refinement function for 1D and a refinement function for 2D meshes. The refinement function can be called without distinguishing between the different dimensions and the interpreter chooses the right function during execution. It is also used to provide geometric quantities or to set reference elements according to a given order.

- Inheritance and Abstract Types

Inheritance for types enables to define a type hierarchy. For example looking on numbers, one could define an abstract type number as a parent of the types integer and float. A function defined for a parameter of type number is defined for parameters of the type integer and float at once. Together with function overloading, this forms Julia into an object-oriented programming language.

In case of the surface finite element code, the type ReferenceElement is the parent of the types ReferenceElement\_Line and ReferenceElement\_Triangle. This allows to differ between the reference elements in 1D and 2D, for example to define sets of quadrature points, but write only one assembling function which is valid for both cases.

---

<sup>1</sup><http://julialang.org/>, 12.03.2017

- Lambda Calculus

Julia supports lambda calculus, sometimes called anonymous functions. A function depending on a variable  $x$  can be given via an instruction  $x \mapsto \dots$ , e.g.  $x \mapsto x + 1$ , without providing a function name. In this way functions can be used like variables and can be passed as function arguments or been attached to objects. An array of anonymous functions is used to represent the basis functions of the finite element spaces and to return geometric quantities as the Gramian determinant.

This allows for an easy evaluation of this functions in a given point. Additionally, the problem formulation itself is provided by anonymous functions representing the bilinear form and the right hand side.

- Extensive Libraries and Easy Connection to External Routines

Julia is equipped with several libraries providing mathematical routines, plotting routines and much more. Especially, solving routines for sparse linear equation systems are provided by Julia and used in the finite element code. Additionally, existing code written in other high-level programming languages, such as C or Python, can easily be interfaced from Julia.

Using these features the basic framework for a multi-dimensional surface finite element code with higher order finite elements is set. Thereby, surface diffusion-convection-reaction equations with variable diffusion parameter, velocity field and reaction parameter are considered as problem class. Until now 1D surfaces embedded in  $\mathbb{R}^2$  and 1D and 2D surfaces embedded in  $\mathbb{R}^3$  can be handled. A linear surface approximation and first and second order finite elements are implemented. The obtained solutions are written to vtk-files and  $L^2$ - and  $H^1$ -errors can be measured. Additionally, the LPS on surfaces for arbitrary finite element and projection spaces is implemented.

The code can easily be extended in different directions. To introduce a higher order surface approximation only new geometric types and the corresponding functions providing the geometric quantities have to be implemented. Higher order finite elements can be provided by defining new reference elements. New diffusion-convection-reaction problems can be inserted by preparing an InitialGeometry-object, which includes the geometric information, and a ProblemData-object, handling the coefficients, the right hand side and the boundary data. Even a completely new problem type can be introduced by simply providing the bilinear form and the right hand side as anonymous functions of given data, test functions and their derivatives. If the complexity or problem size increases, the developed code can be parallelized using the functionalities for distributed computations already provided by Julia.

Julia seems to unite a lot of favourable aspects for modern numerical programming. However, its youth and evolution causes a steady development even in the

syntax. No upward or downward compatibility can be assumed. Further, Julia is not available for all platforms yet. This can lead to problems in code distribution. Another drawback of Julia is owed to its impact from the Python packages NumPy and SciPy. As in the named packages and contrary to the mathematical understanding, a vector or a number is not interpreted as a special case of matrices. Manual type casts are needed, for example to use a number as a parameter of a function expecting a square matrix.

The results presented in the following examples are obtained on a dual socket 16 core Intel Xeon E5-2640v3 with 64 GB RAM. The Julia programming language is used in version 0.4.3, which employs OpenBLAS 0.2.15 and SuiteSparse 4.4.2 for dense and sparse linear algebra operations. All computations are done in IEEE double precision arithmetics.

## 6.2 Example 1: Code Validation

In this section surface diffusion-reaction equations

$$-\varepsilon\Delta_{\Gamma}u + cu = f \quad \text{on } \Gamma$$

with given smooth solutions on 1D and 2D surfaces are considered. The known exact solutions allow for a validation of the implementation. Due to the smoothness of the solution all error estimates proven in the previous sections are applicable and the obtained convergence orders can be expected.

As 1D and 2D geometries  $\Gamma$  a unit circle in  $\mathbb{R}^2$  and a unit sphere in  $\mathbb{R}^3$  are considered. The diffusion parameter and the reaction parameter are set to  $\varepsilon \in \{10^{-2}, 10^{-6}\}$  and  $c = 1$  for both problems. The right hand side is chosen such that  $u = x_1 + x_2$  and  $u = x_1 + x_2 + x_3$  are the solutions of the 1D and 2D problem, respectively.

The calculations are taken out for a linear surface approximation starting with 64 elements in the 1D case and 8 elements in the 2D case for the initial mesh. The unstabilized methods are based on continuous piecewise linear ( $\mathbb{P}_1$ ) and quadratic ( $\mathbb{P}_2$ ) finite elements, respectively. For the LPS stabilized methods the pairs  $\widehat{X}^r = \mathbb{P}_1^{\text{bubble}}$ ,  $\widehat{D}^r = \mathbb{P}_0^{\text{disc}}$  (referred to as:  $\mathbb{P}_1^{\text{stab}}$ ) and  $\widehat{X}^r = \mathbb{P}_2^{\text{bubble}}$ ,  $\widehat{D}^r = \mathbb{P}_1^{\text{disc}}$  (referred to as:  $\mathbb{P}_2^{\text{stab}}$ ) as described in Section 4.1.4 are used. The stabilization parameter is taken as  $\alpha \in \{1.0, 0.001\}$ .

The obtained convergence errors measured in the  $L^2$ -norm and the  $H^1$ -semi-norm together with the calculated convergence rates for all methods are presented over the number of degrees of freedom in Tables 6.1 – 6.8. Thereby, a uniform refinement is used over the whole surface. Newly introduced points of the refinements are projected to the surface  $\Gamma$  making use of the closest point projection  $\mathbf{p}$ .

Having a look at Tables 6.1 and 6.5 it can be seen that in the 1D and the 2D case for low values of the diffusion coefficient  $\varepsilon$  the unstabilized methods reach the predicted convergence orders. The higher order obtained in the  $L^2$ -norm for the



$\varepsilon = 10^{-2}$	#dof	$L^2$ -norm		$H^1$ -semi-norm	
		error	order	error	order
$\mathbb{P}_1$	64	9.01697e-4	-	7.10925e-2	-
	128	2.25342e-4	2.00053	3.55263e-2	1.00081
	256	5.63303e-5	2.00013	1.77607e-2	1.00020
	512	1.40823e-5	2.00003	8.88003e-3	1.00005
	1024	3.52054e-6	2.00001	4.43998e-3	1.00001
	2048	8.80135e-7	2.00000	2.21998e-3	1.00000
$\mathbb{P}_2$	128	4.55170e-5	-	2.70218e-3	-
	256	7.14147e-6	2.67211	6.75362e-4	2.00039
	512	1.40036e-6	2.35042	1.68829e-4	2.00010
	1024	3.21555e-7	2.12266	4.22065e-5	2.00003
	2048	7.85045e-8	2.03422	1.05516e-5	2.00001
	4096	1.95067e-8	2.00880	2.63789e-6	2.00000

Table 6.1: Error and convergence orders of  $u^E - u_h$  measured in the  $L^2$ -norm and the  $H^1$ -semi-norm for the solutions of the 1D problem with  $\varepsilon = 10^{-2}$  using the unstabilized methods.

$\varepsilon = 10^{-6}$	#dof	$L^2$ -norm		$H^1$ -semi-norm	
		error	order	error	order
$\mathbb{P}_1$	64	9.00814e-4	-	7.10936e-2	-
	128	2.25121e-4	2.00053	3.55265e-2	1.00083
	256	5.62752e-5	2.00013	1.77607e-2	1.00021
	512	1.40685e-5	2.00003	8.88003e-3	1.00005
	1024	3.51710e-6	2.00001	4.43997e-3	1.00001
	2048	8.79273e-7	2.00000	2.21998e-3	1.00000
$\mathbb{P}_2$	128	4.08731e-5	-	2.70501e-3	-
	256	5.11339e-6	2.99880	6.75525e-4	2.00155
	512	6.39307e-7	2.99970	1.68836e-4	2.00039
	1024	7.99176e-8	2.99992	4.22060e-5	2.00010
	2048	9.98983e-9	2.99998	1.05513e-5	2.00003
	4096	1.24873e-9	2.99999	2.63782e-6	2.00001

Table 6.2: Error and convergence orders of  $u^E - u_h$  measured in the  $L^2$ -norm and the  $H^1$ -semi-norm for the solutions of the 1D problem with  $\varepsilon = 10^{-6}$  using the unstabilized methods.

$\varepsilon = 10^{-2}$	#dof	$L^2$ -norm		$H^1$ -semi-norm	
		error	order	error	order
$\mathbb{P}_1^{\text{stab}}$ $\alpha = 1.0$	128	8.17127e-3	-	6.44256e-2	-
	256	1.87109e-4	2.12668	2.94942e-2	1.12720
	512	4.00288e-5	2.22477	1.26157e-2	1.22521
	1024	7.76594e-6	2.36581	4.89243e-3	1.36659
	2048	1.34170e-6	2.53310	1.68832e-3	1.53496
	4096	2.07821e-7	2.69065	5.21184e-4	1.69572
$\mathbb{P}_1^{\text{stab}}$ $\alpha = 0.01$	128	9.02667e-5	-	6.79414e-3	-
	256	1.26887e-5	2.83065	1.78521e-3	1.92820
	512	1.95707e-6	2.69678	4.56987e-4	1.96587
	1024	3.66988e-7	2.41489	1.15563e-4	1.98348
	2048	8.18282e-8	2.16506	2.90535e-5	1.99189
	4096	1.97500e-8	2.05074	7.28364e-6	1.99598
$\mathbb{P}_2^{\text{stab}}$ $\alpha = 1.0$	192	4.55170e-5	-	2.70218e-3	-
	384	7.14147e-6	2.67211	6.75362e-4	2.00039
	768	1.40035e-6	2.35042	1.68829e-4	2.00010
	1536	3.21555e-7	2.12266	4.22065e-5	2.00003
	3072	7.85045e-8	2.03422	1.05516e-5	2.00001
	6144	1.95067e-8	2.00880	2.63789e-6	2.00000
$\mathbb{P}_2^{\text{stab}}$ $\alpha = 0.01$	192	4.55170e-5	-	2.70218e-3	-
	384	7.14147e-6	2.67211	6.75362e-4	2.00039
	768	1.40036e-6	2.35042	1.68829e-4	2.00010
	1536	3.21555e-7	2.12266	4.22065e-5	2.00003
	3072	7.85043e-8	2.03422	1.05516e-5	2.00001
	6144	1.95071e-8	2.00877	2.63789e-6	2.00000

Table 6.3: Error and convergence orders of  $u^E - u_h$  measured in the  $L^2$ -norm and the  $H^1$ -semi-norm for the solutions of the 1D problem with  $\varepsilon = 10^{-2}$  using the stabilized methods.

$\varepsilon = 10^{-6}$	#dof	$L^2$ -norm		$H^1$ -semi-norm		
		error	order	error	order	
$\mathbb{P}_1^{\text{stab}}$	128	8.99331e-4	-	7.09767e-2	-	
	256	2.24933e-4	1.99936	3.54967e-2	0.99966	
	512	5.62499e-5	1.99957	1.77527e-2	0.99965	
	1024	1.40644e-5	1.99980	8.87749e-3	0.99982	
	$\alpha = 1.0$	2048	3.51616e-6	1.99998	4.43880e-3	0.99998
	4096	8.78942e-7	2.00016	2.21915e-3	1.00016	
$\mathbb{P}_1^{\text{stab}}$	128	7.73357e-4	-	6.10458e-2	-	
	256	2.07700e-4	1.89663	3.27780e-2	0.89716	
	512	5.38526e-5	1.94741	1.69962e-2	0.94752	
	1024	1.36773e-5	1.97724	8.63311e-3	0.97726	
	$\alpha = 0.01$	2048	3.42622e-6	1.99709	4.32525e-3	0.99710
	4096	8.47322e-7	2.01563	2.13931e-3	1.01563	
$\mathbb{P}_2^{\text{stab}}$	192	4.08731e-5	-	2.70498e-3	-	
	384	5.11339e-6	2.99880	6.75515e-4	2.00155	
	768	6.39308e-7	2.99970	1.68833e-4	2.00039	
	1536	7.99177e-8	2.99992	4.22056e-5	2.00009	
	$\alpha = 1.0$	3072	9.98985e-9	2.99998	1.05513e-5	2.00002
	6144	1.24874e-9	2.99999	2.63782e-6	2.00000	
$\mathbb{P}_2^{\text{stab}}$	192	4.08731e-5	-	2.70497e-3	-	
	384	5.11339e-6	2.99880	6.75515e-4	2.00155	
	768	6.39308e-7	2.99970	1.68833e-4	2.00039	
	1536	7.99177e-8	2.99992	4.22056e-5	2.00009	
	$\alpha = 0.01$	3072	9.98985e-9	2.99998	1.05513e-5	2.00002
	6144	1.24874e-9	2.99999	2.63782e-6	2.00000	

Table 6.4: Error and convergence orders of  $u^E - u_h$  measured in the  $L^2$ -norm and the  $H^1$ -semi-norm for the solutions of the 1D problem using with  $\varepsilon = 10^{-6}$  using the stabilized methods.

$\varepsilon = 10^{-2}$	#dof	$L^2$ -norm		$H^1$ -semi-norm	
		error	order	error	order
$\mathbb{P}_1$	6	3.28478e-1	-	2.08761e+0	-
	18	1.20544e-1	1.44624	1.07480e+0	0.95778
	66	3.45003e-2	1.80488	5.42437e-1	0.98655
	258	8.59929e-3	2.00432	2.72668e-1	0.99231
	1026	2.14508e-3	2.00319	1.36626e-1	0.99691
	4098	5.36049e-4	2.00059	6.83796e-2	0.99860
$\mathbb{P}_2$	20	1.99290e-1	-	1.59026e+0	-
	66	5.24769e-2	1.92511	4.92844e-1	1.69006
	258	8.46228e-3	2.63256	1.26804e-1	1.95853
	1026	1.37004e-3	2.62682	3.20465e-2	1.98436
	4098	2.61332e-4	2.39027	8.04849e-3	1.99338
	16386	5.87175e-5	2.15402	2.01635e-3	1.99697

Table 6.5: Error and convergence orders of  $u^E - u_h$  measured in the  $L^2$ -norm and the  $H^1$ -semi-norm for the solutions of the 2D problem with  $\varepsilon = 10^{-2}$  using the unstabilized methods.

$\varepsilon = 10^{-6}$	#dof	$L^2$ -norm		$H^1$ -semi-norm	
		error	order	error	order
$\mathbb{P}_1$	6	3.24615e-1	-	2.11767e+0	-
	18	1.19496e-1	1.44176	1.08004e+0	0.97139
	66	3.36873e-2	1.82669	5.53239e-1	0.96511
	258	8.26292e-3	2.02748	2.75518e-1	1.00575
	1026	2.02655e-3	2.02762	1.37390e-1	1.00387
	4098	5.00022e-4	2.01897	6.85665e-2	1.00270
$\mathbb{P}_2$	20	1.92976e-1	-	1.60929e+0	-
	66	4.95076e-2	1.96270	5.31169e-1	1.59918
	258	7.45518e-3	2.73133	1.32625e-1	2.00182
	1026	1.00620e-3	2.88933	3.29551e-2	2.00878
	4098	1.30636e-4	2.94529	8.19244e-3	2.00814
	16386	1.66401e-5	2.97281	2.03689e-3	2.00793

Table 6.6: Error and convergence orders of  $u^E - u_h$  measured in the  $L^2$ -norm and the  $H^1$ -semi-norm for the solutions of the 2D problem with  $\varepsilon = 10^{-6}$  using the unstabilized methods.

$\varepsilon = 10^{-2}$	#dof	$L^2$ -norm		$H^1$ -semi-norm		
		error	order	error	order	
$\mathbb{P}_1^{\text{stab}}$	14	3.24996e-1	-	2.06413e+0	-	
	50	1.19491e-1	1.44352	1.06431e+0	0.95562	
	194	3.42182e-2	1.80407	5.36440e-1	0.98842	
	770	8.49890e-3	2.00941	2.67876e-1	1.00185	
	$\alpha = 1.0$	3074	2.10057e-3	2.01650	1.32282e-1	1.01795
	12290	5.15733e-4	2.02608	6.44299e-2	1.03780	
$\mathbb{P}_1^{\text{stab}}$	14	2.35003e-1	-	1.54534e+0	-	
	50	8.75539e-2	1.42444	7.83653e-1	0.97964	
	194	2.62433e-2	1.73822	3.98795e-1	0.97457	
	770	6.57996e-3	1.99580	1.98695e-1	1.00509	
	$\alpha = 0.01$	3074	1.61714e-3	2.02464	9.88124e-2	1.00779
	12290	3.99047e-4	2.01881	4.92994e-2	1.00312	
$\mathbb{P}_2^{\text{stab}}$	36	1.97787e-1	-	1.57165e+0	-	
	130	5.21350e-2	1.92362	4.88870e-1	1.68476	
	514	8.42876e-3	2.62886	1.26109e-1	1.95478	
	2050	1.36569e-3	2.62569	3.18542e-2	1.98512	
	$\alpha = 1.0$	8194	2.60767e-4	2.38880	7.97838e-3	1.99732
	32770	5.86497e-5	2.15257	1.98708e-3	2.00545	
$\mathbb{P}_2^{\text{stab}}$	36	1.46561e-1	-	1.05185e+0	-	
	130	4.19979e-2	1.80312	3.88977e-1	1.43517	
	514	7.47251e-3	2.49065	1.10316e-1	1.81804	
	2050	1.28085e-3	2.54450	2.88196e-2	1.93652	
	$\alpha = 0.01$	8194	2.54177e-4	2.33319	7.30862e-3	1.97938
	32770	5.82180e-5	2.12630	1.83386e-3	1.99472	

Table 6.7: Error and convergence orders of  $u^E - u_h$  measured in the  $L^2$ -norm and the  $H^1$ -semi-norm for the solutions of the 2D problem with  $\varepsilon = 10^{-2}$  using the stabilized methods.

$\varepsilon = 10^{-6}$	#dof	$L^2$ -norm		$H^1$ -semi-norm		
		error	order	error	order	
$\mathbb{P}_1^{\text{stab}}$	14	3.22107e-1	-	2.10071e+0	-	
	50	1.18874e-1	1.43811	1.07474e+0	0.96689	
	194	3.36034e-2	1.82275	5.51949e-1	0.96138	
	770	8.25462e-3	2.02533	2.75223e-1	1.00393	
	$\alpha = 1.0$	3074	2.02564e-3	2.02682	1.37318e-1	1.00307
	12290	4.99916e-4	2.01862	6.85486e-2	1.00233	
$\mathbb{P}_1^{\text{stab}}$	14	2.34721e-1	-	1.58164e+0	-	
	50	9.08949e-2	1.36868	8.36222e-1	0.91946	
	194	2.83674e-2	1.67996	4.71505e-1	0.82661	
	770	7.59256e-3	1.90158	2.51587e-1	0.90621	
	$\alpha = 0.01$	3074	1.94418e-3	1.96542	1.30911e-1	0.94247
	12290	4.89941e-4	1.98849	6.68595e-2	0.96938	
$\mathbb{P}_2^{\text{stab}}$	36	1.92077e-1	-	1.59933e+0	-	
	130	4.93163e-2	1.96155	5.28819e-1	1.59662	
	514	7.44073e-3	2.72855	1.32367e-1	1.99823	
	2050	1.00512e-3	2.88808	3.29208e-2	2.00747	
	$\alpha = 1.0$	8194	1.30560e-4	2.94458	8.18798e-3	2.00742
	32770	1.66351e-5	2.97242	2.03632e-3	2.00754	
$\mathbb{P}_2^{\text{stab}}$	36	1.39756e-1	-	1.10337e+0	-	
	130	3.93135e-2	1.82982	4.16960e-1	1.40394	
	514	6.44335e-3	2.60914	1.16374e-1	1.84114	
	2050	9.19830e-4	2.80837	3.04198e-2	1.93568	
	$\alpha = 0.01$	8194	1.24048e-4	2.89047	7.82133e-3	1.95952
	32770	1.61739e-5	2.93915	1.98579e-3	1.97770	

Table 6.8: Error and convergence orders of  $u^E - u_h$  measured in the  $L^2$ -norm and the  $H^1$ -semi-norm for the solutions of the 2D problem with  $\varepsilon = 10^{-6}$  using the stabilized methods.

linear ( $r = 1$ ) unstabilized method is expected and could be proven for any fixed  $\varepsilon$  using the Aubin-Nitsche trick. For the quadratic ( $r = 2$ ) unstabilized method an increased convergence order in the  $L^2$ -norm is prohibited by the error coming from the geometric approximation of the surface. Only surface approximations of first order ( $k = 1$ ) are used. Therefore, only second order convergence in both, the  $L^2$ - and the  $H^1$ -norm can be expected.

Comparing Tables 6.2 and 6.6, the same conclusions hold true, but the order seems to be independent of the geometric approximation. The highest impact of the geometric error is received from the approximation of the surface gradients. Hence, the influence of the geometric error is scaled down by the diffusion parameter and becomes quantitatively small enough to be neglectable for the studied refinement levels.

The same difference can be observed for the stabilized methods in Tables 6.3–6.4 and 6.7–6.8. For small diffusion values, the impact of the geometric error becomes neglectable, whereas for higher diffusion values all convergence orders are limited to two by the geometric error. The obtained convergence orders coincide with the convergence orders of the corresponding unstabilized methods. The proven advance of half an order in the convergence error is in general not visible. This improvement can only be visualized in simulations if the part of the error scaled by  $\varepsilon$  in the analytically obtained error bounds is quantitatively small enough.

A special case is the stabilized method  $\mathbb{P}_1^{\text{stab}}$  in the 1D case with the diffusion coefficient  $\varepsilon = 10^{-2}$ , compare Table 6.3. For a small stabilization parameter  $\alpha = 0.001$  the method reaches convergence orders expected for methods based on quadratic finite element spaces, especially the error in the  $H^1$ -semi-norm is of second order. This can be explained recognizing that in 1D the space  $\mathbb{P}_1^{\text{bubble}}$  is exactly the space  $\mathbb{P}_2$ . Additionally, the method is only slightly influenced by the stabilization term due to the small stabilization parameter. Hence, the obtained method behaves similarly to an unstabilized quadratic method. Studying the same method with a bigger stabilization parameter  $\alpha = 1.0$  the behaviour of the quadratic method cannot longer be assumed and a convergence of second order in the  $L^2$ -norm and first order in the  $H^1$ -semi-norm would be expected. But in this particular problem setting even the increased convergence orders for the LPS stabilized methods are visible.

Concluding the results, the analytically predicted convergence orders are met by the simulations. Thereby, different diffusion and stabilization parameter for the 1D and 2D problem are considered. The potential of LPS stabilization does not lie in a substantial improvement of the convergence order but in reduction and localization of oscillations around internal and boundary layers. This is shown in the following examples.

### 6.3 Example 2: Non-smooth Right Hand Side

In this section the equation from the 1D case of Example 1

$$-\varepsilon \Delta_{\Gamma} u + cu = f \quad \text{on } \Gamma$$

on the unit sphere  $\Gamma$  with reaction parameter  $c = 1$  and the non-smooth right hand side  $f(\mathbf{x}) = \text{sign}(x_2)$  is studied.

If the diffusion parameter  $\varepsilon$  tends to zero, the exact solution  $u$  tends to the non-smooth function  $f$ . The slope at  $x_2 = 0$  becomes steeper and an internal layer develops at this point. In the following calculations the diffusion parameter is set to  $\varepsilon = 10^{-4}$  and the behaviour of the numerical solutions around the layer is studied. The plots present the obtained solution plotted over the arc length  $s$  starting in  $(-1, 0)$  and moving clockwise.

Figure 6.1 shows the numerical solutions of the unstabilized surface finite element method using continuous linear ( $P_1$ ) and quadratic ( $P_2$ ) basis functions for different refinement levels. It can be seen that on coarse meshes the solution oscillates on a small number of elements around the layer. Whereas the width of the oscillation area decreases with the element size, the height of the oscillations stays fixed.

The same problem is solved using the LPS stabilized finite element method with ansatz space  $\hat{X}^r = \mathbb{P}_1^{\text{bubble}}$  and projection space  $\hat{D}^r = \mathbb{P}_0^{\text{disc}}$  with a set of stabilization parameters. The obtained numerical solutions for different stabilization parameters are compared to the linear and quadratic unstabilized solutions in Figure 6.2.

If the stabilization parameter is chosen too small (compare  $\alpha = 0.001$ ) the solution tends toward the unstabilized quadratic solution. This is reasonable because the stabilization term is neglectable for small stabilization parameter and the spaces  $\mathbb{P}_2$  and  $\mathbb{P}_1^{\text{bubble}}$  are identical in the 1D case. For big values of the parameters (compare  $\alpha = 1.0$ ) the solution tends towards the unstabilized linear solution. This can be understood by recognizing that the fluctuation of the gradient is the gradient of the bubble function. The strong penalization of the stabilization term hence leads to a suppression of the bubble parts. Using a suitable stabilization parameter (compare  $\alpha = 0.01$ ) the stabilization is able to localize the oscillations and reduce their amplitude.

An other possible reason for internal layers on closed surfaces are discontinuous velocity fields. An example considering and discussing LPS for such kind of layer is presented in [65].

### 6.4 Example 3: Circular Flow

Boundary layers can also occur due to non-smooth boundary conditions. This situation is studied in this example. The example is inspired by Example 2 in [38]



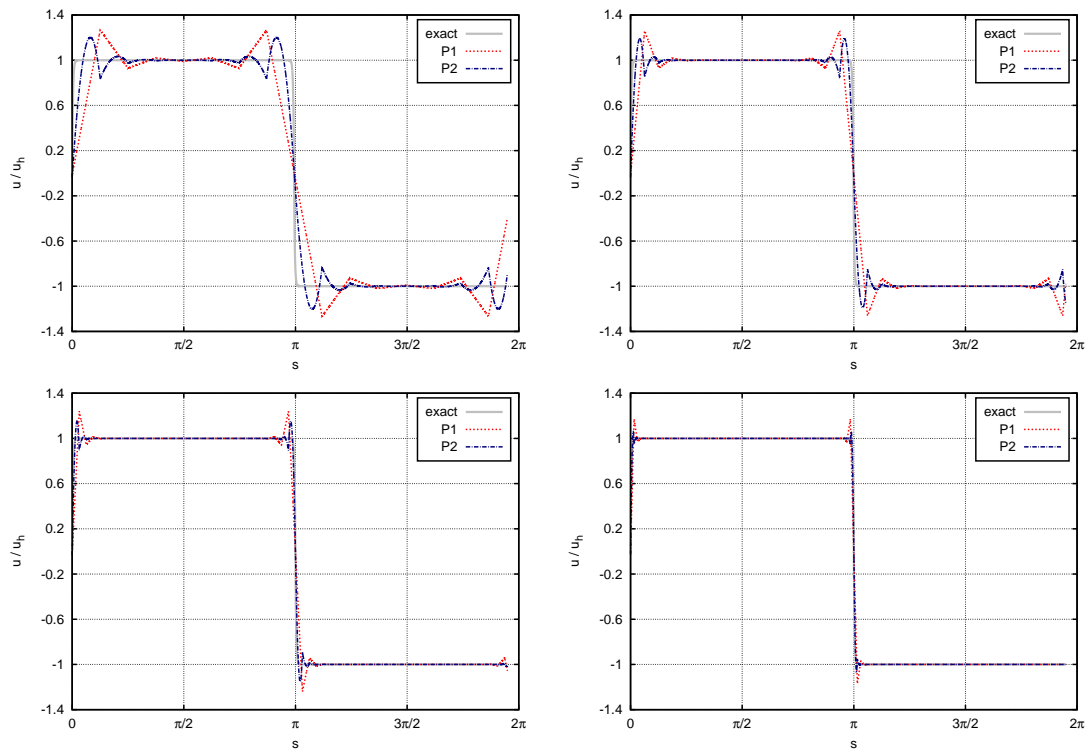


Figure 6.1: Exact solution (exact) and numerical solutions using linear (P1) and quadratic (P2) unstabilized finite elements for increasing refinement levels. From top left to bottom right: 16, 32, 64 and 128 elements.

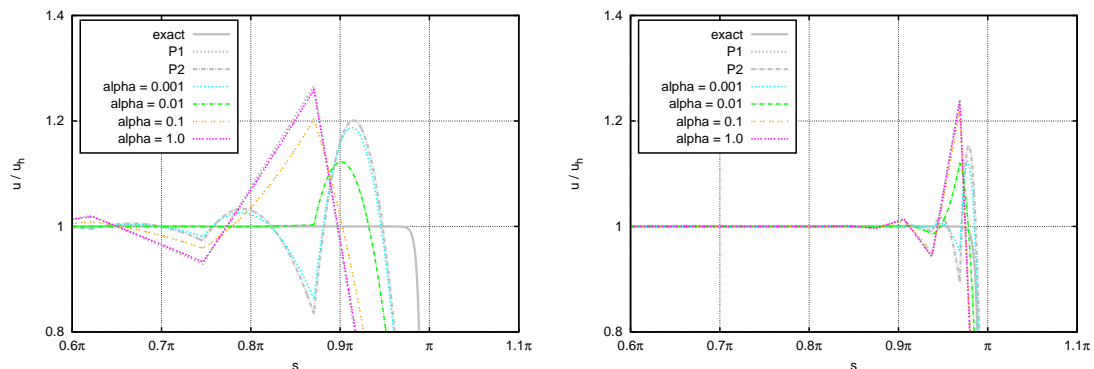


Figure 6.2: Exact solution (exact), numerical solutions using linear (P1) and quadratic (P2) unstabilized finite elements and numerical solution using LPS stabilization with different stabilization parameters  $\alpha_0$  for refinement levels 1 (left) and 3 (right).

and mapped to a curved surface. Considering the cylinder

$$Z = \{\mathbf{x} \in \mathbb{R}^3 \mid (x_1 - 0.5)^2 + x_2^2 = 0.5^2, 0 \leq x_3 \leq 1\}$$

with radius 0.5 and height 1, the given surface  $\Gamma$  is set to

$$\Gamma = \{\mathbf{x} \in Z \mid x_3 \geq 0\}.$$

Hence,  $\Gamma$  is half of the lateral surface of a cylinder, compare Figure 6.3. The velocity field  $\mathbf{w}$  is given by a mapping of the plane circular flow around  $(0, 0)^T$ ,  $\mathbf{w}_{2D}(\phi, \psi) = (-\psi, \phi)^T$ , used in [38] onto the surface. Therefore, we introduce a parametrization of the surface  $\Gamma$  over  $[0, 1]^2$  via:

$$\begin{aligned} x_1(\phi, \psi) &= 0.5(1 - \cos(\pi\phi)), \\ x_2(\phi, \psi) &= \psi, \\ x_3(\phi, \psi) &= 0.5 \sin(\pi\phi). \end{aligned}$$

Further, the directional vectors  $(\phi, 0)^T$  and  $(0, \psi)^T$  map to the tangential directional vectors  $(\pi x_3, 0, \pi(0.5 - x_1))^T$  and  $(0, 1, 0)^T$ . This leads to the following surface divergence free velocity field  $\mathbf{w}$ :

$$\begin{aligned} \mathbf{w} &= -\psi(\pi x_3, 0, \pi(0.5 - x_1))^T + \phi(0, 1, 0)^T \\ &= \left( -\pi x_2 x_3, \frac{1}{\pi} \arccos(1 - 2x_1), -\frac{\pi}{2} x_2(1 - 2x_1) \right). \end{aligned}$$

The diffusion coefficient is chosen as  $\varepsilon = 10^{-6}$  and the reaction coefficient and the right hand side are set to zero:

$$-\varepsilon \Delta_\Gamma u + \mathbf{w} \cdot \nabla_\Gamma u = 0 \quad \text{on } \Gamma.$$

To fully describe the problem, boundary conditions have to be stated. The boundary is divided into a Dirichlet and a homogeneous Neumann boundary part. The Neumann boundary part  $(\partial\Gamma)_N$  is the inner of the intersection of  $\Gamma$  with the  $x_2$  axis and the Dirichlet boundary part  $(\partial\Gamma)_D$  includes the rest of the boundary:

$$(\partial\Gamma)_N = \{\mathbf{x} \in \partial\Gamma \mid x_1 = x_3 = 0, 0 < x_2 < 1\} \quad \text{and} \quad (\partial\Gamma)_D = \partial\Gamma \setminus (\partial\Gamma)_N.$$

The Dirichlet boundary conditions are given as follows:

$$u(1, \cdot, \cdot) = 0, \quad u(\cdot, 1, \cdot) = 0, \quad \text{and} \quad u(x_1, 0, \cdot) = \begin{cases} 1, & \frac{1}{3} \leq x_1 \leq \frac{2}{3} \\ 0, & \text{else} \end{cases}.$$

To solve this problem, again the surface finite element method stabilized by Local Projection is considered. Thereby,  $P_1^{\text{stab}}$  refers to the method using  $\mathbb{P}_1^{\text{bubble}}$  and

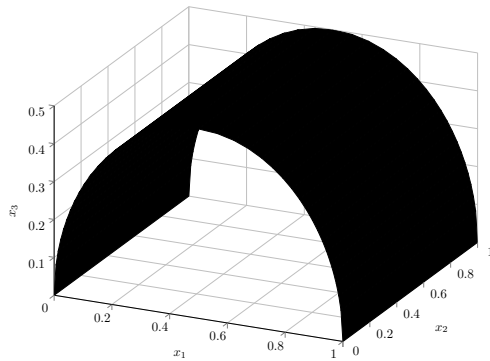


Figure 6.3: Smooth surface  $\Gamma$  used in Examples 3 and 4.

$\mathbb{P}_0^{\text{disc}}$  as finite element and projection space and  $P_2^{\text{stab}}$  equivalently names the method with  $\mathbb{P}_2^{\text{bubble}}$  and  $\mathbb{P}_1^{\text{disc}}$  as finite element and projection space. They are compared to the linear ( $P_1$ ) and the quadratic ( $P_2$ ) unstabilized finite element method.

The jump in the boundary condition on the inflow boundary is transported counter-clockwise by the velocity field. In the convection-dominated case the steep gradients are not smeared out by diffusion, but they develop along the streamline. For the unstabilized finite element method oscillations over the whole domain occur, compare Figure 6.4 left. Using the LPS stabilized techniques the oscillations can be damped and localized as seen in Figure 6.4 right.

For a better visualisation Figure 6.5 and Figure 6.6 show the solutions along the intersection of the surface with the plane  $x_1 = x_2$  starting in the point  $(0, 0, 0)$ . A closer look is also taken at the solution at the Neumann boundary. For missing diffusion ( $\varepsilon = 0$ ) the outflow profile is given as a step function mirroring the Dirichlet boundary condition at the inflow. Thus, for  $\varepsilon \ll 1$  a similar behaviour can be expected. The different outflow profiles obtained by the different solution methods are presented in Figure 6.7 and Figure 6.8 starting in  $(0, 0)$  again.

It can be seen from Figures 6.4 – 6.6 that the linear and the quadratic unstabilized finite element methods lead to strong oscillations in the surface area around the point  $(0, 0, 0)$  enclosed by the streamline starting at the inflow boundary at  $x_1 = 1/3$  (area A1) and the area enclosed by the streamlines starting in  $x_1 = 1/3$  and  $x_1 = 2/3$  (area A2). LPS is able to suppress the oscillations in area A1 up to a few elements near the streamline. In area A2 the oscillations can not be suppressed but their amplitude is decreased. Having a closer look at the impact of the stabilization parameter one can see that high values for the parameter (compare  $\alpha = 1.0$ ) lead to oscillations around the layer as seen for the unstabilized methods but reduced in amplitude and width. If the parameter is chosen too small (see  $\alpha = 0.001$ ) in the linear case the layer is smeared out. In the quadratic case on the contrary a small stabilization parameter produces oscillations again.

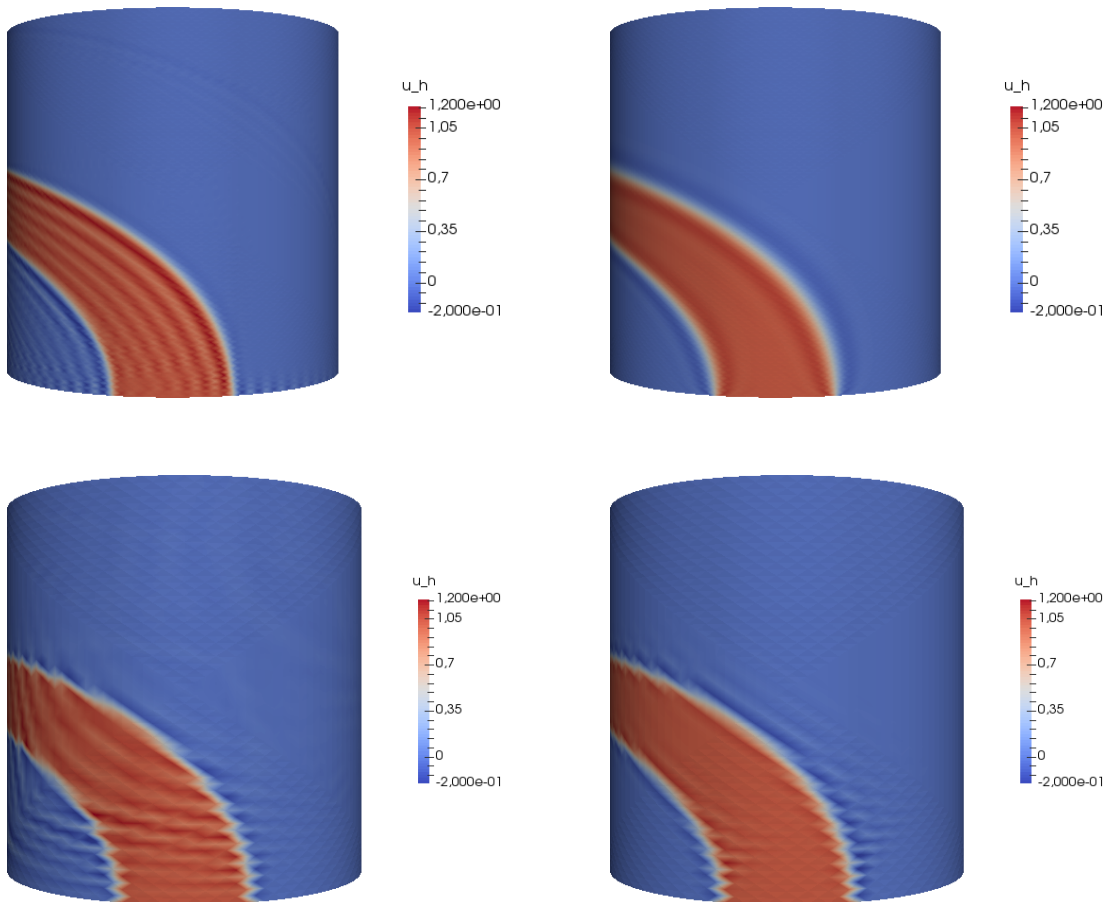


Figure 6.4: Plot of the solutions obtained using unstabilized linear (top left) and quadratic (bottom left) finite element methods and the LPS stabilized methods  $P_1^{\text{stab}}$  (top right) and  $P_2^{\text{stab}}$  (bottom right) with a stabilization parameter  $\alpha_0 = 0.01$ .

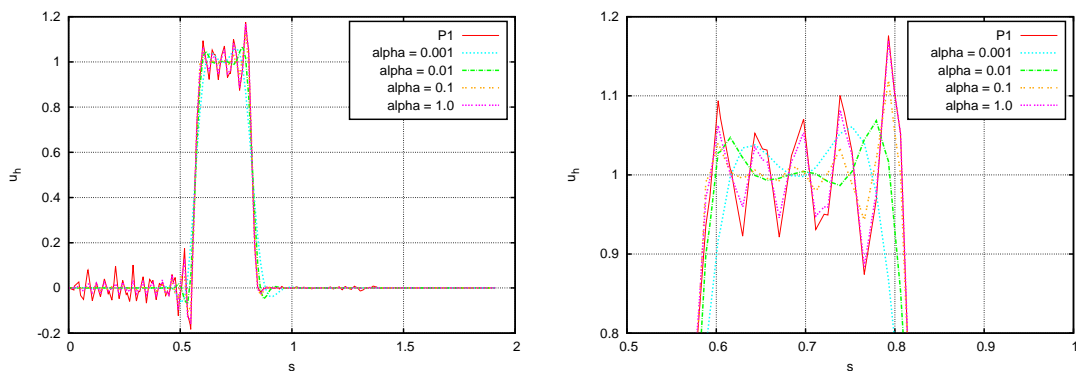


Figure 6.5: Solutions using the unstabilized (P1) and the LPS stabilized  $P_1^{\text{stab}}$  method plotted over the intersection curve of  $\Gamma$  and the  $(x_1 = x_2)$ -plane. Left: complete intersection curve. Right: detailed view.

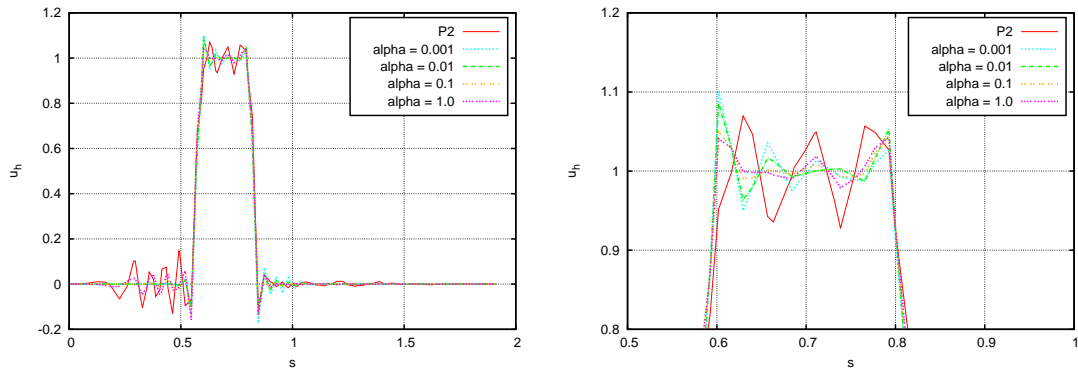


Figure 6.6: Solutions using the unstabilized (P2) and the LPS stabilized  $P_2^{\text{stab}}$  method plotted over the intersection curve of  $\Gamma$  and the  $(x_1 = x_2)$ -plane. Left: complete intersection curve. Right: detailed view.

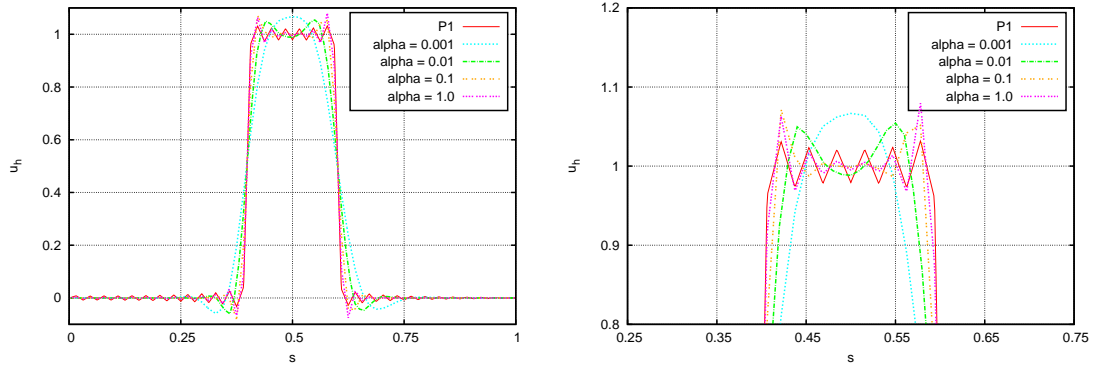


Figure 6.7: Solutions using the unstabilized (P1) and the LPS stabilized  $P_1^{\text{stab}}$  method plotted over the outflow boundary. Left: complete intersection curve. Right: detailed view.

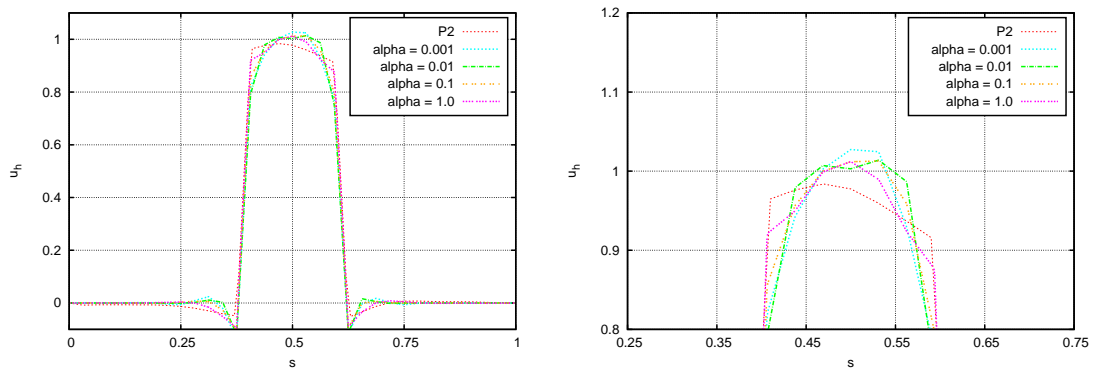


Figure 6.8: Solutions using the unstabilized (P2) and the LPS stabilized  $P_2^{\text{stab}}$  method plotted over the outflow boundary. Left: complete intersection curve. Right: detailed view.

The flow profile at the outflow boundary in the linear case, see Figure 6.7, behaves similarly and the same order of magnitude seems to be optimal for the stabilization parameter. In the quadratic case the profile is hardly influenced by the size of the stabilization parameter but all LPS stabilized methods produce a slightly better capturing of the height 1.

## 6.5 Example 4: Boundary layer

The last example considers not internal but boundary layers. The same geometry as in Example 3 is used but equipped with different boundary conditions. Setting the velocity field to  $\mathbf{w} = 2(x_3, 0, 0.5 - x_1)^T$  leads to a flow from the inflow boundary part:

$$(\partial\Gamma)^- = \{\mathbf{x} \in \Gamma \mid x_1 = 0, 0 \leq x_2 \leq 1\}$$

to the outflow boundary part:

$$(\partial\Gamma)^+ = \{\mathbf{x} \in \Gamma \mid x_1 = 1, 0 \leq x_2 \leq 1\}$$

parallel to the remaining boundary:

$$(\partial\Gamma)^0 = \{\mathbf{x} \in \Gamma \mid 0 < x_1 < 1, x_2 \in \{0, 1\}\}.$$

At the inflow and the outflow boundary Dirichlet boundary conditions are used:

$$u = 1 \quad \text{at } (\partial\Gamma)^- \quad \text{and} \quad u = 0 \quad \text{at } (\partial\Gamma)^+.$$

The remaining boundary is equipped with homogeneous Neumann conditions. By setting the reaction coefficient to zero  $c = 0$  and choosing a small diffusion parameter  $\varepsilon = 10^{-4}$  the solution of the problem is mainly given by the convection process. The profile given at the inflow boundary is transported over the surface by the velocity field. This leads to a layer at the outflow boundary because the transported value ( $u = 1$ ) does not match the given Dirichlet boundary conditions at the outflow ( $u = 0$ ).

This problem is solved using linear ( $P1$ ) and quadratic ( $P2$ ) unstabilized finite elements. Additionally, the same LPS stabilized methods as in Example 3 with varying stabilization parameters are considered. Again,  $P_1^{\text{stab}}$  and  $P_2^{\text{stab}}$  names the methods using either  $\mathbb{P}_1^{\text{bubble}}$  and  $\mathbb{P}_0^{\text{disc}}$  or  $\mathbb{P}_2^{\text{bubble}}$  and  $\mathbb{P}_1^{\text{disc}}$  as finite element and projection spaces. The plots presented below show the numerical solutions along the intersection curve of  $\Gamma$  with the plane  $x_2 = 0.5$ .

Using linear unstabilized finite element methods to get a solution of the problem leads to oscillations around the layer, compare Figure 6.9. Whereas, unstabilized quadratic finite elements tend to smear out the layer, which can be seen in Figure 6.10.

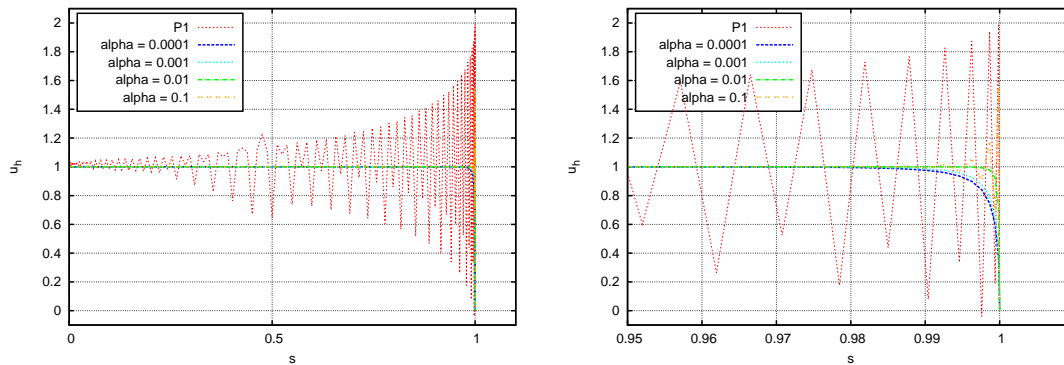


Figure 6.9: Solutions obtained with  $P_1$  and  $P_1^{\text{stab}}$  finite elements with different stabilization parameter ( $\alpha$ ) plotted along the whole intersection curve (left) and near the layer (right).

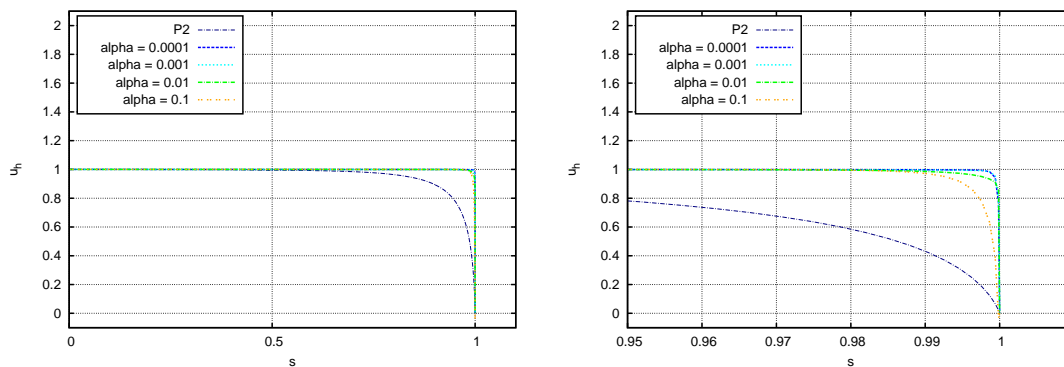


Figure 6.10: Solutions obtained with  $P_2$  and  $P_2^{\text{stab}}$  finite elements with different stabilization parameter ( $\alpha$ ) plotted along the whole intersection curve (left) and near the layer (right).

In the case of linear finite elements the LPS stabilization can fully suppress the oscillations if the stabilization parameter is chosen small enough. But even higher stabilization parameters (compare  $\alpha = 0.1$  in Figure 6.9) still localize the oscillations to a fraction of its initial width. Parameters, that are too small, smear the layer, but the impact of the smearing is neglectable compared to the quadratic unstabilized case.

Figure 6.10 shows the improvement of the solution using LPS in the quadratic case. Although there are no oscillations in the unstabilized solutions, an improvement is achieved by reducing the smearing of the layer. The best results are obtained with small stabilization parameters, but even higher ones still improve the behaviour of the solution significantly.





# Chapter 7

## Conclusion

In this thesis, surface finite elements for diffusion-convection-reaction equations have been studied and stabilization on surfaces using the Local Projection Stabilization and Streamline Upwind Petrov-Galerkin methods have been introduced. At first a geometric discretization technique has been presented, which is able to approximate a given smooth curvilinear surface with a freely selectable order  $k$ . On the discrete surface finite element methods of arbitrary order  $r$  have been defined.

The numerical methods arising have been studied for diffusion-convection-reaction equations on surfaces. Under an assumption on the data of the given problem,  $c + \frac{1}{2} \nabla_{\Gamma} \cdot \mathbf{w}$ , a semi-robust estimate of the convergence error of order  $\min(r, k + 1)$  has been proven.

This result has been improved by stabilization techniques. The Local Projection Stabilization approach has been transferred to the setting of surface finite elements. The Streamline-Upwind-Petrov-Galerkin method for surfaces has been extended to higher order finite elements. Both ansätze have led to an improvement in the error estimates. In case of convection dominated problems an order of  $\min(r + \frac{1}{2}, k + 1)$  has been obtained.

Another class of diffusion-convection-reaction equations studied in this setting is indicated by the assumptions  $c = 0$  and  $\nabla_{\Gamma} \cdot \mathbf{w} = 0$ . In this case no semi-robust estimates are possible, due to missing  $L^2$ -control. In the convection-dominated case a convergence error of order  $\min(r + 1, k + 1)$  but scaled with the factor  $\varepsilon^{-1/2}$  has been proven. The stabilization techniques do not lead to an improvement of the convergence error in this case. Nevertheless, they can be used to obtain more stable solutions of the problem.

The presented analysis have been rounded out by the consideration of surfaces with Dirichlet and Neumann boundaries. The obtained results could be transferred to this setting.

Several numerical examples have shown the potential of the Local Projection Stabilization to suppress and localize oscillations occurring for standard surface finite elements around internal and boundary layers. Thereby, both above described

classes of diffusion-convection-reaction equations have been considered. Nevertheless, several aspects are still unresolved and can be topic of future work in this area. An open question is the geometric approximation of surfaces, that are not curvilinear, and the construction of a suitable projection operator for this case. In the context of the Local Projection Stabilization, the exploration of a surface variant of the two-level approach would be interesting. Further, a detailed study of the influence of the stabilization parameter should be taken out but would have exceeded the scope of this work.

# Bibliography

- [1] Naveed Ahmed, Simon Becher, and Gunar Matthies. Higher-order discontinuous Galerkin time stepping and local projection stabilization techniques for the transient Stokes problem. *Computer Methods in Applied Mechanics and Engineering*, 313:28–52, 2017.
- [2] Paola F. Antonietti, Andreas Dedner, Pravin Madhavan, Simone Stangalino, Björn Stinner, and Marco Verani. High order discontinuous Galerkin methods for elliptic problems on surfaces. *SIAM Journal on Numerical Analysis*, 53(2):1145–1171, 2015.
- [3] Daniel Arndt, Helene Dallmann, and Gert Lube. Local projection FEM stabilization for the time-dependent incompressible Navier–Stokes problem. *Numerical Methods for Partial Differential Equations*, 31(4):1224–1250, 2015.
- [4] Roland Becker and Malte Braack. A finite element pressure gradient stabilization for the Stokes equations based on local projections. *Calcolo*, 38(4):173–199, 2001.
- [5] Roland Becker and Malte Braack. A two-level stabilization scheme for the Navier-Stokes equations. In *Numerical Mathematics and Advanced Applications*, pages 123–130. Springer, 2004.
- [6] Christine Bernardi. Optimal finite-element interpolation on curved domains. *SIAM Journal on Numerical Analysis*, 26(5):1212–1240, 1989.
- [7] Jeff Bezanson, Alan Edelman, Stefan Karpinski, and Viral B. Shah. Julia: a fresh approach to numerical computing. *SIAM Review*, 59(1):65–98, 2017.
- [8] Malte Braack and Erik Burman. Local projection stabilization for the Oseen problem and its interpretation as a variational multiscale method. *SIAM Journal on Numerical Analysis*, 43(6):2544–2566, 2006.
- [9] Malte Braack and Thomas Richter. Local projection stabilization for the Stokes system on anisotropic quadrilateral meshes. In *Numerical Mathematics and Advanced Applications*, pages 770–778. Springer, 2006.

- 
- [10] Alexander N. Brooks and Thomas J.R. Hughes. Streamline upwind/Petrov-Galerkin formulations for convection dominated flows with particular emphasis on the incompressible Navier-Stokes equations. *Computer Methods in Applied Mechanics and Engineering*, 32(1-3):199–259, 1982.
- [11] Martin Burger. Finite element approximation of elliptic partial differential equations on implicit surfaces. *Computing and Visualization in Science*, 12(3):87–100, 2009.
- [12] Erik Burman. A unified analysis for conforming and nonconforming stabilized finite element methods using interior penalty. *SIAM Journal on Numerical Analysis*, 43(5):2012–2033, 2005.
- [13] Erik Burman. Consistent SUPG-method for transient transport problems: Stability and convergence. *Computer Methods in Applied Mechanics and Engineering*, 199(17):1114–1123, 2010.
- [14] Erik Burman and Alexandre Ern. Continuous interior penalty hp-finite element methods for advection and advection-diffusion equations. *Mathematics of Computation*, 76(259):1119–1140, 2007.
- [15] Erik Burman and Miguel A. Fernández. Continuous interior penalty finite element method for the time-dependent Navier–Stokes equations: space discretization and convergence. *Numerische Mathematik*, 107(1):39–77, 2007.
- [16] Erik Burman, Miguel A. Fernández, and Peter Hansbo. Continuous interior penalty finite element method for Oseen’s equations. *SIAM Journal on Numerical Analysis*, 44(3):1248–1274, 2006.
- [17] Erik Burman and Peter Hansbo. Edge stabilization for the generalized Stokes problem: a continuous interior penalty method. *Computer Methods in Applied Mechanics and Engineering*, 195(19):2393–2410, 2006.
- [18] Erik Burman, Peter Hansbo, and Mats G. Larson. A stabilized cut finite element method for partial differential equations on surfaces: The Laplace–Beltrami operator. *Computer Methods in Applied Mechanics and Engineering*, 285:188–207, 2015.
- [19] Philippe G. Ciarlet. *The finite element method for elliptic problems*. Studies in mathematics and its applications. North-Holland, Amsterdam, New-York, 1980.
- [20] Klaus Deckelnick, Gerhard Dziuk, Charles M. Elliott, and Claus-Justus Heine. An h-narrow band finite-element method for elliptic equations on implicit surfaces. *IMA Journal of Numerical Analysis*, 2009.

- [21] Klaus Deckelnick, Charles M. Elliott, and Thomas Ranner. Unfitted finite element methods using bulk meshes for surface partial differential equations. *SIAM Journal on Numerical Analysis*, 52(4):2137–2162, 2014.
- [22] Alan Demlow. Higher-order finite element methods and pointwise error estimates for elliptic problems on surfaces. *SIAM Journal on Numerical Analysis*, 47(2):805–827, 2009.
- [23] Alan Demlow and Gerhard Dziuk. An adaptive finite element method for the Laplace-Beltrami operator on implicitly defined surfaces. *SIAM Journal on Numerical Analysis*, 45(1):421–442, 2007.
- [24] Udo Diewald, Tobias Preußer, and Martin Rumpf. Anisotropic diffusion in vector field visualization on euclidean domains and surfaces. *IEEE Transactions on Visualization and Computer Graphics*, 6(2):139–149, 2000.
- [25] Jim Douglas and Todd Dupont. Interior penalty procedures for elliptic and parabolic Galerkin methods. In *Computing Methods in Applied Sciences*, pages 207–216. Springer, 1976.
- [26] Gerhard Dziuk. Finite elements for the Beltrami operator on arbitrary surfaces. In *Partial Differential Equations and Calculus of Variations*, volume 1357 of *Lecture Notes in Math.*, pages 142–155. Springer, Berlin, 1988.
- [27] Gerhard Dziuk and Charles M. Elliott. Finite elements on evolving surfaces. *IMA Journal of Numerical Analysis*, 27(2):262–292, 2007.
- [28] Gerhard Dziuk and Charles M. Elliott. Surface finite elements for parabolic equations. *Journal of Computational Mathematics*, pages 385–407, 2007.
- [29] Gerhard Dziuk and Charles M. Elliott. An eulerian approach to transport and diffusion on evolving implicit surfaces. *Computing and Visualization in Science*, 13(1):17–28, 2010.
- [30] Gerhard Dziuk and Charles M. Elliott. Finite element methods for surface PDEs. *Acta Numerica*, 22:289–396, 2013.
- [31] Gerhard Dziuk and Charles M. Elliott.  $L^2$ -estimates for the evolving surface finite element method. *Mathematics of Computation*, 82(281):1–24, 2013.
- [32] Charles M. Elliott and Björn Stinner. Modeling and computation of two phase geometric biomembranes using surface finite elements. *Journal of Computational Physics*, 229(18):6585–6612, 2010.
- [33] Charles M. Elliott, Björn Stinner, Vanessa Styles, and Richard Welford. Numerical computation of advection and diffusion on evolving diffuse interfaces. *IMA Journal of Numerical Analysis*, 2010.

- [34] Yurun Fan, Roger I. Tanner, and Nhan Phan-Thien. Galerkin/least-square finite-element methods for steady viscoelastic flows. *Journal of Non-Newtonian Fluid Mechanics*, 84(2):233–256, 1999.
- [35] Leopoldo P. Franca and Eduardo G. D. Do Carmo. The galerkin gradient least-squares method. *Computer Methods in Applied Mechanics and Engineering*, 74(1):41–54, 1989.
- [36] Leopoldo P. Franca and Rolf Stenberg. Error analysis of Galerkin least squares methods for the elasticity equations. *SIAM Journal on Numerical Analysis*, 28(6):1680–1697, 1991.
- [37] Sashikumaar Ganesan, Gunar Matthies, and Lutz Tobiska. Local projection stabilization of equal order interpolation applied to the Stokes problem. *Mathematics of Computation*, 77(264):2039–2060, 2008.
- [38] Sashikumaar Ganesan and Lutz Tobiska. Stabilization by local projection for convection–diffusion and incompressible flow problems. *Journal of Scientific Computing*, 43(3):326–342, 2010.
- [39] Vivette Girault and Pierre-Arnaud Raviart. *Finite element methods for Navier-Stokes equations : theory and algorithms*. Springer series in computational mathematics. Springer-Verlag, Berlin, New York, 1986.
- [40] Jörg Grande, Christoph Lehrenfeld, and Arnold Reusken. Analysis of a high order Trace Finite Element Method for PDEs on level set surfaces. 2016. arXiv:1611.01100.
- [41] Jörg Grande and Arnold Reusken. A higher order finite element method for partial differential equations on surfaces. *SIAM Journal on Numerical Analysis*, 54(1):388–414, 2016.
- [42] Wolfgang Hackbusch. *Theorie und Numerik elliptischer Differentialgleichungen*. Springer, 1986.
- [43] Lianhua He and Lutz Tobiska. The two-level local projection stabilization as an enriched one-level approach. *Advances in Computational Mathematics*, 36(4):503–523, 2012.
- [44] Thomas J.R. Hughes and Alec Brooks. A multidimensional upwind scheme with no crosswind diffusion. *Finite Element Methods for Convection Dominated Flows*, 34:19–35, 1979.
- [45] Thomas J.R. Hughes, Leopold P. Franca, Gregory M. Hulbert, Zdenek Johan, and Farzin Shakib. The Galerkin/least-squares method for advective-diffusive equations. In *Recent Developments in Computational Fluid Dynamics*, volume 1, pages 75–99, 1988.

- [46] Thomas J.R. Hughes, Leopoldo P. Franca, and Michel Mallet. A new finite element formulation for computational fluid dynamics: VI. Convergence analysis of the generalized SUPG formulation for linear time-dependent multidimensional advective-diffusive systems. *Computer Methods in Applied Mechanics and Engineering*, 63(1):97–112, 1987.
- [47] Volker John and Julia Novo. Error analysis of the SUPG finite element discretization of evolutionary convection-diffusion-reaction equations. *SIAM Journal on Numerical Analysis*, 49(3):1149–1176, 2011.
- [48] Petr Knobloch. A generalization of the local projection stabilization for convection-diffusion-reaction equations. *SIAM Journal on Numerical Analysis*, 48(2):659–680, 2010.
- [49] Petr Knobloch and Gert Lube. Local projection stabilization for advection–diffusion–reaction problems: One-level vs. two-level approach. *Applied Numerical Mathematics*, 59(12):2891–2907, 2009.
- [50] Petr Knobloch and Lutz Tobiska. On the stability of finite-element discretizations of convection–diffusion–reaction equations. *IMA Journal of numerical analysis*, 31:147–164, 2009.
- [51] Peter D. Lax and Arthur N. Milgram. *Parabolic Equations*, volume 33, pages 167–190. Princeton University Press, 1954.
- [52] Arif Masud and Thomas J.R. Hughes. A space-time Galerkin/least-squares finite element formulation of the Navier-Stokes equations for moving domain problems. *Computer Methods in Applied Mechanics and Engineering*, 146(1-2):91–126, 1997.
- [53] Gunar Matthies. Local projection methods on layer-adapted meshes for higher order discretisations of convection–diffusion problems. *Applied Numerical Mathematics*, 59(10):2515–2533, 2009.
- [54] Gunar Matthies. Local projection stabilisation for higher order discretisations of convection-diffusion problems on Shishkin meshes. *Advances in Computational Mathematics*, 30(4):315–337, 2009.
- [55] Gunar Matthies, Piotr Skrzypacz, and Lutz Tobiska. A unified convergence analysis for local projection stabilisations applied to the Oseen problem. *ESAIM: Mathematical Modelling and Numerical Analysis*, 41(4):713–742, 2007.
- [56] Gunar Matthies, Piotr Skrzypacz, and Lutz Tobiska. Stabilization of local projection type applied to convection-diffusion problems with mixed boundary conditions. *Electronic Transactions on Numerical Analysis*, 32:90–105, 2008.

- [57] Gunar Matthies and Lutz Tobiska. The Inf-Sup Condition for the Mapped  $Q_k$ - $P_{k-1}^{disc}$  Element in Arbitrary Space Dimensions. *Computing*, 69(2):119–139, 2002.
- [58] Uno Nävert. *A finite element method for convection-diffusion problems*. Chalmers Tekniska Högskola/Göteborgs Universitet. Department of Computer Science, 1982.
- [59] Maxim A. Olshanskii, Arnold Reusken, and Jörg Grande. A finite element method for elliptic equations on surfaces. *SIAM Journal on Numerical Analysis*, 47(5):3339–3358, 2009.
- [60] Maxim A. Olshanskii, Arnold Reusken, and Xianmin Xu. An Eulerian space-time finite element method for diffusion problems on evolving surfaces. *SIAM Journal on Numerical Analysis*, 52(3):1354–1377, 2014.
- [61] Maxim A. Olshanskii, Arnold Reusken, and Xianmin Xu. A stabilized finite element method for advection-diffusion equations on surfaces. *IMA Journal of Numerical Analysis*, 34(2):732–758, 2014.
- [62] Thomas Ranner. *Computational surface partial differential equations*. ProQuest LLC, Ann Arbor, MI, 2013. Thesis (Ph.D.)—University of Warwick (United Kingdom).
- [63] Andreas Rätz and Axel Voigt. PDE’s on surfaces—a diffuse interface approach. *Communications in Mathematical Sciences*, 4(3):575–590, 2006.
- [64] Hans-Görg Roos, Martin Stynes, and Lutz Tobiska. *Robust Numerical methods for singularly perturbed differential equations: convection-diffusion-reaction and flow problems*, volume 24. Springer Science & Business Media, 2008.
- [65] Kristin Simon and Lutz Tobiska. Local projection stabilization for convection-diffusion-reaction equations on surfaces. *BAIL 2016 proceedings (accepted)*, 2017.
- [66] Lonny L Thompson and Peter M. Pinsky. A Galerkin least-squares finite element method for the two-dimensional Helmholtz equation. *International Journal for Numerical Methods in Engineering*, 38(3):371–397, 1995.
- [67] Lutz Tobiska and Rüdiger Verfürth. Analysis of a streamline diffusion finite element method for the Stokes and Navier-Stokes equations. *SIAM Journal on Numerical Analysis*, 33(1):107–127, 1996.
- [68] Lutz Tobiska and Christian Winkel. *The Two-level Local Projection Stabilization as an Enriched One-level Approach: A One-dimensional Study*. Univ., Fak. für Mathematik, 2009.